WRINKLING OF THE FACINGS OF SANDWICH CONSTRUCTION SUBJECTED TO EDGEWISE COMPRESSION

Information Reviewed and Reaffirmed

April 1961

No. 1810

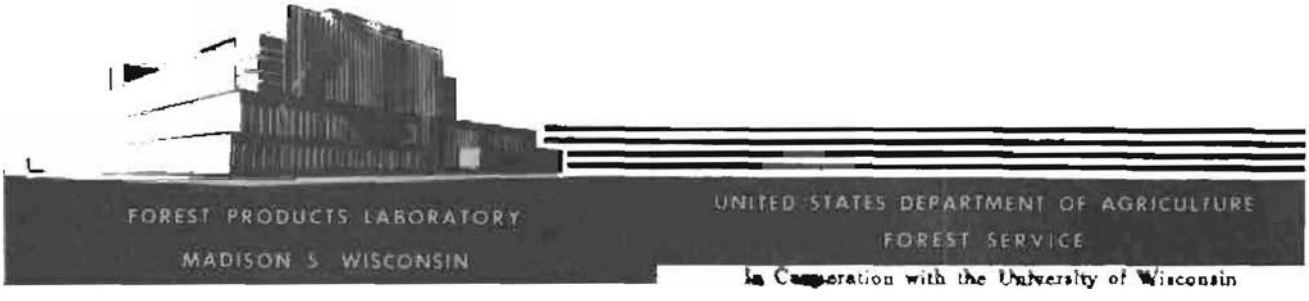

WRINKLING OF THE FACINGS OF SANDWICH CONSTRUCTIONS SUBJECTED TO EDGEWISE COMPRESSION[1]

By

CHARLES B. NORRIS, Engineer
WILHELM S. ERICKSEN, Mathematician
H. W. MARCH, Mathematician
C. B. SMITH, Mathematician
KENNETH H. BOLLER, Engineer

Forest Products Laboratory,[2] Forest Service
U. S. Department of Agriculture

SYNOPSIS

This report, which includes a theoretical and an experimental investigation of the stability of the facings of sandwich columns in endwise compression, is divided into three parts. Part I contains the mathematical analysis. It makes use of the simplifying assumptions of Gough, Elam, and deBruyne and applies to orthotropic as well as to isotropic materials. Comparison is made with the more accurate but more complicated results of Williams, Leggett, and Hopkins, of Cox, and of others.

Part II gives the data from a series of tests and a comparison of the theoretical predictions with the results of tests.

Part III gives suggested design criteria. It is complete in itself, so that the designer need not be familiar with the other two parts. He should, however, read the introduction to Part I and all of Part II.

[1] This progress report is one of a series prepared and distributed by the Forest Products Laboratory under U.S. Navy, Bureau of Aeronautics No. NBA-PO-NAer 00619 and USAF-PO-(33-038)49-4696E. Results here reported are preliminary and may be revised as additional data become available. Previous report dated November 1949.

[2] Maintained at Madison, Wis., in cooperation with the University of Wisconsin.

PART I. MATHEMATICAL ANALYSIS

Introduction

The problem of the wrinkling of the facings of a sandwich column under compressive end load is essentially the problem of the stability of two elastically supported sheets, of which the elastic support of one is influenced to a greater or less extent by the presence of the other. In the mathematical treatment of the problem, it has been customary to consider types of instability of the facings involving fully developed sinusoidal wave patterns of a definite wave length that is so chosen that the compressive wrinkling stress is a minimum for the type of instability considered. The two types of instability that are commonly considered are the following:

(a) Antisymmetrical wrinkling. --The sinusoidal wrinkles of the two facings are in phase as shown in figure 1, A.

(b) Symmetrical wrinkling. --The faces are displaced symmetrically with respect to the undistorted middle plane of the core as shown in figure 1, B.

It is probable that none of these idealized types is realized in a test of a sandwich column under compressive end load. What actually occurs is the result of the modification of the magnitude and forms of the initial irregularities in the facings. If the facings were perfectly flat and the core perfectly homogeneous, the theoretical critical stress would be the lowest of the stresses associated with the various possible types of wrinkling instability, or the stress associated with the buckling of the column into a single half wave if the stress would be still lower. If initial irregularities are present, those in each facing can be considered to be resolved into their Fourier sine components. As the stress in the facings increases, the amplitude of each of the Fourier components will grow, with the one whose wave length is nearest to that of the ideal wave length corresponding to the critical stress, being ultimately the one most greatly amplified. It will be found, however, that in addition to the one component whose wave length is closest to that of the ideal wave length, there are other Fourier components whose wave lengths differ but little from the ideal. The amplitudes of such components will be amplified nearly as much as the amplitude associated with the ideal wave length. It will only be true when the stress in the facings is almost equal to the critical stress, that the amplitude of the ideal wave form is magnified out of all proportion to those of other component waves. Consequently, it may very well happen that the combination of the magnified amplitudes of a group of waves of nearly the same wave length as

the ideal one, will result in a local deformation of the facing from its plane of such magnitude that failure will occur as the result of local stresses that exceed the strength of the core or the glue line. Such stresses, which may be tensile or compressive stresses in the direction perpendicular to the facings or may be shear stresses, will cause failure of the sandwich before the predicted wrinkling stress is reached.

The load carried by the core of a sandwich column with a light core and strong facings is usually a very small fraction of that carried by the facings. It is possible, however, depending on the core material, that this load will stress the core beyond its proportional limit or cause failure before the stress in the facings is equal to that predicted for wrinkling failure. While this stress is present in a perfectly flat sandwich in compression, it is augmented in the vicinity of an initial irregularity and may locally exceed that computed from the strains in the facings of a flat sandwich.

It is evident, then, that the wrinkling stress that is the lowest for the various possible modes considered in the mathematical analysis, will not usually be attained in an actual test. The effect of initial irregularities will be to lower the stress for each mode and to lower each by a different amount. Thus local failure may occur at a stress that is lower than the lowest predicted for any idealized type of wrinkling failure. Other types of failure, such as buckling of the column as a whole or shear failure in the core, may also occur at loads lower than those associated with wrinkling failure.

The first theoretical study of the wrinkling of sandwich columns of isotropic materials in compression was made by Gough, Elam, and deBruyne (4). [3] To obtain relatively simple formulas for the critical compressive stress, they introduced certain simplifying assumptions. It was noted by Williams, Leggett, and Hopkins (10) that these formulas lead to incorrect results for wrinkles of long wave lengths. They introduced more suitable boundary conditions and developed formulas for sandwiches with both isotropic and orthotropic cores. For sandwiches with isotropic cores and antisymmetrical wrinkling, they found that, except for wrinkles of the longer wave lengths, where buckling of the column as a whole rather than wrinkling may be expected, the formulas of Gough, Elam, and deBruyne led to results in satisfactory agreement with those obtained by their own formulas. The formulas of Williams, Leggett, and Hopkins are exceedingly complicated and are net suited to the numerical computations required for an extensive series of sandwich constructions. Cox (2), in his study of sandwiches with orthotropic cores, introduced parameters that are very well suited to the problem

[3] Underlined numbers in parenthesis refer to papers or reports listed under Literature Cited at the end of this report.

at hand, and discussed extensively both symmetrical and antisymmetrical wrinkling. For antisymmetrical wrinkling, his formulas are in agreement with those of Williams, Leggett, and Hopkins. For large core thicknesses, he derived satisfactory approximate formulas, Van der Neut (7) undertook to improve the boundary conditions used by Gough, Elam, and deBruyne, but, as pointed out by Bijlaard (1), he tacitly retained one of their assumptions. Bijlaard made the necessary modifications to remove this restriction and carried out an analysis for isotropic facings and core that is in essential agreement with that of Williams, Leggett, and Hopkins. Hoff and Mautner (5) considered symmetrical and other types of wrinkling under assumptions similar to those of Gough, Elam, and deBruyne. An estimate of the destabilizing effect of the compressive stress in the core was made by Williams, Leggett, and Hopkins (10).

Other papers that should be mentioned are that of Wan (8), who derived formulas having special reference to sandwich columns such as metal-faced balsa, where the Young's modulus of the core in the direction perpendicular to the facings is very large compared to that in the direction of the load and to the shear modulus in planes parallel to the load and perpendicular to the facings; and that of Williams (9), whose aim was to present simplified methods for the use of the designer. Both of these writers considered the effect of initial irregularities. In papers by Goodier (3) and Neuber (6), the destabilizing effect of the compressive stress in the core is analyzed.

In sections 1 through 10 that follow, the wrinkling of an initially flat sandwich with either orthotropic or isotropic facings and cores is discussed by making use of the assumptions of Gough, Elam, and deBruyne. In the treatment of this problem, it is assumed that the loads carried by the two facings are equal. It is shown that under these assumptions two dimensionless parameters, β and σ, which are functions of the elastic constants of the core, specify completely the elastic properties of the core. These parameters were introduced by Cox (2). The prediction of stress at failure is based upon two quantities, Q_f and q, which are proportional, respectively, to the theoretical wrinkling stress, p_f, and the ratio, c/f, of the thickness of the core to that of the facings, as shown by the following equations:

$$p_f = Q_f \overline{E},$$

$$q = \frac{c}{f} x,$$

where $\overline{E}$ and x are determined by the elastic properties of the core and facings. A series of curves relating q and Q_f for various combinations of β and σ are given. The introduction of these parameters makes it possible

to take into account in a comparatively simple manner the wide variation in the relative magnitudes of the elastic constants of orthotropic cores, among which no relation exists corresponding to that connecting the Young's modulus, the modulus of rigidity, and Poisson's ratio for isotropic cores.

The derived relations between Q_f and q apply equally well under either an assumed state of plane stress or plane strain in the core. The desired state is imposed by the definition of constants upon which depend the quantity $\overline{E}$ and the quantities β, σ, and x, as well.

In section 11 a comparison is made between the formulas derived by Cox (2) and the corresponding formulas developed in this report. It is shown that—for a given sandwich the difference between the results obtained by the formulas compared depends upon the parameter x. The degree to which the present results approximate those of Cox therefore depends upon the magnitude of this parameter.

Sections 12, 13, and 14 are devoted to the analysis of stresses in the core when the faces have initial irregularities. In section 12 formulas for the stresses are derived, under an assumption of initial irregularities, of a general class which have been resolved into their Fourier sine components. In sections 13 and 14 these formulas are applied to special cases.

In section 15 a possible application of the formulas to predicting failure at stresses above the proportional limit of the face material is discussed.

A summary of the results and suggestions for their applications are given in part III of the report.

Development of Formulas

1. Orientation of Axes

The axes of reference x, y, z (fig. 2) are so oriented that the x, z plane is the middle surface of the core in its undeformed state, with the x axis being parallel to the direction of loading. By designating the thickness of the core by c and that of each facing by f, the planes

$y = \pm \frac{c}{2}$ separate the core and the facings, and the planes

$y = \pm \frac{c + f}{2}$ are the middle surfaces of the facings prior to loading.

2. Assumed Form of Wrinkles

It is assumed that the planes $y = \pm \frac{c}{2}$ are deformed under the compressive end load into sinusoidal surfaces and that this deformation takes place without displacement in the direction of loading. The conditions imposed at these surfaces are:

$$\left.\begin{aligned} u_1 &= u_2 = 0 \\ v_1 &= a \sin \frac{\pi}{L} x \\ v_2 &= \delta\, a \sin \frac{\pi}{L} x \end{aligned}\right\} \qquad 1.2.1$$

where the subscripts 1 and 2 associate the components u and v of displacement with the surfaces $y = \frac{c}{2}$ and $y = -\frac{c}{2}$, respectively. The value assigned to δ is either +1 or -1. The former value prescribes wrinkles in the two facings that are antisymmetrical, and the latter, those that are symmetrical, with respect to the undeformed middle surface of the core.

3. Stress-strain Relations of the Core

The core of the sandwich is assumed to be orthotropic, with the orthotropic axes coinciding with the axes of reference. The components of stress and strain are then connected by the relations[4]

$$\left.\begin{aligned} e_{xx} &= \frac{1}{E_x} X_x - \frac{\sigma_{yx}}{E_y} Y_y - \frac{\sigma_{zx}}{E_z} Z_z \\ e_{yy} &= -\frac{\sigma_{xy}}{E_x} X_x + \frac{1}{E_y} Y_y - \frac{\sigma_{zy}}{E_z} Z_z \\ e_{zz} &= -\frac{\sigma_{xz}}{E_x} X_x - \frac{\sigma_{yz}}{E_y} Y_y + \frac{1}{E_z} Z_z \\ e_{xy} &= \frac{1}{\mu_{xy}} X_y, \quad e_{yz} = \frac{1}{\mu_{yz}} Y_z, \quad e_{zx} = \frac{1}{\mu_{zx}} Z_x \end{aligned}\right\} \qquad 1.3.1$$

---

[4] March, H. W. Flat Plates of Plywood Under Uniform or Concentrated Loads. U. S. Forest Products Laboratory Report No. 1312, page 34. Love's notations for stress and strain components are used. (A. E. Love, The Mathematical Theory of Elasticity, Cambridge University Press, 1920.)

In these equations E_x, E_y, and E, are Young's moduli in the directions x, y, and z, respectively. Poisson's ratio, σ_{xy}, is the ratio of the contraction parallel to the y-axis to the extension parallel to the x-axis associated with a tension parallel to the x-direction. The quantity μ_{xz}, is the modulus of rigidity associated with the directions x and z.

The problem is reduced to one in two dimensions by assuming either a state of plane stress or of plane strain with respect to the x, y plane. In the former the stress components, Z_z, Y_z, and Z_x, and in the latter the strain components, e_{zz}, e_{yz}, and e_{zx}, are assumed to vanish. Under either assumption the relations required below may be derived from 1.3.1 in the forms

$$\left.\begin{aligned} e_{xx} &= a_{11} X_x - a_{12} Y_y \\ e_{yy} &= -a_{12} X_x + a_{22} Y_y \\ e_{xy} &= \frac{1}{\mu_{xy}} X_y \end{aligned}\right\} \qquad 1.3.2$$

For the state of plane stress,

$$a_{11} = \frac{1}{E_x}, \quad a_{12} = \frac{\sigma_{xy}}{E_x}, \quad a_{22} = \frac{1}{E_y} \qquad 1.3.3$$

and for plane strain,

$$\left.\begin{aligned} a_{11} &= \frac{1 - \sigma_{xz}\,\sigma_{zx}}{E_x} \\ a_{12} &= \frac{\sigma_{xy} + \sigma_{xz}\,\sigma_{zy}}{E_x} \\ a_{22} &= \frac{1 - \sigma_{zy}\,\sigma_{yz}}{E_y} \end{aligned}\right\} \qquad 1.3.4$$

4. The Stress Function and Stress Components

The compatibility of strains in the x, y plane requires that

$$\frac{\partial^2 e_{xx}}{\partial y^2} + \frac{\partial^2 e_{yy}}{\partial x^2} - \frac{\partial^2 e_{xy}}{\partial x\,\partial y} = 0 \qquad 1.4$$

Introducing a stress function, F (x, y), such that

$$X_x = \frac{\partial^2 F}{\partial y^2}, \quad Y_y = \frac{\partial^2 F}{\partial x^2}, \quad X_y = -\frac{\partial^2 F}{\partial x \partial y} \tag{1.4.1}$$

and by applying the relations (1.3.2), it is found from the above compatibility condition that

$$a_{22} \frac{\partial^4 F}{\partial x^4} + \left\{ \frac{1}{\mu_{xy}} - 2a_{12} \right\} \frac{\partial^4 F}{\partial x^2 \partial y^2} + a_{11} \frac{\partial^4 F}{\partial y^4} = 0$$

This equation is transformed into the more convenient form

$$\frac{\partial^4 F}{\partial x^4} + 2\kappa \frac{\partial^4 F}{\partial x^2 \partial \eta^2} + \frac{\partial^4 F}{\partial \eta^4} = 0 \tag{1.4.2}$$

where

$$\kappa = \frac{1}{2\sqrt{a_{11} a_{22}}} \left\{ \frac{1}{\mu_{xy}} - 2a_{12} \right\} \tag{1.4.3}$$

by the transformation

$$\eta = \epsilon y \tag{1.4.4}$$

with

$$\epsilon = \sqrt[4]{\frac{a_{22}}{a_{11}}} \tag{1.4.5}$$

For the problem here considered, a suitable form of the solution of 1.4.2 is

$$F = \left[A_1 \sinh \nu y + A_2 \sinh \bar{\nu} y + B_1 \cosh \nu y + B_2 \cosh \bar{\nu} y \right] \sin \frac{\pi x}{L} \tag{1.4.6}$$

with

$$\nu = \frac{\pi \epsilon \alpha}{L}, \quad \bar{\nu} = \frac{\pi \epsilon \bar{\alpha}}{L}, \tag{1.4.7}$$

$$\alpha = \alpha_1 + \alpha_2, \quad \bar{\alpha} = \alpha_1 - \alpha_2, \tag{1.4.8}$$

$$\alpha_1 = \sqrt{\frac{\kappa + 1}{2}}, \quad \alpha_2 = \sqrt{\frac{\kappa - 1}{2}} \tag{1.4.9}$$

5. Components of Stress and Displacement in the Core

By applying the relations 1.4.1, the following expressions for the stress components in the core are obtained from expression 1.4.6.

$$X_x = \left[A_1 \nu^2 \sinh \nu y + A_2 \bar{\nu}^2 \sinh \bar{\nu} y + B_1 \nu^2 \cosh \nu y + B_2 \bar{\nu}^2 \cosh \bar{\nu} y \right] \sin \frac{\pi}{L} x \qquad 1.5.1$$

$$Y_y = - \left(\frac{\pi}{L}\right)^2 F \qquad 1.5.2$$

$$X_y = \frac{\pi}{L} \left[A_1 \nu \cosh \nu y + A_2 \bar{\nu} \cosh \bar{\nu} y + B_1 \nu \sinh \nu y + B_2 \bar{\nu} \sinh \bar{\nu} y \right] \cos \frac{\pi}{L} x \qquad 1.5.3$$

By substituting these into 1.3.2, it is found that

$$e_{xx} = \left(\frac{\pi}{L}\right)^2 \left[A_1 g_1 \sinh \nu y + A_2 \bar{g}_1 \sinh \bar{\nu} y + B_1 g_1 \cosh \nu y + B_2 \bar{g}_1 \cosh \bar{\nu} y \right] \sin \frac{\pi x}{L} \qquad 1.5.4$$

$$e_{yy} = - \left(\frac{\pi}{L}\right)^2 \left[A_1 g_2 \sinh \nu y + A_2 \bar{g}_2 \sinh \bar{\nu} y + B_1 g_2 \cosh \nu y + B_2 \bar{g}_2 \cosh \bar{\nu} y \right] \sin \frac{\pi x}{L} \qquad 1.5.5$$

where

$$g_1 = a_{11} \epsilon^2 \alpha^2 + a_{12}, \quad g_2 = a_{12} \epsilon^2 \alpha^2 + a_{22},$$
$$\bar{g}_1 = a_{11} \epsilon^2 \bar{\alpha}^2 + a_{12}, \quad \bar{g}_2 = a_{12} \epsilon^2 \bar{\alpha}^2 + a_{22}. \qquad 1.5.6$$

Since

$$e_{xx} = \frac{\partial u}{\partial x}, \quad e_{yy} = \frac{\partial v}{\partial y}, \qquad 1.5.7$$

$$u = - \frac{\pi}{L} \left[A_1 g_1 \sinh \nu y + A_2 \bar{g}_1 \sinh \bar{\nu} y + B_1 g_1 \cosh \nu y + B_2 \bar{g}_1 \cosh \bar{\nu} y \right] \cos \frac{\pi x}{L} \qquad 1.5.8$$

and

$$v = -\left(\frac{\pi}{L}\right)^2 \left[\frac{A_1 g_2}{\nu} \cosh \nu y + \frac{A_2 \bar{g}_2}{\bar{\nu}} \cosh \bar{\nu} y + \frac{B_1 g_2}{\nu} \sinh \nu y + \frac{B_2 \bar{g}_2}{\bar{\nu}} \sinh \bar{\nu} y \right] \sin \frac{\pi x}{L} \qquad 1.5.9$$

These expressions for the components of displacements satisfy the conditions imposed by the relations 1.2.1 at the boundaries $y = \pm \frac{c}{2}$ provided

$$\left.\begin{aligned} A_1 &= \frac{(1+\delta)\, a\epsilon\, L\, \bar{g}_1 \sinh \frac{\bar{\nu} c}{2}}{2\pi \left\{ g_1 \bar{g}_2\, \alpha \sinh \frac{\nu c}{2} \cosh \frac{\bar{\nu} c}{2} - \bar{g}_1 g_2\, \bar{\alpha} \sinh \frac{\bar{\nu} c}{2} \cosh \frac{\nu c}{2} \right\}} \\ A_2 &= \bar{A}_1 \\ B_1 &= \frac{(1-\delta)\, a\epsilon\, L\, \bar{g}_1 \cosh \frac{\bar{\nu} c}{2}}{2\pi \left\{ g_1 \bar{g}_2\, \alpha \sinh \frac{\bar{\nu} c}{2} \cosh \frac{\nu c}{2} - \bar{g}_1 g_2\, \bar{\alpha} \sinh \frac{\nu c}{2} \cosh \frac{\bar{\nu} c}{2} \right\}} \\ B_2 &= \bar{B}_1 \end{aligned}\right\} \qquad 1.5.10$$

where $\bar{A}_1$ and $\bar{B}_1$ denote the quantities A_1 and B_1, respectively, with a and $\bar{\alpha}$ interchanged. The following expressions for the stress component Y_y at the boundaries $y \pm \frac{c}{2}$ are obtained by substituting 1.5.10 into 1.5.2.

$$\left.\begin{aligned} (Y_y)_{y = \frac{c}{2}} &= a\gamma_1 \sin \frac{\pi}{L} x \\ (Y_y)_{y = -\frac{c}{2}} &= a\gamma_2 \sin \frac{\pi}{L} x \end{aligned}\right\} \qquad 1.5.11$$

with

$$\gamma_i = \frac{\pi\epsilon}{2L} (g_1 - \bar{g}_1) \left[\frac{(-1)^{i+1} (1+\delta)}{g_1 \bar{g}_2\, \alpha \coth \frac{\bar{\nu} c}{2} - \bar{g}_1 g_2\, \bar{\alpha} \coth \frac{\nu c}{2}} + \frac{(1-\delta)}{g_1 \bar{g}_2\, \alpha \tanh \frac{\bar{\nu} c}{2} - \bar{g}_1 g_2\, \bar{\alpha} \tanh \frac{\nu c}{2}} \right]_{i = 1, 2} \qquad 1.5.12$$

Similarly, the shear stress component, X_y, given by 1.5.3 may be expressed in the form

$$\left.\begin{aligned}(X_y)_{y=\frac{c}{2}} &= a\tau_1 \cos\frac{\pi}{L}x,\\ (X_y)_{y=-\frac{c}{2}} &= a\tau_2 \cos\frac{\pi}{L}x,\end{aligned}\right\} \qquad 1.5.13$$

with

$$\tau_i = \frac{\pi\epsilon^2}{2L}\left[\frac{(1+\delta)\left\{g_1\bar{\alpha}\coth\frac{\bar{\nu}c}{2} - \bar{g}_1\alpha\coth\frac{\nu c}{2}\right\}}{g_1\bar{g}_2\alpha\coth\frac{\nu c}{2} - \bar{g}_1 g_2\bar{\alpha}\coth\frac{\nu c}{2}}\right.$$

$$\left. + (-1)^{i+1}\frac{(1-\delta)\left\{g_1\bar{\alpha}\tanh\frac{\bar{\nu}c}{2} - \bar{g}_1\alpha\tanh\frac{\nu c}{2}\right\}}{g_1\bar{g}_2\alpha\tanh\frac{\bar{\nu}c}{2} - \bar{g}_1 g_2\bar{\alpha}\tanh\frac{\nu c}{2}}\right]_{i=1,2} \qquad 1.5.14$$

6. Expressions for Strain Energy in the Core and Faces and the Work Done by the Applied Load

The strain energy in the core is expressed as the integral of the quantity

$$\frac{1}{2}(X_n u + Y_n v)$$

taken around the entire boundary. In this expression

$$X_n = X_x \cos(x,n) + X_y \cos(y,n),$$

$$Y_n = X_y \cos(x,n) + Y_y \cos(y,n)$$

where cos (x, n), cos (y, n) are direction cosines of the external normal to the boundary considered. Since the components of stress and displacement are periodic in x, it suffices to consider the integral over any half period. By taking a strip of unit width, and denoting the energy by W_c,

$$W_c = \frac{1}{2}\int_0^L (vY_y)_{y=\frac{c}{2}}\,dx - \frac{1}{2}\int_0^L (vY_y)_{y=-\frac{c}{2}}\,dx \qquad 1.6.1$$

When formulas 1.2.1 and 1.5.11 are substituted into this expression, it is found that

$$W_c = \frac{a^2 L}{4}\left\{\gamma_1 - \delta\gamma_2\right\} \qquad 1.6.2$$

The strain energy in bending in the faces over one-half wave length of a strip of unit width is

$$W_B = \frac{E_f f^3}{24\lambda_f}\int_0^L \left(\frac{d^2 v_1}{dx^2}\right)^2 dx + \frac{E_f f^3}{24\lambda_f}\int_0^L \left(\frac{d^2 v_2}{dx^2}\right)^2 dx \qquad 1.6.3$$

where E_f denotes the Young's modulus of the facing material in the direction of the compressive load and

$$\lambda_f = 1 - \sigma_{xzf}\,\sigma_{zxf}$$

where σ_{xzf} and σ_{zxf} are Poisson's ratios.

By substituting expression 1.2.1

$$W_B = \frac{E_f f^3 \pi^4 a^2}{24\lambda_f L^3}. \qquad 1.6.4$$

The work done by the applied compressive load, calculated for the same portion of the strip, is given by the expression

$$W_P = \frac{P}{2}\int_0^L \left(\frac{dv_1}{dx}\right)^2 dx + \frac{P}{2}\int_0^L \left(\frac{dv_2}{dx}\right)^2 dx \qquad 1.6.5$$

where P denotes the load applied to each face. In this expression displacements at the surfaces of the core in the direction of loading are made use of in order to account for the work done by the applied load. These displacements were neglected in deriving the expression for the energy in the core, since in that case they lead to additional quantities that are infinitesimals of higher order than those already derived and that are therefore neglected in finding the critical load. By substituting expressions 1.2.1 into 1.6.5, it is found that

$$W_P = \frac{P \pi^2 a^2}{2L} \qquad 1.6.6$$

7. Expressions for the Wrinkling Stress

The condition that a facing be in unstable equilibrium under the compressive load, P, is that

$$W_P = W_B + W_C \qquad 1.7.1$$

It is found on substituting expressions 1.6.2, 1.6.4, and 1.6.6 into 1.7.1 that

$$P = \frac{E_f f^3 \pi^2}{12\lambda_f L^2} + \frac{L^2}{2\pi^2}\left\{\gamma_1 - \delta\,\gamma_2\right\} \qquad 1.7.2$$

and on substituting for γ_1, and γ_2 from 1.5.12

$$P = \frac{E_f f^3 \pi^2}{12\lambda_f L^2} + \frac{\epsilon L(g_1 - \bar{g}_1)}{2\pi}\left[\frac{(1+\delta)}{g_1\bar{g}_2\,\alpha\coth\frac{\bar{\nu}c}{2} - \bar{g}_1 g_2\,\bar{\alpha}\coth\frac{\nu c}{2}} + \frac{1-\delta}{g_1\bar{g}_2\,\alpha\tanh\frac{\bar{\nu}c}{2} - \bar{g}_1 g_2\,\bar{\alpha}\tanh\frac{\nu c}{2}}\right] \qquad 1.7.3$$

Since P is the load per inch of edge on each face,

$$p = \frac{P}{f} \qquad 1.7.4$$

is an expression for the compressive stress. By introducing this notation and letting

$$r = \frac{c}{f} \qquad 1.7.5$$

$$\zeta = \frac{\epsilon \pi c}{L} \qquad 1.7.6$$

so that

$$\nu c = \alpha\zeta, \qquad \bar{\nu}c = \bar{\alpha}\zeta,$$

$$p = \frac{E_f \zeta^2}{12\lambda_f \epsilon^2 r^2} + \frac{r\epsilon^2 (g_1 - \bar{g}_1)}{2\zeta} \left[\frac{1+\delta}{g_1 \bar{g}_2 \alpha \coth \frac{\bar{\alpha}\zeta}{2} - \bar{g}_1 g_2 \bar{\alpha} \coth \frac{\alpha\zeta}{2}} \right.$$

$$\left. + \frac{1-\delta}{g_1 \bar{g}_2 \alpha \tanh \frac{\bar{\alpha}\zeta}{2} - \bar{g}_1 g_2 \bar{\alpha} \tanh \frac{\alpha\zeta}{2}} \right] \qquad 1.7.7$$

The above expression for p is always real, for in the event that α is complex, the last term on the right consists of the quotients of two quantities, each of which is the difference between conjugate functions of α. It is, however, desirable to reduce the expression to one containing no complex quantities by separating into parts in α_1 and α_2. It also proves to be advantageous to replace p, the stress in the facings, and r, the ratio of the thickness of the core to that of each facing, by quantities proportional to them and to introduce certain combinations of elastic constants. All these changes are made in accordance with the following equations.

$$p = Q\bar{E} \qquad 1.7.8$$

$$r = \frac{q}{x} \qquad 1.7.9$$

$$\bar{E} = \sqrt[3]{\frac{E_f}{\lambda_f} \frac{\mu_{xy}}{a_{22}}} \qquad 1.7.10$$

$$x = \frac{\mu_{xy}}{\bar{E}} \qquad 1.7.11$$

$$\left.\begin{aligned} E &= \frac{1}{\sqrt{a_{11} a_{22}}} \\ \sigma &= a_{12} E \\ \beta &= \frac{\mu_{xy}}{E} \end{aligned}\right\} \qquad 1.7.12$$

The combinations 1.7.12 are due to Cox (2). Gough, Elam, and deBruyne (4), Hoff and Mautner (5), and Williams (9) used a parameter quite similar to 1.7.8.

The various steps taken to introduce the above changes are the following. By definitions 1.4.3 and 1.7.12,

$$\kappa = \frac{1}{2\beta} - \sigma \qquad 1.7.13$$

and from 1.4.5 and 1.7.12,

$$a_{11} = \frac{1}{\epsilon^2 E}, \quad a_{22} = \frac{\epsilon^2}{E} \qquad 1.7.14$$

Therefore, by substitution into 1.5.6

$$g_1 = \frac{1}{E}\left\{\alpha^2 + \sigma\right\} \qquad 1.7.15$$

and

$$g_2 = \frac{\epsilon^2}{E}\left\{\alpha^2\sigma + 1\right\} \qquad 1.7.16$$

From 1.7.15 with the application of relations 1.4.8,

$$g_1 - \bar{g}_1 = \frac{4\alpha_1\alpha_2}{E} \qquad 1.7.17$$

By using the relation

$$\alpha\,\bar{\alpha} = 1,$$

1.7.15 and 1.7.16 yield

$$g_1\bar{g}_2\,\alpha = \frac{\epsilon^2}{E^2}\left\{\alpha^3 + 2\sigma\alpha + \sigma^2\bar{\alpha}\right\}$$

$$\bar{g}_1 g_2\,\bar{\alpha} = \frac{\epsilon^2}{E^2}\left\{\bar{\alpha}^3 + 2\sigma\bar{\alpha} + \sigma^2\alpha\right\}$$

After substituting the values of α and $\bar{\alpha}$ from 1.4.8, and applying relations 1.4.9 and 1.7.13, it is found that

$$\left.\begin{aligned} g_1\bar{g}_2\alpha &= \frac{\alpha_1\alpha_2\epsilon^2}{\mu_{xy}E}\left\{\frac{G}{\alpha_1}+\frac{H}{\alpha_2}\right\} \\ \text{and}\quad \bar{g}_1 g_2\bar{\alpha} &= \frac{\alpha_1\alpha_2\epsilon^2}{\mu_{xy}E}\left\{-\frac{G}{\alpha_1}+\frac{H}{\alpha_2}\right\} \end{aligned}\right\} \qquad 1.7.18$$

where

$$\left.\begin{aligned} G &= 1+(1-\sigma^2)\beta \\ H &= 1-(1-\sigma^2)\beta \end{aligned}\right\} \qquad 1.7.19$$

The hyperbolic functions appearing in formula 1.7.7 are separated into parts in α_1 and α_2 by the relations

$$\coth(\alpha_1 \pm \alpha_2)\frac{\zeta}{2} = \frac{\sinh\alpha_1\zeta \pm \sinh\alpha_2\zeta}{\cosh\alpha_1\zeta - \cosh\alpha_2\zeta} \qquad 1.7.20$$

$$\tanh(\alpha_1 \pm \alpha_2)\frac{\zeta}{2} = \frac{\sinh\alpha_1\zeta \pm \sinh\alpha_2\zeta}{\cosh\alpha_1\zeta + \cosh\alpha_2\zeta} \qquad 1.7.21$$

From 1.7.18 and 1.7.20,

$$g_1\bar{g}_2\,\alpha\coth\bar{\alpha}\frac{\zeta}{2} - \bar{g}_1 g_2\,\bar{\alpha}\coth\alpha\frac{\zeta}{2} = \frac{2\alpha_1\alpha_2\epsilon^2}{\mu_{xy}E}\left[\frac{G\dfrac{\sinh\alpha_1\zeta}{\alpha_1}+H\dfrac{\sinh\alpha_2\zeta}{\alpha_2}}{\cosh\alpha_1\zeta-\cosh\alpha_2\zeta}\right] \qquad 1.7.22$$

and from 1.7.18 and 1.7.21,

$$g_1\bar{g}_2\,\alpha\tanh\bar{\alpha}\frac{\zeta}{2} - \bar{g}_1 g_2\,\bar{\alpha}\tanh\alpha\frac{\zeta}{2} = \frac{2\alpha_1\alpha_2\epsilon^2}{\mu_{xy}E}\left[\frac{G\dfrac{\sinh\alpha_1\zeta}{\alpha_1}-H\dfrac{\sinh\alpha_2\zeta}{\alpha_2}}{\cosh\alpha_1\zeta+\cosh\alpha_2\zeta}\right] \qquad 1.7.23$$

With the substitution of 1.7.8, 1.7.9, 1.7.17, 1.7.22, and 1.7.23 into 1.7.7,

$$Q = \frac{\zeta^2}{12q^2}\frac{\mu_{xy}}{E} + \frac{2q}{\zeta}\left[\frac{(1+\delta)}{2}\left\{\frac{\cosh\alpha_1\zeta - \cosh\alpha_2\zeta}{G\frac{\sinh\alpha_1\zeta}{\alpha_1} + H\frac{\sinh\alpha_2\zeta}{\alpha_2}}\right\}\right.$$

$$\left. + \frac{(1-\delta)}{2}\left\{\frac{\cosh\alpha_1\zeta + \cosh\alpha_2\zeta}{G\frac{\sinh\alpha_1\zeta}{\alpha_1} - H\frac{\sinh\alpha_2\zeta}{\alpha_2}}\right\}\right] \qquad 1.7.24$$

In the event that $\kappa < 1$,

$$i\alpha_2 = \sqrt{\frac{1-\kappa}{2}} \qquad 1.7.25$$

is real and the relations

$$\left.\begin{aligned}\cosh\alpha_2\zeta &= \cos i\alpha_2\zeta\\ \frac{\sinh\alpha_2\zeta}{\alpha_2} &= \frac{\sin i\alpha_2\zeta}{i\alpha_2}\end{aligned}\right\} \qquad 1.7.26$$

are used to eliminate the pure imaginary arguments appearing in 1.7.24.

If the core is isotropic, $\alpha_1 = 1$ and $\alpha_2 = 0$. Formula 1.7.24 applies in this case after taking the limit as $\alpha_2 \to 0$.

Reference to formulas 1.4.9, 1.7.13, and 1.7.19 shows that α_1, α_2, G and H are functions of ß and σ alone. While the quantity ζ, 1.7.6, contains the factor E, one is usually only interested in the minimum value of Q with respect to L (or ζ) for a specified value of q in the problem of wrinkling. The variable ζ is thus eliminated, and, therefore, the elastic properties of the core are completely specified by the two parameters ß and σ.

For reference below, it is convenient to have on hand the forms of γ_i and τ_i when separated into parts in α_1 and α_2. The expression

$$\gamma_i = \frac{2\pi\,\mu_{xy}}{\epsilon\,L}\left[(-1)^{i+1}\,\frac{(1+\delta)}{2}\left\{\frac{\cosh\alpha_1\zeta - \cosh\alpha_2\zeta}{G\frac{\sinh\alpha_1\zeta}{\alpha_1} + H\frac{\sinh\alpha_2\zeta}{\alpha_2}}\right\}\right.$$

$$\left. + \frac{(1-\delta)}{2}\left\{\frac{\cosh\alpha_1\zeta + \cosh\alpha_2\zeta}{G\frac{\sinh\alpha_1\zeta}{\alpha_1} - H\frac{\sinh\alpha_2\zeta}{\alpha_2}}\right\}\right] \qquad 1.7.27$$

is obtained by substituting 1.7.17, 1.7.22, and 1.7.23 into 1.5.12. With the relations

$$g_1\,\bar{\alpha}\coth\bar{\alpha}\frac{\zeta}{2} - \bar{g}_1\,\alpha\coth\alpha\frac{\zeta}{2} =$$

$$\frac{2\alpha_1\alpha_2}{E}\left\{\frac{(1-\sigma)\frac{\sinh\alpha_1\zeta}{\alpha_1} + (1+\sigma)\frac{\sinh\alpha_2\zeta}{\alpha_2}}{\cosh\alpha_1\zeta - \cosh\alpha_2\zeta}\right\}$$

$$g_1\,\bar{\alpha}\tanh\bar{\alpha}\frac{\zeta}{2} - \bar{g}_1\,\alpha\tanh\alpha\frac{\zeta}{2} =$$

$$\frac{2\alpha_1\alpha_2}{E}\left\{\frac{(1-\sigma)\frac{\sinh\alpha_1\zeta}{\alpha_1} - (1+\sigma)\frac{\sinh\alpha_2\zeta}{\alpha_2}}{\cosh\alpha_1\zeta + \cosh\alpha_2\zeta}\right\}$$

derived from 1.7.15, 1.7.16, 1.7.20, and 1.7.21, one obtains, upon substituting 1.7.22 and 1.7.23 into 1.5.14,

$$\tau_i = \frac{\pi\,\mu_{xy}}{L}\left[\frac{(1+\delta)}{2}\left\{\frac{(1-\sigma)\frac{\sinh\alpha_1\zeta}{\alpha_1} + (1+\sigma)\frac{\sinh\alpha_2\zeta}{\alpha_2}}{G\frac{\sinh\alpha_1\zeta}{\alpha_1} + H\frac{\sinh\alpha_2\zeta}{\alpha_2}}\right\}\right.$$

$$\left. + (-1)^{i+1}\,\frac{(1-\delta)}{2}\left\{\frac{(1-\sigma)\frac{\sinh\alpha_1\zeta}{\alpha_1} - (1+\sigma)\frac{\sinh\alpha_2\zeta}{\alpha_2}}{G\frac{\sinh\alpha_1\zeta}{\alpha_1} - H\frac{\sinh\alpha_2\zeta}{\alpha_2}}\right\}\right] \qquad 1.7.28$$

8. The Critical Wrinkling Stress

When given the elastic constants of the faces and the core, p and r are constant multiples of Q and q, respectively, as defined by 1.7.8 and 1.7.9. Therefore the relative minimum values of p with respect to ζ with r held constant may be found by using the variables Q and q with q held constant.

Writing formula 1.7.24 in the form

$$Q = \frac{\zeta^2}{12q^2}\beta + \frac{2qR}{\zeta} \qquad 1.8.1$$

with

$$R = \frac{(1+\delta)}{2}\left\{\frac{\cosh\alpha_1\zeta - \cosh\alpha_2\zeta}{G\frac{\sinh\alpha_1\zeta}{\alpha_1} + H\frac{\sinh\alpha_2\zeta}{\alpha_2}}\right\} + \frac{(1-\delta)}{2}\left\{\frac{\cosh\alpha_1\zeta + \cosh\alpha_2\zeta}{G\frac{\sinh\alpha_1\zeta}{\alpha_1} - H\frac{\sinh\alpha_2\zeta}{\alpha_2}}\right\} \qquad 1.8.2$$

the condition

$$\frac{\partial Q}{\partial \zeta} = 0 \qquad 1.8.3$$

is expressed by the relation

$$q^3 = \frac{\frac{\zeta^3}{12}\frac{\mu xy}{E}}{R - \zeta\frac{dR}{d\zeta}} \qquad 1.8.4$$

By means of this expression, together with 1.8.1. Q is defined as a function of q with ζ as a parameter. The values of Q determined by means of these equations include those that are relative minima with respect to ζ, as well as possibly others for which $\frac{\partial Q}{\partial \zeta} = 0$. The minima are denoted by Q_f. To devise a means of selecting these minima, consider the expression

$$\frac{d}{d\zeta}\frac{\partial Q}{\partial \zeta} = \frac{\partial^2 Q}{\partial \zeta^2} + \frac{\partial^2 Q}{\partial \zeta\,\partial q}\frac{dq}{d\zeta} \qquad 1.8.5$$

Now, in view of the condition 1.8.3, this total derivative must vanish. Hence,

$$\frac{\partial^2 Q}{\partial \zeta^2} = - \frac{\partial^2 Q}{\partial \zeta \partial q} \frac{dq}{d\zeta} \qquad 1.8.6$$

From 1.8.1 and 1.8.4, it is found that

$$\frac{\partial^2 Q}{\partial \zeta \partial q} = - \frac{\zeta}{2q^3} \beta \qquad 1.8.7$$

and therefore

$$\frac{\partial^2 Q}{\partial \zeta^2} = \frac{\zeta}{2q^3} \beta \frac{dq}{d\zeta} \qquad 1.8.8$$

In the right member of this relation all quantities except $\frac{dq}{d\zeta}$ are necessarily positive. Therefore, for a relative minimum of Q with respect to ζ, the slope of q plotted as a function of ζ is positive.

The method of constructing plots of Q_f as a function of q for antisymmetrical and symmetrical wrinkling is discussed in the two following sections. With such plots on hand for a given core material, the procedure in finding the theoretical wrinkling stress of a sandwich with this core is first to compute q by the relation 1.7.9, which is written as

$$q = rx = \frac{c}{f} \sqrt[3]{\frac{\mu_{xy}}{\frac{E_f}{\lambda_f} \frac{\mu_{xy}}{a_{22}}}} \qquad 1.8.9$$

The expression on the right is determined by the ratio of the core thickness to the face thickness and the elastic constants of the core and faces. The value of a_{22} depends upon the assumed state of stress in the core and is obtained from either formula 1.3.3 or 1.3.4. If the sandwich is wide compared to the thickness of the core, the state of plane strain is the proper choice. The state of plane stress is appropriate for sandwiches that are narrow in comparison to the core thickness. With q determined, the corresponding value of Q_f yields the predicted wrinkling stress by means of the relation

$$p_f = Q_f \overline{E} = Q_f \sqrt[3]{\frac{E_f}{\lambda_f} \frac{\mu_{xy}}{a_{22}}} \qquad 1.8.10$$

which is the same as 1.7.8, with the symbol p_f now denoting the least critical stress.

As an example of the way in which the predicted wrinkling stress is found, consider a sandwich for which

$$c = 0.5 \text{ in.}, \qquad f = 0.012 \text{ in.}$$

and for which the core and face materials, both assumed to be isotropic, have the elastic constants

$$E_f = 3 \times 10^7 \text{ p. s. i.} \qquad \sigma_f = 0.3$$

$$E_c = 10^4 \text{ p. s. i.} \qquad \sigma_c = 0.2$$

Assuming a state of plane strain in the core,

$$a_{22} = \frac{1 - \sigma_c^2}{E_c} = 9.6 \times 10^{-5}$$

$$\overline{E} = \sqrt[3]{\frac{E_f}{\lambda_f} \frac{\mu_c}{a_{22}}} = 1.125 \times 10^5$$

$$x = \frac{\mu_c}{\overline{E}} = 0.037$$

and

$$q = rx = 1.54$$

Since the core material is isotropic,

$$E = \frac{1}{\sqrt{a_{11} a_{22}}} = \frac{E_c}{1 - \sigma_c^2}$$

also

$$\mu_c = \frac{E_c}{2(1 + \sigma_c)}$$

so that

$$\beta = \frac{\mu_c}{E} = \frac{1 - \sigma_c}{2} = 0.4$$

and

$$\sigma = a_{12}E = \frac{\sigma_c (1 + \sigma_c)}{E_c} \frac{E_c}{1 - \sigma_c^2} = \frac{\sigma_c}{1 - \sigma_c} = 0.25$$

Curves relating Q and q for symmetrical and antisymmetrical wrinkling are given in figures 3, 4, and 5. Those corresponding to the computed values of β and σ are found in figure 4. Evidently, the curve for antisymmetrical wrinkling gives the lower values of Q_f which, corresponding to the computed value of q, is

$$Q_f = 0.72$$

and, therefore,

While the above example has been selected to yield values of β and σ for which a curve relating Q_f and q had been constructed, it is shown in the following section that such curves do not change greatly with changes in β and σ (and that a single curve may be used for practical purposes) in certain specified ranges.

9. Discussion of Formulas and Plots for Predicting the Critical Antisymmetrical Wrinkling Stress

For antisymmetrical wrinkles $\delta = 1$. The formula

$$Q = \frac{\zeta^2}{12q^2}\beta + \frac{2q}{\zeta}\left\{\frac{\cosh \alpha_1\zeta - \cosh \alpha_2\zeta}{G\frac{\sinh \alpha_1\zeta}{\alpha_1} + H\frac{\sinh \alpha_2\zeta}{\alpha_2}}\right\} \qquad 1.9.1$$

as obtained from 1.7.24, applies in the present case, and the condition 1.8.4 takes the form

$$q^3 = \frac{\frac{\zeta^3}{12}\beta}{\left\{\frac{\cosh\alpha_1\zeta - \cosh\alpha_2\zeta}{G\frac{\sinh\alpha_1\zeta}{\alpha_1} + H\frac{\sinh\alpha_2\zeta}{\alpha_2}}\right\}\left[1 - \zeta\left\{\frac{\alpha_1\sinh\alpha_1\zeta - \alpha_2\sinh\alpha_2\zeta}{\cosh\alpha_1\zeta - \cosh\alpha_2\zeta} - \frac{G\cosh\alpha_1\zeta + H\cosh\alpha_2\zeta}{G\frac{\sinh\alpha_1\zeta}{\alpha_1} + H\frac{\sinh\alpha_2\zeta}{\alpha_2}}\right\}\right]} \qquad 1.9.2$$

These two formulas define Q as a function of q with ζ as a parameter. That is, a value of ζ substituted into 1.9.2 determines a value of q, from which, together with ζ, Q is determined by 1.9.1. Among the values of Q paired with q in this manner are those that are relative minima with respect to ζ and that are denoted by Q_f. Plots of Q_f as a function of q are given in figures 3, 4, and 5 for a number of combinations of β and σ. The ranges chosen for these parameters include values for balsa, cellular cellulose acetate cork, and cellular hard rubber, Values of the parameters for these core materials are listed in table 1.

In figures 3, 4, and 5 the point at which a given curve begins at the left is called the "cut-off point." The value $q = q_o$ at this point divides the range of q into two parts. On the basis of the present assumptions, a sandwich that is originally flat and for which $q < q_o$, will not wrinkle antisymmetrically but will fail in some other way. On the interval $q > q_o$ wrinkling is possible. In figure 6, where q and ζ are related according to formula 1.9.2, it is seen that q has a lower limit below which $\frac{\partial Q}{\partial \zeta} = 0$ is not satisfied. The existence of a cut-off point was observed by Gough, Elam, and deBruyne.

Analytically, q_o is the smallest value of q for which Q has a minimum with respect to ζ. It has been found in the ranges of β and σ considered herein, that this value of q is either identical with

$$\lim_{\zeta \to 0} q = \sqrt[3]{\frac{2}{1 - \sigma^2}} \qquad 1.9.3$$

as obtained from formula 1.9.2, or is so close to this value that there is no practical difference. The corresponding value of Q is obtained from 1.9.1 as

$$\lim_{\zeta \to 0} Q = \lim_{\zeta \to 0} \frac{q}{2} = \frac{1}{2} \sqrt[3]{\frac{2}{1 - \sigma^2}} \qquad 1.9.4$$

In figures 3 and 4 the cut-off point is located by the coordinates given by equations 1.9.3 and 1.9.4. This is also true for the curves β = 0.6 and 0.8 in figure 5. For β = 0.2 and 0.4 in figure 5, the smallest of q for which Q has a relative minimum does not coincide exactly with that given by 1.9.3. The greatest discrepancy occurs when β = 0.2. In those cases in which q at the cut-off point does not coincide with that determined by 1.9.3, the plot of Q as a function of ζ has a relative maximum point between ζ = 0 and the relative minimum for values of q in a narrow range lying to the right of the true cut-off point.

In the more exact theory of Cox and Williams, Leggett, and Hopkins, a cut-off point evidently exists for antisymmetrical wrinkling. While no simple means of determining its location has been found, figures 7 or 8 and a number of computations indicate that the point determined by equations 1.9.3 and 1.9.4 is a good approximation to its position. The value of ζ at the cut-off point, in using the more accurate formulas, is some finite value other than zero, as indicated in figure 8.

The limiting values of equations 1.9.3 and 1.9.4, as well as the values of q and Q_f when ζ is near zero, may be questioned from a practical standpoint because the value ζ = 0 for a finite core implies that the sandwich buckles into waves of infinite length. In this case it is expected that the critical load, and therefore Q, should be zero rather than the value determined by equation 1.9.4. On the basis of comparisons with the more rigorous theory such as that made in section 11, however, one is led to conclude that the present theory errs in the predicted wave length at failure when q is near the cut-off value rather than in the value of Q_f.

When q becomes infinite, Q_f approaches a finite asymptotic value. This value is found from formulas 1.9.1 and 1.9.2 by taking limits as ζ becomes infinite. From 1.9.2,

$$\lim_{\zeta \to \infty} \frac{q}{\zeta} = \sqrt[3]{\frac{G\beta}{12\alpha_1}} \qquad 1.9.5$$

and with the use of this expression, 1.9.1 yields

$$\lim_{\zeta \to \infty} Q_f = \frac{3}{2} \sqrt[3]{\frac{1 + 2(1 - \sigma)\beta}{6G^2}} \qquad 1.9.6$$

Reference to figures 3, 4, and 5 show that this value of Q_f is approximately correct even for moderately small values of q.

Figures 3, 4, and 5 indicate that the variation of Q_f with respect to Q for any given value of q is quite insignificant. Moreover, the variation of Q_f with respect to β is not large, and from a practical point of view one can choose mean values of both parameters and base predictions upon a single curve. For example, if $\frac{\mu_{xy}}{E} \leq 0.6$, as it is for the core materials mentioned above, the curve for $\beta = 0.4$, $\sigma = 0.25$ gives values of Q_f that differ at most by 5 percent from those from any other curve.

For a given value of β, the value of ζ at which Q is a minimum may be obtained from a curve, or by interpolation between the curves, shown in figure 6. These are denoted by ζ_{cr}. Computations indicate that for a given β there is not a great variation in these values of ζ with σ for any q, and, therefore, only the curves corresponding to $\sigma = 0.25$ are given. The critical half-wave length, L_{cr}, is obtained from ζ_{cr} and corresponds to a given q by relation 1.7.6, viz. :

$$L_{cr} = \frac{\epsilon \pi c}{\zeta_{cr}} \qquad 1.9.7$$

The plots of ζ_{cr} as a function of q indicate that the slope $\frac{dq}{d\zeta_{cr}}$ is positive for the given combinations of β and σ, and, therefore, according to 1.8.8, the corresponding values of Q_f are relative minima.

10. Discussion of the Formulas and Plots for Predicting the Critical Symmetrical Wrinkling Stress

For symmetrical wrinkles, $\delta = -1$, the formula for Q as obtained from 1.7.24 is

$$Q = \frac{\zeta^2}{12q^2}\frac{\mu_{xy}}{E} + \frac{2q}{\zeta}\left\{\frac{\cosh \alpha_1\zeta + \cosh \alpha_2\zeta}{G\frac{\sinh \alpha_1\zeta}{\alpha_1} - H\frac{\sinh \alpha_2\zeta}{\alpha_2}}\right\} \qquad 1.10.1$$

and expression 1.8.4 may be written in the form

$$q^3 = \frac{\frac{\zeta^3 \mu_{xy}}{12E}}{\left\{\frac{\cosh \alpha_1\zeta + \cosh \alpha_2\zeta}{G\frac{\sinh \alpha_1\zeta}{\alpha_1} - H\frac{\sinh \alpha_2\zeta}{\alpha_2}}\right\}\left[1-\zeta\left\{\frac{\alpha_1 \sinh \alpha_1\zeta + \alpha_2 \sinh \alpha_2\zeta}{\cosh \alpha_1\zeta + \cosh \alpha_2\zeta}\right.\right.}$$

$$\left.\left. - \frac{G \cosh \alpha_1\zeta - H \cosh \alpha_2\zeta}{G\frac{\sinh \alpha_1\zeta}{\alpha_1} - H\frac{\sinh \alpha_2\zeta}{\alpha_2}}\right\}\right] \qquad 1.10.2$$

For the present mode of wrinkling there is no cut-off point, since Q, as defined by 1.10.1, has a minimum with respect to < for any value of q. When q is small, i.e., when the core is relatively thin, the values of Q_f are large, and Q_f becomes infinite as q approaches zero. Obviously, some other type of failure, such as failure by column buckling or by shear failure in the core, will occur when q is small. As q becomes large, Q_f approaches the same asymptotic value that it does in the antisymmetrical case. This value is given by formula 1.9.6.

When ϰ, expression 1.7.13, is greater than or equal to unity, the value of Q_f for the present mode of wrinkling is larger than, or at least equal to, the corresponding value for antisymmetrical wrinkling. This is shown as follows. For a given value of q, the value of Q for antisymmetrical wrinkling is less than that for symmetrical wrinkling whenever

$$\frac{\cosh \alpha_1\zeta - \cosh \alpha_2\zeta}{G\frac{\sinh \alpha_1\zeta}{\alpha_1} + H\frac{\sinh \alpha_2\zeta}{\alpha_2}} < \frac{\cosh \alpha_1\zeta + \cosh \alpha_2\zeta}{G\frac{\sinh \alpha_1\zeta}{\alpha_1} - H\frac{\sinh \alpha_2\zeta}{\alpha_2}}$$

This relation holds for all ζ provided α_2 is real. But α_2 is real when $\varkappa \geq 1$. For such values of ϰ, therefore, it follows from consideration of the curves relating Q to ζ for the two modes of wrinkling, that the relative minimum values of Q for antisymmetrical wrinkles are the smaller. When ϰ is less than unity, it is found, when q is sufficiently large, that Q_f for symmetrical wrinkling may be less than that for antisymmetrical wrinkling. This is shown in a number of the curves in figures 3, 4, and 5. The difference is not significant, however, if ß is moderately small, at most equal to 0.6, with σ

being less than 0.5. The difference may be of importance for sandwich constructions having certain honeycomb cores.

The plots of Q_f as a function of q for the present mode of wrinkling are shown in figures 3, 4, and 5, where the corresponding curves for antisymmetrical wrinkling are also given. In figure 4 a curve for symmetrical wrinkling is given for each of the four values of ß. In figures 3 and 5, however, the curves for symmetrical wrinkling given are only those for which Q_f, symmetrical, is noticeably less than the corresponding Q_f, antisymmetrical, over a range of values of q. It is seen from the given curves that for the combinations of ß and σ considered, that Q_f, antisymmetrical, never exceeds Q_f, symmetrical, by a very large amount.

The values of ζ_{cr} for σ = 0.25 and various values of ß are plotted against q in figure 6.

11. Discussion of Results by More Accurate Analyses

The analysis of the present report is considered approximate for three main reasons, as follows: (a) the component, u, of displacement at the glue line is taken as zero, (b) the core is considered as attached directly to the middle surfaces of the faces, and (c) the effect of the compressive stress in the core upon the stability of the faces has been disregarded. These are restrictions that limit the range of applicability of the theory in certain respects. It is the purpose of the present section to discuss these limitations, with the results from more accurate analyses being used as a basis.

The analyses of Williams, Leggett, and Hopkins (10) and of Cox (2) dispense with restrictions (a) and (b). Considering, for the present, only the effect of these two assumptions, the work of Cox, which is in a form particularly suited to the purpose, is chosen as a basis for comparison. It is, however, proposed to make one slight change in the equations that he has developed. The proposed modification is the one that is brought about by assuming a state of plane strain in the faces when imposing the condition of continuity of strain at the glue line. According to Cox, this condition is written

$$\frac{du_1}{dx} = \frac{f}{2}\frac{d^2v_1}{dx^2} - \frac{P_1}{fE_f} \qquad 1.11.1$$

where P_1 denotes the direct stress in the face and v_1, u_1, components of displacement at the glue line. It now is changed to the form

$$\frac{du_1}{dx} = \frac{f}{2}\frac{d^2v_1}{dx^2} - \frac{P_1\lambda_f}{fE_f} \qquad 1.11.2$$

This change has the effect of introducing λ_f as a divisor of E_f wherever the latter occurs in the formulas for the critical strains that Cox develops. While this modification produces no perceptible change in the Cox results, the difference between those results and predictions by the present theory now becomes a function of the single parameter

$$x = \frac{\mu_{xy}}{\overline{E}}$$

that was introduced in section 7. This is the main reason for the modification. In addition, the assumed state of plane strain in the facings seems to be the more plausible assumption.

The formula developed by Cox for antisymmetrical wrinkling failure (equation 27 of (2), transformed after making the above modification to the variables used in the present report, takes the form

$$p = Q_x\overline{E} \qquad 1.11.3$$

where p is the stress in each facing (as a function of ζ),

$$Q_x = \frac{\zeta^2\beta}{12q^2} + \frac{\frac{2q}{\zeta}R + \frac{x^2}{\beta^2}\frac{q^2}{\zeta^2}S + xT + \frac{\zeta}{2q}x^2U}{1 + \frac{2q}{\zeta}\frac{x^2}{\beta}U} \qquad 1.11.4$$

and

$$\left.\begin{aligned} R &= \frac{\cosh\alpha_1\zeta - \cosh\alpha_2\zeta}{G\frac{\sinh\alpha_1\zeta}{\alpha_1} + H\frac{\sinh\alpha_2\zeta}{\alpha_2}} \\ S &= \frac{\frac{\sinh\alpha_1\zeta}{\alpha_1} - \frac{\sinh\alpha_2\zeta}{\alpha_2}}{G\frac{\sinh\alpha_1\zeta}{\alpha_1} + H\frac{\sinh\alpha_2\zeta}{\alpha_2}} \end{aligned}\right\} \qquad 1.11.5$$

$$T = \frac{(1 - \sigma)\dfrac{\sinh \alpha_1 \zeta}{\alpha_1} + (1 + \sigma)\dfrac{\sinh \alpha_2 \zeta}{\alpha_2}}{G\dfrac{\sinh \alpha_1 \zeta}{\alpha_1} + H\dfrac{\sinh \alpha_2 \zeta}{\alpha_2}}$$

$$U = \frac{\cosh \alpha_1 \zeta + \cosh \alpha_2 \zeta}{G\dfrac{\sinh \alpha_1 \zeta}{\alpha_1} + H\dfrac{\sinh \alpha_2 \zeta}{\alpha_2}}.$$

1.11.5 contd.

It now appears that formula 1.11.4 reduces to that derived for Q for antisymmetrical wrinkling in section 7 when x, as it appears explicitly, is set equal to zero. The reduced form is

$$Q = \frac{\zeta^2 \beta}{12q^2} + \frac{2q}{\zeta} R \qquad 1.11.6$$

which is the same as 1.7.24 with $\delta = 1$. In fact, Q_x can be expressed in the form

$$Q_x = Q + \frac{\dfrac{\zeta}{2q} x^2 U + xT - \dfrac{q^2}{\zeta^2}\dfrac{x^2}{\beta} T^2}{1 + \dfrac{2q}{\zeta}\dfrac{x^2}{\beta} U} \qquad 1.11.7$$

where Q denotes expression 1.11.6,

In figure 9, a comparison of the compressive stress in the facings as obtained by formulas 1.11.4 and 1.11.6 is made, In this figure, the compressive stress,

$$p = Q\overline{E} \quad \text{or} \quad p = Q_x\overline{E},$$

is given as a function of ζ with q held constant. The constants used in making the computations were

$$\frac{E_f}{\lambda_f} = 3 \times 10^7$$

$$\mu_c = 3 \times 10^3$$

$$\sigma_c = 0.25$$

with the core being taken to be isotropic and in a state of plane strain, These values yield

$$\overline{E} = 8.96 \times 10^{4},$$

$$E = 8 \times 10^{3},$$

$$\beta = 0.375,$$

$$\sigma = 1/3,$$

and

$$x = 0.0335.$$

Two values of q were used, namely,

$$q = 1.31 \quad \text{and} \quad q = 3.35.$$

These correspond respectively to

$$r = 39.2 \quad \text{and} \quad r = 100$$

of which the former is the cut-off value and the latter is well above it. For the value q = 3.35, both curves show a well-defined relative minimum; and for q = 1.31, each has a horizontal tangent but no relative minimum. Had the curves been constructed for a value of q less than 1.31, the one obtained from formula 1.11.4 would have a point of inflection with a tangent of nonzero slope, while that obtained from 1.11.6 would start at a point on the axis where $\zeta = 0$ with a horizontal tangent and would have no point of inflection. The curves show good agreement between the results from the two formulas, except for very small values of ζ, where column buckling is expected. This type of failure is discussed below. While the curves have been constructed for a sandwich with an isotropic core, they nevertheless have the general characteristics of the curves for sandwiches with orthotropic cores.

In section 7 it was shown that the relation between Q_f, the relative minima of Q, and q depends on the two parameters β and σ. It is now seen from 1.11.4 and 1.1 1.5 that the relation between the minimum values of Q_x, to be denoted by Q_{xf}, and q depends upon β, σ, and x. For given values of β, σ, and q, i.e., for a given sandwich, the difference between the Cox results and those from the present report therefore depends upon x and the present theory is applicable, provided the value of x is sufficiently small.

Since the expressions

$$\frac{\partial Q}{\partial \zeta} = 0 \quad \text{and} \quad \frac{\partial Q_x}{\partial \zeta} = 0$$

are polynomials in q with function of ζ as coefficients, it is not possible to express Q_f and Q_{xf}, and, therefore, their difference, as functions of q directly. For this reason the dependence of the difference $Q_{xf} - Q_f$ upon x must be investigated by computations. Figure 7, where curves are shown for Q_f, and for Q_{xf} with x = 0.05 and 0.1, and with β = 0.4 and σ = 0.25 in all cases, gives the results of such computations. Values of ζ, denoted by ζ_{cr}, at which the relative minima occur, are plotted against q in figure 8. The extreme values used for x include its range for a number of sandwiches with soft cores and stiff facings. For such combinations as spring-steel or clad-aluminum-alloy facings with balsa, cork, cellular cellulose acetate or cellular hard-rubber cores, the range of x is approximately

$$0.01 \leq x \leq 0.05.$$

Combinations of the above core materials with papreg or glass-cloth facings yield higher values of x, but these values are usually within the range $0.01 \leq x < 0.1$. Values of x for various combinations of facing and core materials are listed in table 1.

The difference $Q_{xf} - Q_f$, which depends only on x for a given sandwich, varies with the parameters β, σ, and q. The curves shown in figure 7 therefore apply only when β = 0.4 and σ = 0.25. One of the features of those curves that appears to be general, however, is that Q_f is smaller than Q_{xf}, and, consequently, predictions by the present theory are conservative with respect to those from the more exact analysis. In fact, it can be deduced from 1.1 1.7, together with a consideration of the geometry of the curve of Q plotted as a function of ζ, that Q_x has a minimum in the vicinity of the point where Q has one, provided q is sufficiently large, and that the difference between the two minimum values lies in the range

$$0 \leq Q_{xf} - Q_f \leq \Delta \qquad 1.11.8$$

where

$$\Delta = \frac{\zeta}{2q} x^2 U + xT \qquad 1.11.9$$

is evaluated at the value of ζ that makes Q a minimum.

When the value of q is large, it is found in many cases that the difference $Q_{xf} - Q_f$ is nearly equal to A, In the limit as q becomes large, Δ is given by the expression

$$\lim_{\zeta \to \infty} \Delta = \frac{x^2 \alpha_1}{2G} \sqrt[3]{\frac{12\alpha_1}{G\beta}} + \frac{x(1 - \sigma)}{G} \qquad 1.11.10$$

which is obtained from 1.11.9 by using equation 1.9.5 for the limit form of $\frac{\zeta}{q}$. This formula exhibits the dependence of the difference $Q_{xf} - Q_f$ upon β and σ and upon x as well. Its evaluation for the values of β, σ, and x given in figure 7 shows that it yields a good approximation to the difference between the asymptotic values of Q_{xf} and Q_f. In fact, it gives a good approximation to the difference in most of the wrinkling range.

While the preceding discussion has been confined to antisymmetrical wrinkling, formulas analogous to 1.11.4 and 1.11.7 can be derived from the Cox results for symmetrical wrinkling, so that the same discussion applies for the two cases. In particular, formula 1.11.10 is applicable when the wrinkles are symmetrical.

The effect of the compressive stress in the core upon the stability of the facings is accounted for in an approximate manner by Williams, Leggett, and Hopkins (10). In their treatment of the problem they obtained an expression for the critical stress in the faces that, with the same modification as made above in the Cox equation, may be reduced to the form

$$p = \frac{Q_x \overline{E}}{1 + \frac{CE_x}{2fE_f}\psi} \qquad 1.11.11$$

The quantity Q_x in this expression is defined by 1.11.4, and ψ is a parameter depending on the ratio of the length of the buckle to the core thickness, L/c. The manner in which ψ depends upon L/c is not given, beyond the specification that ψ increases from 0 to 1 as L/c increases from 0 to infinity.

In the work of Goodier (3) the effect of the compressive stress in the core upon the stability of the facings has been incorporated in the analysis. The results apply to a sandwich with an isotropic core and are in such form that the effect must be evaluated by computations for individual specimens. Neuber (6) carried out an analysis that is similar to that of Goodier in many respects. The work of Neuber, who made some comparisons of his results with those of Gough, Elam, and deBruyne, is, however, not available in complete form at present.

The destabilizing effect of the compressive stress in the core has thus not been investigated in sufficient detail to make a general statement at the present time concerning its possible magnitude. By making use of the formula derived by Williams, Leggett, and Hopkins, and by taking $\psi = 1$ for the entire buckling range of the column, the largest reduction in the buckling load of the column is found to be about 1 percent for such sandwich constructions as aluminum - end-grain balsa, steel - cellular cellulose acetate, and aluminum - cellular hard rubber. In the wrinkling range, the reduction remains to be evaluated, but it appears to be small.

The preceding discussion indicates that for a wide variety of sandwich columns with light cores and stiff facings the predicted wrinkling stresses by the present theory are in good agreement with those from the more exact analyses. When the half-wave length at failure is long, however, the present formulas give incorrect results, a fact that is attributed mainly to assumption (a). In such cases however, the failure will be by column buckling or by shear failure in the core. The critical stress in the former case can be found from formula (32) of U. S. Forest Products Laboratory Report No. 1583. This formula, which applies to the buckling of a simply supported panel, is applicable to a column after taking the limit as the width, a, becomes infinite. A similar formula, (46), is found for panels with clamped edges in Forest Products Laboratory Report No. 1583.

The possibility of failure of a sandwich column in column buckling should always be considered. Below the cut-off point, this mode of failure seems always to be associated with a lower load than that which causes symmetrical wrinkling. Above the cut-off point it is a possible mode of failure if the column is sufficiently long.

12. The Stresses in the Core When the Faces are Not Initially Flat

In the mathematical treatment of the problem of the wrinkling of a flat sandwich, the core is considered to be free of all stresses except those associated with the compressive load until the point of instability is reached. It is therefore customary to assume that the core material remains elastic until the point of instability is reached. When the facings are not originally flat, the irregularities initially present grow with the increase in load and the core is stressed locally throughout the loading process. The problem of predicting failure under these circumstances is one of determining the load at which the core or the glue line is stressed to its ultimate at some point, rather than one of instability.

For the discussion of this problem, which cannot be carried out in full generality, it is assumed that the initial irregularities in the two facings are either

symmetrical or antisymmetrical with respect to the middle plane of the core, or that just one face has an irregularity and that the other is flat. The last-named case is of some interest because it approximates that in which the irregularities in the two facings are not located opposite each other and in which the growth of the irregularities in one face is not greatly influenced by the growth of those in the other. In the treatment of this case it is assumed that the face that is originally flat is constrained from wrinkling. The stress in the opposite face is alone considered. The three cases will be treated simultaneously in the present section by means of introducing a factor δ as defined below,

It is assumed that the initial irregularities in the facings have been resolved into their Fourier sine components. Specifically, let the initial form of the faces at the glue line be given by

$$\left.\begin{aligned} v_{10} &= \sum_{n=1}^{\infty} a_n \sin \frac{n\pi x}{\iota} \\ v_{20} &= \sum_{n=1}^{\infty} \delta a_n \sin \frac{n\pi k}{\iota} \end{aligned}\right\} \qquad 1.12.1$$

where the first subscripts 1 and 2 refer to the facings $y = \frac{c}{2}$ and $y = \frac{c}{2}$, respectively, and ι denotes the length of the column. The factor δ is assigned the values 1, -1, or 0, respectively, according to whether the irregularities are antisymmetrical, symmetrical, or appear in just one face.

The surfaces of the facings at a load P per inch of edge on each facing are assumed to be expressible in the forms

$$\left.\begin{aligned} v_1 &= \sum_{n=1}^{\infty} b_n \sin \frac{n\pi x}{\iota} \\ v_2 &= \sum_{n=1}^{\infty} \delta b_n \sin \frac{n\pi x}{\iota} \end{aligned}\right\} \qquad 1.12.2$$

The components of displacement of each point in the core when the facings are loaded are measured from the position of the point prior to loading. At the surfaces that separate the core and facings these displacements are

$$\left.\begin{aligned} v = v_1 - v_{10} &= \sum_{n=1}^{\infty} (b_n - a_n) \sin \frac{n\pi x}{\iota} \text{ at } y = \frac{c}{2} \\ v = v_2 - v_{20} &= \sum_{n=1}^{\infty} (b_n - a_n) \sin \frac{n\pi x}{\iota} \text{ at } y = -\frac{c}{2} \end{aligned}\right\} \qquad 1.12.3$$

A suitable form for the stress function in the core under the present assumption is

$$F = \sum_{n=1}^{\infty} \left\{ A_{1n} \sinh \nu_n y + A_{2n} \sinh \bar{\nu}_n y + B_{1n} \cosh \nu_n y + B_{2n} \cosh \bar{\nu}_n y \right\} \sin \frac{n\pi x}{\iota} \qquad 1.12.4$$

where

$$\nu_n = \frac{n\pi\epsilon\alpha}{\iota}, \qquad \bar{\nu}_n = \frac{n\pi\epsilon\bar{\alpha}}{\iota} \qquad 1.12.5$$

The determination of the coefficients in this expansion is carried out by assuming, as has previously been done, that the component of displacement in the direction of the compressive load associated with the bending of the facing into sinusoidal waves of half length $\frac{\iota}{n}$ is zero for each value of n.[5] The coefficients may then be obtained from 1.5.10 by replacing L in that formula by $\frac{\iota}{n}$ for each integral n and a by $a_n - b_n$ for all three values of δ.

The components of stress at the surfaces separating the core and facings take the forms

$$\left.\begin{aligned} (Y_y)_{y = \frac{c}{2}} &= \sum_{n=1}^{\infty} (b_n - a_n) \gamma_{1n} \sin \frac{n\pi x}{\iota} \\ (Y_y)_{y = -\frac{c}{2}} &= -\sum_{n=1}^{\infty} (b_n - a_n) \gamma_{2n} \sin \frac{n\pi x}{\iota} \end{aligned}\right\} \qquad 1.12.6$$

[5] It has been observed above that this assumption leads to an incorrect estimate of the compressive load necessary to bend the facings into this form when the half-wave length is long. It is observed below, however, that the effects under discussion are influenced only to a small degree by the longer waves.

$$\left.\begin{aligned}(X_y)_{y=\frac{c}{2}} &= \sum_{n=1}^{\infty} (b_n - a_n)\,\tau_{1n} \cos\frac{n\pi x}{\iota} \\ (X_y)_{y=-\frac{c}{2}} &= \sum_{n=1}^{\infty} (b_n - a_n)\,\tau_{2n} \cos\frac{n\pi x}{\iota}\end{aligned}\right\} \qquad 1.12.7$$

where γ_{in}, τ_{in}, $i = 1, 2$ are obtained from 1.7.27 and 1.7.28, respectively, by substituting $\frac{\iota}{n}$ for L.

It is desired to find expressions for the above stress components in terms of the compressive load to which the column is subjected. These expressions are most easily obtained through the equations of equilibrium of an element of each of the facings. Consider such an element of the face at $y = \frac{c}{2}$ subjected to forces and moments as indicated in figure 10. By conditions of equilibrium of forces parallel and normal to the face of the element, respectively, one obtains

$$\frac{dP_1}{dx} - \frac{N}{\rho} + (X_y)_{y=\frac{c}{2}} = 0 \qquad 1.12.8$$

$$\frac{dN}{dx} + \frac{P_1}{\rho} - (Y_y)_{y=\frac{c}{2}} = 0 \qquad 1.12.9$$

and by the condition that the moments vanish,

$$\frac{dM}{dx} - N + \frac{f}{2}(X_y)_{y=\frac{c}{2}} = 0 \qquad 1.12.10$$

Under the assumption that the core may be considered to be attached directly to the middle surface of the face, the last term in 1.12.10 is neglected. Then eliminating N between 1.12.9 and 1.12.10,

$$\frac{d^2M}{dx^2} + \frac{P}{\rho} - (Y_y)_{y=\frac{c}{2}} = 0 \qquad 1.12.11$$

where P denotes the compressive load applied to the facing. For small displacements the approximations

$$\frac{1}{\rho} = -\frac{d^2v_1}{dx^2}$$

and

$$M = - \frac{E_f f^3}{12\lambda_f} \frac{d^2(v_1 - v_{10})}{dx^2}$$

may be used, where the moment depends on the increase in curvature on the assumption that the face is initially free of stress. By substituting these expressions into 1.12.11,

$$\frac{E_f f^3}{12\lambda_f} \frac{d^4(v_1 - v_{10})}{dx^4} + P \frac{d^2 v_1}{dx^2} + (Y_y)_{y = \frac{c}{2}} = 0 \qquad 1.12.12$$

At the opposite face the equation

$$\frac{E_f f^3}{12\lambda_f} \frac{d^4(v_2 - v_{20})}{dx^4} + P \frac{d^2 v_2}{dx^2} - (Y_y)_{y = -\frac{c}{2}} = 0 \qquad 1.12.13$$

replaces 1.12.12. It is observed from 1.12.6, however, that

$$(Y_y)_{-\frac{c}{2}} = - \delta (Y_y)_{y = \frac{c}{2}} \quad \text{when } \delta = + 1 \text{ and } \delta = - 1$$

and from 1.12.2 and 1.12.3 that

$$v_2 = \delta v_1, \quad v_2 - v_{20} = \delta (v_1 - v_{10}).$$

Therefore 1.12.12 is equivalent to 1.12.13 when $\delta = \pm 1$. In the case $\delta = 0$, 1.12.12 again applies. It is therefore taken to apply for all three values of δ.

By substituting the expressions for v_1, $(v_1 - v_{10})$ and $(Y_y)_{y = \frac{c}{2}}$ given by 1.12.2, 1.12.3, and 1.12.6 respectively, equation 1.12.12 takes the form

$$\frac{E_f f^3}{12\lambda_f} \sum_{n=1}^{\infty} \left(\frac{n\pi}{\iota}\right)^4 (b_n - a_n) \sin \frac{n\pi x}{\iota} - P \sum_{n=1}^{\infty} \left(\frac{n\pi}{\iota}\right)^2 b_n \sin \frac{n\pi x}{\iota}$$
$$+ \sum_{n=1}^{\infty} (b_n - a_n) \gamma_{1n} \sin \frac{n\pi x}{\iota} = 0$$

The coefficient of $\sin \frac{n\pi x}{\iota}$ in this series is zero for each n, since the series must vanish identically. Thus

$$\frac{E_f f^3}{12\lambda_f}\left(\frac{n\pi}{\iota}\right)^4 (b_n - a_n) - P\left(\frac{n\pi}{\iota}\right)^2 b_n + (b_n - a_n)\,\gamma_{1n} \qquad 1.12.14$$

Let

$$P_n = \frac{E_f f^3}{12\lambda_f}\left(\frac{n\pi}{\iota}\right)^2 + \left(\frac{\iota}{n\pi}\right)^2 \gamma_{1n} \qquad 1.12.15$$

then from 1.12.14

$$P_n (b_n - a_n) - P b_n = 0 \qquad 1.12.16$$

and

$$b_n = \frac{a_n}{1 - \frac{P}{P_n}} \qquad 1.12.17$$

also,

$$b_n - a_n = \frac{a_n \frac{P}{P_n}}{1 - \frac{P}{P_n}} \qquad 1.12.18$$

The two preceding formulas give respectively the amplitude and the increase in amplitude of the nth Fourier sine component when the load on each face is P. The quantity P_n is the wrinkling load for each face associated with wrinkles of half-wave length $\frac{\iota}{n}$. This is seen by comparing expressions 1.12.15 and 1.7.2. Expression 1.12.18 shows that as P approaches the critical load for sandwich, the amplitudes of the waves of critical length are magnified out of all proportion to those of waves of other lengths. For values of P that are less than the critical load, however, the relative increase in amplitude of a number of the components whose wave lengths are near critical may be nearly as great as that of the critical. This is due to the fact that a_n and P_n for a group of waves whose lengths are near critical often do not differ greatly from the corresponding quantities associated with the waves of critical length.

By means of formula 1.12.18, together with formulas 1.12.6 and 1.12.7, it is now possible to compute the stress components at the glue line at a given compressive load when there is a given initial irregularity of the facings. If

it is desired to express the increase in amplitude given by formulas 1.12.18 in terms of variables defined in section 7, let p_n denote the stress associated with a compressive load P_n. Then, according to 1.7.8,

$$p_n = Q_n \overline{E} \qquad 1.12.19$$

where Q_n is obtained from 1.7.24 by replacing L by $\frac{\iota}{n}$. Defining Q_p by the relation

$$Q_p = \frac{p}{\overline{E}} \qquad 1.12.20$$

where p is the stress in a face associated with a load P per inch of edge, formulas 1.12.17 and 1.12.18 take the forms

$$b_n = \frac{a_n}{1 - \frac{Q_p}{Q_n}} \qquad 1.12.21$$

and

$$b_n - a_n = \frac{a_n \frac{Q_p}{Q_n}}{1 - \frac{Q_p}{Q_n}} \qquad 1.12.22$$

These two formulas are somewhat easier to apply than 1.12.17 and 1.12.18 since the expressions for Q_n are simpler than those for p_n.

The formulas derived above are applied to special cases in the two following sections.

13. The Distribution of Stresses at the Glue Line for an Irregularity in One Face

It is assumed that one face is flat and that the other has an irregularity at midheight extending across the width of the specimen that is represented by

$$\left.\begin{aligned} f(x) &= A \cos^2 \frac{\pi}{2e}\left(x - \frac{\iota}{2}\right) \text{ on } \frac{\iota}{2} - e < x < \frac{\iota}{2} + e \\ &= 0 \text{ elsewhere on } 0 \leq x \leq \iota \end{aligned}\right\} \qquad 1.13.1$$

This function has the expansion

$$f(x) = \sum_{1}^{\infty} a_n \sin \frac{n\pi x}{\iota} \qquad 1.13.2$$

with

$$\left.\begin{aligned} a_n &= \frac{2A\iota^2 (-1)^{\frac{n+1}{2}}}{n\pi(ne^2 - \iota^2)} \sin \frac{n\pi e}{\iota} \quad \text{when n is odd} \\ &= 0 \text{ when n is even} \end{aligned}\right\} \qquad 1.13.3$$

That the irregularity is taken at the center of the specimen is probably not of great importance if the length of the specimen is several times the length 2e of the bump.

The formulas of the preceding section apply to the present example when $\delta = 0$. When this substitution is made, the conditions 1.12.1 reduce to

$$\left.\begin{aligned} v_{10} &= f(x) \\ v_{20} &= 0 \end{aligned}\right\} \qquad 1.13.4$$

With the coefficients a_n given by formula 1.13.3, the increase in amplitude $b_n - a_n$ is obtained from formula 1.12.22. In that expression the quantity Q_p is associated with the assumed stress in the faces through formula 1.12.20, and Q_n is obtained from 1.7.24 with $\delta = 0$ in the form

$$Q_n = \frac{\zeta_n^2}{12q^2}\beta + \frac{q}{\zeta_n}\left[\frac{\cosh \alpha_1\zeta_n - \cosh \alpha_2\zeta_n}{G\frac{\sinh \alpha_1\zeta_n}{\alpha_1} + H\frac{\sinh \alpha_2\zeta_n}{\alpha_2}} + \frac{\cosh \alpha_1\zeta_n + \cosh \alpha_2\zeta_n}{G\frac{\sinh \alpha_1\zeta_n}{\alpha_1} - H\frac{\sinh \alpha_2\zeta_n}{\alpha_2}}\right] \qquad 1.13.5$$

where

$$\zeta_n = \frac{n\epsilon\,\pi c}{\iota} \qquad 1.13.6$$

Formula 1.12.6 in the present case reduces to

$$Y_y\Big|_{y=\frac{c}{2}} = \sum_{n=1}^{\infty} (Y_y)_n = \sum_{n=1}^{\infty} (b_n - a_n)\, \gamma_{1n} \sin \frac{n\pi x}{\iota} \qquad 1.13.7$$

with γ_{1n} given by the expression

$$\gamma_{1n} = \frac{n\pi\mu_{xy}}{\epsilon\iota}\left[\frac{\cosh \alpha_1\zeta_n - \cosh \alpha_2\zeta_n}{G\frac{\sinh \alpha_1\zeta_n}{\alpha_1} + H\frac{\sinh \alpha_2\zeta_n}{\alpha_2}} + \frac{\cosh \alpha_1\zeta_n + \cosh \alpha_2\zeta_n}{G\frac{\sinh \alpha_1\zeta_n}{\alpha_2} - H\frac{\sinh \alpha_2\zeta_n}{\alpha_2}}\right] \qquad 1.13.8$$

which is obtained from 1.7.27.

As an illustration, the above formulas will be applied to a sandwich with the following dimensions and elastic constants:

Core	Facings
$\frac{1}{a_{11}} = \frac{E_x}{1 - \sigma_{xz}\sigma_{zx}} = 5{,}000$ pounds per square inch	$E_f = 3 \times 10^7$ pounds per square inch
$\frac{1}{a_{22}} = \frac{E_y}{1 - \sigma_{zy}\sigma_{yz}} = 20{,}000$ pounds per square inch	$\lambda_f = 0.91$
$\mu_{xy} = 4{,}000$ pounds per square inch	$f = 0.01$ inch
$\frac{1}{a_{12}} = 40{,}000$ pounds per square inch	$\iota = 4.5$ inches
Y_y ultimate $= 200$ pounds per square inch	
$e = 0.3$ inch	
$c = 0.75$ inch	

These constants, which were chosen with a view to making the computations as simple as possible, are those for a sandwich with spring-steel facings and a core similar to cellular cellulose acetate. A state of plane strain is assumed to exist in the core. From the above constants it is found that

$$E = 10^4$$

$$\beta = 0.4$$

$$\sigma = 0.25$$

$$\overline{E} = 1.38 \times 10^5$$

and

$$q = 2.175$$

A number of plots showing the results of computations are given in figures 11, 12, and 13. From the plot of Q_n, as obtained from formula 1.13.5 and given in figure 11, it is seen that the minimum value of Q_n is 0.78 and that it occurs at n = 17. The critical wrinkling stress in one face of an initially flat sandwich, assuming that the other face is restrained from wrinkling, is therefore approximately

$$p_f = 0.78\ \overline{E} = 1.08 \times 10^5 \text{ pounds per square inch}$$

and the critical wave length is approximately

$$\frac{4.5}{17} = 0.265 \text{ inch.}$$

Plots of $|a_n|$ and $|b_n|$ in units of the amplitude, A, of the original imperfection are given in figure 12. Values of $\frac{|b_n|}{A}$, obtained from formula 1.12.21, were computed for a number of values of Q_p, namely, $\frac{Q_f}{4}$, $\frac{Q_f}{2}$, $\frac{3Q_f}{4}$, and $\frac{9}{10}Q_f$, with the value of Q_f being taken as 0.78, as obtained from the plot of Q_n, (fig. 11). The plotted values of $\frac{|b_n|}{A}$ give some indication of the manner in which the irregularity grows with increasing load. It is observed that the wave whose half length equals the length of the specimen (n=1), and likewise those of short length (n large), do not change greatly in amplitude. At all fractions of the critical load, a number of waves, whose lengths are both greater than and less than the critical length, show growth in amplitude. At small fractions of the critical load, it appears that the greatest amplification takes place in waves of length somewhat longer than the critical length, but as the critical load is approached, the length of the most greatly amplified wave approaches that of the critical length.

The plots of $\frac{(Y_y)_n}{A}$ given in figure 11 show the relative magnitude of the direct-stress components at the glue line at midspan associated with waves of various lengths. It is seen that the waves of greatest lengths, and those of short lengths as well, do not contribute greatly to the total direct stress

and that those whose lengths are slightly greater than the critical length, contribute most, The total direct stress is found by using formula 1.13.7. By summing to n=31, it is found that

$$Y_y \Big|_{\substack{x = \frac{\iota}{2} \\ y = \frac{c}{2}}} = 14{,}000 \text{ A p. s. i. at } \frac{1}{4} \text{ the critical load}$$

$$= 39{,}000 \text{ A p. s. i. at } \frac{1}{2} \text{ the critical load}$$

$$= 102{,}000 \text{ A p. s. i. at } \frac{3}{4} \text{ the critical load}$$

These values indicate that the failing load may well be determined by the strength of the bond or of the core. For instance, failure would be possible at three-fourths the critical load if the initial amplitude, A, was 0.002 inch and the strength of the bond was 200 pounds per square inch of the facing.

Figure 13 shows the profiles at various fractions of the critical load as obtained by computations, together with the initial profile. Examination of these profiles gives some indication that the distance between points of contraflexure at the larger fractions of the critical load is approximately equal to the critical half-wave length, To investigate this as a further possibility, an initial irregularity of twice the length given above, with other constants remaining the same, was assumed. The profiles of the facing as obtained by computations at 0.75 and at 0.95 of the critical load are shown in figure 14 for this case. The critical half-wave length is again approximately 0.265 inch, and there is an indication that the distance between points of contraflexure is approximately of this magnitude at the larger fraction of the critical load.

14. The Stress at Failure When the Facings are Initially in the Forms of Fully Developed Sinusoidal Surfaces

In this case a_n and b_n for some value of n are the only nonzero coefficients in 1.12.1 and 1.12.2 and each summation of section 13 reduces to a single term. For the present, the value of n, and therefore of the half-wave length, is not specified. At a later point, the value of $\frac{\iota}{n}$ will be so chosen that failure will occur at a minimum stress.

From 1.12.22 it is found that

$$Q_p = \frac{Q_n}{1 + \frac{a_n}{b_n - a_n}} \qquad 1.14.1$$

Let it now be assumed that failure occurs when the stress reaches its ultimate at some point on the surface of the core. From 1.12.6,

$$Y_y \Big|_{\substack{x = \frac{\iota}{2} \\ y = \frac{c}{2}}} = (b_n - a_n)\, \gamma_{1n}$$

where γ_{1n} is obtained from 1.7.27 by replacing L in that formula by $\frac{\iota}{n}$.

For a given value of n, the ultimate, t, of Y_y is reached when

$$b_n - a_n = \frac{t}{\gamma_{1n}} \qquad 1.14.2$$

and with the substitution of this quantity into 1.14.1

$$Q_p = \frac{Q_n}{1 + \frac{a_n \gamma_{1n}}{t}} \qquad 1.14.3$$

If it be assumed that failure of the sandwich is due to the core (or glue line) being stressed in shear to its ultimate, then 1.12.7 is used to obtain the expression

$$b_n - a_n = \frac{X_{y\ ult.}}{\tau_{1n}} \qquad 1.14.4$$

where τ_{1n} is obtained from 1.7.28 by replacing L in that formula by $\frac{\iota}{n}$, which gives the increase in amplitude at which the ultimate stress in shear is reached. Substituting this expression into 1.14.1

$$Q_p = \frac{Q_n}{1 + \frac{a_n \tau_{1n}}{X_{y\ ult.}}} \qquad 1.14.5$$

Various assumptions have been made in the literature concerning the nature of the initial wave pattern. Williams (9) assumes that the amplitude is proportional to the wave length, and Wan (8) assumes that the amplitude is proportional to the square of the wave length and that it varies inversely as the face thickness. The assumptions of both associate large amplitudes with large wave lengths, and that of Wan implies that sandwiches with thick facings

$$Q_p = \frac{\frac{\zeta^2}{12q^2}\frac{\mu_{xy}}{E} + \frac{2q}{\zeta}\left\{\frac{\cosh \alpha_1\zeta - \cosh \alpha_2\zeta}{G\frac{\sinh \alpha_1\zeta}{\alpha_1} + H\frac{\sinh \alpha_2\zeta}{\alpha_2}}\right\}}{1 + K_s\left\{\frac{(1-\sigma)\frac{\sinh \alpha_1\zeta}{\alpha_1} + (1+\sigma)\frac{\sinh \alpha_2\zeta}{\alpha_2}}{G\frac{\sinh \alpha_1\zeta}{\alpha_1} + H\frac{\sinh \alpha_2\zeta}{\alpha_2}}\right\}} \qquad 1.14.10$$

For any assumed values of K_t and K_s it is possible to locate the relative minimum points of Q_p by the method of section 8. The relative minima are denoted by Q_{pf}, and these are, of course, the relative minima of Q_p consistent with the assumed value of K_t or K,. Computations of Q_{pf} have been carried out for the special case $\beta = 0.4$ and $\sigma = 0.25$ for three values of K_t and K,. The results of these computations are shown in figure 15.

To discuss a possible use for the curves in figure 15, assume that the elastic constants of the core and faces, the proportionality factor K_o, and the ultimate values of Y_y and X_y are known. With this information the values of q, K_t, and K_s may be determined. From the value of q and K_t a value of Q_{pf} is selected from a curve or by interpolation. The predicted stress at tension failure is then found from the relation,

$$p_f = Q_{pf}\overline{E} \qquad 1.14.11$$

The predicted stress at shear failure is similarly determined by using K_s in place of K_t. Under the assumed conditions the lower of the two stresses is the predicted stress at failure.

Another possible approach to predicting the stress at failure when irregularities are initially present, is to use the assumption made by Wan (8), namely,

$$a_n = \frac{K_t^2}{\pi^2 f} \qquad 1.14.12$$

In his use of this assumption Wan also assumed that E_x and μ_{xy} are small in comparison with E_y, and derived a relatively simple formula or the stress at failure. While the form (1.14.12) appears to be reasonable, the assumption that E_x and μ_{xy} are small in comparison with E_y is not generally applicable. In the absence of this simplification the formulas are quite difficult to apply and will not be considered herein.

are smoother than those with thin facings. As far as the analysis is concerned, one can also assume that waves with amplitude independent of the wave length are initially present,

The choice of making one of the above assumptions, or some other possible assumption, concerning the initial wave pattern is quite arbitrary since it does not appear possible to determine which best describes the initial state of sandwiches in general. In view of this situation, a number of possibilities will be considered, the first of which is that antisymmetrical waves with amplitude proportional to the wave length are initially present. Specifically, let

$$a_n = \frac{K_o \iota}{\pi n} \qquad 1.14.6$$

where K_o is a proportionality factor. Since the wave length is to be determined so that Q_p in 1.14.3 or 1.14.5 is a minimum, $\frac{\iota}{n}$ will now be replaced by L and it will be assumed that L varies continuously.

Consider the case of tension failure and define

$$K_t = \frac{2\mu_{xy} K_o}{\epsilon t} \qquad 1.14.7$$

Then with the substitution of 1.7.24 and 1.7.27, with $\delta = 1$, into 1.14.3

$$Q_p = \frac{\frac{\zeta^2}{12q^2}\frac{\mu_{xy}}{E} + \frac{2q}{\zeta}\left\{\frac{\cosh \alpha_1\zeta - \cosh \alpha_2\zeta}{G\frac{\sinh \alpha_1\zeta}{\alpha_1} + H\frac{\sinh \alpha_2\zeta}{\alpha_2}}\right\}}{1 + K_t\left\{\frac{\cosh \alpha_1\zeta - \cosh \alpha_2\zeta}{G\frac{\sinh \alpha_1\zeta}{\alpha_1} + H\frac{\sinh \alpha_2\zeta}{\alpha_2}}\right\}} \qquad 1.14.8$$

For the case of shear failure let

$$K_s = \frac{K_o \mu_{xy}}{X_{y\ ult.}} \qquad 1.14.9$$

Then with the substitution of 1.7.24 and 1.7.28, with $\delta = 1$, into 1.14.5,

Tests of sandwich columns at the Forest Products Laboratory indicate that specimens with thick cores and given thickness of facings tend to fail at smaller fractions of the predicted critical load when the faces are assumed to be initially flat, than do specimens with thin cores. Examination of a number of profiles of the specimens (part II) gave some indication that those with thick cores were rougher than those with thin cores. This result would be expected if the major proportion of the irregularities were due to the differences in recovery of hard and soft spots in the core from plastic deformations induced by the normal pressure on the facings during fabrication (part III). It therefore seems plausible in the analysis of these tests to assume that the original amplitude is proportional to the core thickness. As to the mode of failure, predictions most consistent with test results were obtained by assuming the wrinkles to be antisymmetrical.

To obtain formulas for predicting the failing stress under the above assumptions, it is convenient to define

$$a_n = Kc\, a_{22} t \qquad 1.14.13$$

where K is a dimensionless proportionality factor. Then with the substitution of 1.7.24 and 1.7.27, with $\delta = 1$, into 1.14.3

$$Q_p = \frac{\frac{\zeta^2}{12q^2}\beta + \frac{2q}{\zeta}\left[\frac{\cosh \alpha_1\zeta - \cosh \alpha_2\zeta}{G\frac{\sinh \alpha_1\zeta}{\alpha_1} + H\frac{\sinh \alpha_2\zeta}{\alpha_2}}\right]}{1 + 2K\beta\zeta\left[\frac{\cosh \alpha_1\zeta - \cosh \alpha_2\zeta}{G\frac{\sinh \alpha_1\zeta}{\alpha_1} + H\frac{\sinh \alpha_2\zeta}{\alpha_2}}\right]} \qquad 1.14.14$$

Values of the relative minima of Q_p, denoted by Q_{pf}, have been computed for a number of values of K. These are given in figure 16. While these curves were constructed for the values $\beta = 0.4$ and $\sigma = 0.25$, earlier discussion indicated that other combinations of these parameters for which $\kappa \geq 0.5$ would yield essentially the same results.

If the curves obtained under the above tentative assumption are applicable, the values to assign to K for a given combination of core and face materials may be determined by compression tests at some chosen value of q. The curve selected in this manner applies only as the core thickness is varied and the thickness of the faces is held constant. With changes in the face thickness the value of K may vary so that it should be determined for each face thickness.

Some confirmation of the assumption 1.14.13, that the amplitude of the initial irregularities is proportional to the thickness of the core, is to be found in figures 29, 31, and 32. These figures, which show the results of tests together with the predictions based on the above formula, are discussed in part II. A discussion of possible applications of the curves obtained by the use of the formula is given in part III.

15. The Predicted Wrinkling Stress when It is Larger than the Proportional-limit Stress of the Face Material

A. The Critical Wrinkling Stress for Initially Flat Specimens

When the stress in the faces is above the proportional limit, the modulus of elasticity of the face material changes with the stress. In order to predict the critical wrinkling stress under this condition, a procedure that is sometimes used is to associate with each stress a modulus that is effective when the faces wrinkle at the stress. Since in wrinkling it is assumed that each face is bent about its own middle plane, the reduced modulus, E_r, [6] appears to be a logical choice for such a modulus. Under the conditions assumed in the following discussion, however, any other appropriate modulus, such as E_t, the tangent modulus, may be used in place of E_r.

When E_f is replaced by E_r, the formulas for predicting the wrinkling stress may be written[7]

$$p_f = \left(\frac{E_r}{E_f}\right)^{1/3} \overline{E} Q_f \qquad 1.15.1$$

$$q = \frac{r\,\mu_{xy}}{\left(\frac{E_r}{E_f}\right)^{1/3} \overline{E}} \qquad 1.15.2$$

with $\overline{E}$ as previously defined, namely,

$$\overline{E} = \sqrt[3]{\frac{E_f\,\mu_{xy}}{\lambda_f\, a_{22}}} \qquad 1.15.3$$

---

[6] U. S. Forest Products Laboratory Report No. 1525-A.

[7] c.f. formulas 1.8.9 and 1.8.10.

In the application of these formulas it is assumed that the elastic constants of the core remain unchanged, Then, by using the same core constants as are used below the proportional limit, the predicted wrinkling stress is a simultaneous solution of 1.15.1, 1.15.2, and the relation that exists between the stress p and the modulus E_r. A plot of p against $(\frac{E_r}{E_f})^{1/3}$, which is a convenient form for use in conjunction with 1.15.1 and 1.15.2, is given in figure 17 for 24ST clad aluminum alloy.

With a curve for Q_f vs. q appropriate to the core material and a plot of p vs. $(\frac{E_r}{E_f})^{1/3}$, one can obtain pairs of values of p_f and r that will satisfy the above conditions by the following process. Select a pair of values of Q_f and q. Then on the same graph as the curve of p vs. $(\frac{E_r}{E_f})^{1/3}$ for the face material plot equation 1.15.1. This is evidently a line with slope $\overline{E}Q_f$. The intersection of the line and the curve gives a pair of values of $p = p_f$ and $(\frac{E_r}{E_f})^{1/3}$ By using the latter value and the selected q, r is determined by equation 1.15.2. With a series of paired values of p_f and r determined in this way, a plot may be constructed from which p_f can be found for any r. Evidently, this process can be reversed and pairs of values of p and $(\frac{E_r}{E_f})^{1/3}$ be selected at the outset. For each of these pairs a value of Q_f is determined by 1.15.1. With the corresponding q selected from an appropriate Q_f vs. q curve, r is determined by 1.15.2. In converting test points to Q_f and q, coordinate p_f and r are known and a modification of the latter process should be used.

A comparison of formulas 1.15.2 and 1.7.9 shows that when the reduced modulus is used

$$x = (\frac{E_f}{E_r})^{1/3} \frac{\mu_{xy}}{\overline{E}}$$

In the applications in which wrinkling occurs below the proportional limit of the face material, the first factor on the right in this expression is unity. When E_r is small compared to E_f, the value of x may be many times as large as that estimated in section 11. The applicability of the values of Q_f computed on the basis of the present theory may therefore not be justified when the stress in the facings is extremely high. Another possible source of error in predictions by the above method is the assumption that the core

remains elastic until failure. For these reasons, and to establish the applicability of the reduced modulus, the results obtained by the procedure should be checked by test.

B. Stress at Failure When the Faces are Not Initially Flat

The above method of determining the critical wrinkling stress when it occurs above the proportional limit of the face material can also be applied to determining the stress at failure when the faces have an initial irregularity. In the application of the process a curve for Q_{pf} vs. q, such as one of those given in figures 15 or 16 is used, together with an appropriate relation between the modulus of the face material and the stress. The procedure is open to same objections, as given for the case of an initially flat sandwich, and the results should again be checked by test.

REFERENCES

(1) Bijlaard, P. P.
1946. On the elastic stability of thin plates supported by a continuous medium. Honinklyke Akodemie von Wetenshappen Te Amsterdam, Section of Sciences, Vol. 49, Nos. 6-10.

(2) Cox, H. L.
1945. Sandwich construction and core materials Part III. Instability of sandwich struts and beams. Report No. 9226, Aeronautical Research Council. Dec.

(3) Goodier, J. N.
1946. Cylindrical buckling of sandwich plates. Journal of Applied Mechanics, Vol. 13, No. 4, Dec.

(4) Gough, C. S., Elam, C. F., and deBruyne, N. A.
1940. The stabilization of a thin sheet by a continuous supporting medium. Journal of the Royal Aeronautical Society. Jan.

(5) Hoff, N. J., and Mautner, S. E.
1945. The buckling of sandwich type panels. Journal of the Aeronautical Sciences, Vol. 12, No. 3. July.

(6) Neuber, H.
Stability theory of compression-stressed sandwich structures. Translation Report No. F-TS-964 PIE, Headquarters, Air Materiel Command, Wright-Patterson Air Force Base, Dayton, Ohio.

(7) Van der Neut, A.
Die stabilitat geschiechteter streifen. National Luchtvaartlabarotorium Amsterdam, Bericht S. 284.

(8) Wan, C. C.
1947. Face buckling and core strength requirements in sandwich construction. Journal of the Aeronautical Sciences. Sept.

(9) Williams, D.
1947. Sandwich construction - A practical approach for the use of designers. Report No. Structures 2, Royal Aircraft Establishment, April.

(10) Williams, D., Leggett, D. M. A., and Hopkins, H. G.
1941. Flat sandwich panels under compressive end loads. Report No. A. D. 3174, Royal Aircraft Establishment. June.

NOTATION

a_{11}, a_{12}, a_{22}	combinations of elastic constants of core defined by 1.3.3 or 1.3.4
c	thickness of the core
$e_{xx}, \ldots\ldots, e_{zy}$	components of strain in the core
f	thickness of each facing
ι	length of the column
p	predicted compressive stress in facings when half-wave length of wrinkles is L
p_f	predicted wrinkling stress
p_n	predicted compressive stress in facings when half-wave length of wrinkles is $\frac{\iota}{n}$
$q = rx$	
$r = \frac{c}{f}$	
t	tensile strength of core (or bond) in the direction perpendicular to the facing
$\zeta = \frac{\epsilon \pi c}{L}$	
$\zeta_n = \frac{\epsilon \pi c n}{\iota}$	
u, v	components of displacement
x, y, z	axes of reference
$E = \frac{1}{\sqrt{a_{11} a_{22}}}$	
$\overline{E} = \sqrt[3]{\frac{E_f \mu_{xy}}{\lambda_f a_{22}}}$	

E_f	Young's modulus of the facing material in the direction of the applied load
E_c	Young's modulus of isotropic core
$E_r = \frac{4E_f E_t}{(\sqrt{E_f} + \sqrt{E_t})^2}$	reduced modulus of facing
E_t	tangent modulus of the facing
E_x, E_y, E_z	Young's moduli of orthotropic core
$G = 1 + (1 - \sigma^2)\beta$	
$H = 1 - (1 - \sigma^2)\beta$	
K	proportionality factor introduced in formula 1.14.12
L	half-wave length of sinusoidal wrinkles
P	compressive load per inch of edge on each facing
P_n	compressive load per inch of edge on each facing when half-wave length of wrinkle is $\frac{\iota}{n}$
Q	quantity given by 1.7.24
Q_f	minimum of Q with respect to ζ
Q_x	quantity given by 1.11.4
Q_{xf}	minimum of Q_x with respect to ζ
Q_n	the expression Q with L replaced by $\frac{\iota}{n}$
Q_p	quantity defined by 1.14.8, 1.14.10, or 1.14.13
Q_{pf}	minimum of Q_p with respect to ζ
$X_x \ldots\ldots X_y$	components of stress

$$\alpha_1 = \sqrt{\frac{\kappa + 1}{2}}$$

$$\alpha_2 = \sqrt{\frac{\kappa - 1}{2}}$$

$$\alpha = \alpha_1 + \alpha_2$$

$$\bar{\alpha} = \alpha_1 - \alpha_2$$

$$\beta = \frac{\mu_{xy}}{E}$$

γ_i, $i = 1, 2$ expressions defined by 1.5.12

δ a constant introduced in expressions 1.2.1 and 1.12.1

$$\epsilon = \sqrt[4]{\frac{a_{22}}{a_{11}}}$$

$$\kappa = \frac{1}{2\beta} - \sigma$$

$$\lambda_f = 1 - \sigma_{xzf}\sigma_{zxf}$$

μ_c = shear modulus of isotropic core

μ_{xy}, μ_{yz}, μ_{zx} shear moduli of orthotropic core

$$\nu = \frac{\alpha\epsilon\,\pi}{L}$$

$$\bar{\nu} = \frac{\bar{\alpha}\epsilon\,\pi}{L}$$

$$\nu_n = \frac{\alpha\epsilon\,\pi n}{\iota}$$

$$\bar{\nu}_n = \frac{\bar{\alpha}\epsilon\,\pi n}{\iota}$$

$$\sigma = a_{12}E$$

σ_f Poisson's ratio of isotropic face

σ_{xzf}, σ_{zxf} Poisson's ratios of orthotropic faces

σ_c Poisson's ratio of isotropic core

$\sigma_{xy}, \ldots \sigma_{yz}$ Poisson's ratios of orthotropic cores

τ_i, $i = 1, 2$ expressions defined by 1.5.14

$$x = \frac{\mu_{xy}}{E}$$

PART II. COMPARISON OF THE RESULTS OF TESTS WITH RESULTS OBTAINED FROM THE MATHEMATICAL DEVELOPMENT

Introduction

Experimental data are presented for comparison with the mathematical development discussed in part I. Edgewise-compression tests and related strength tests were made on a large number of different sandwich constructions. The edgewise tests were made on short columns to determine the maximum loads and to observe the local wrinkling of the facings. The related tests were made on the components of the sandwich constructions to determine their elastic properties.

The manner in which the different sandwich constructions failed is the key to this presentation. The types of failure can be classified in five groups:

(1) Sandwich columns may fail due to local instability of the facings, commonly called wrinkling. This type of failure is the major subject of this report and was analyzed in part I. Illustrations are presented in this, the second part, of the report.

(2) Sandwich columns may become elastically unstable as a whole. These instabilities are commonly called column failures. Such failures may occur at loads insufficient to cause local instability of the individual facings. The stability of such columns is a special case of the stability of flat sandwich plates and is dealt with in Forest Products Laboratory Report No. 1583. A few specimens in the following presentation illustrate this type of failure.

(3) Sandwich columns, which are not flat but slightly curved as a whole, will deflect as the load is applied. They may fail due to transverse shear at loads lees than those that cause either wrinkling or column failures.

(4) Sandwich columns may fail due to stresses in the facings equal to the maximum compressive stress of the facing material.

(5) Sandwich columns may fail when the core fails in direct compression at loads insufficient to cause other types of failure.

The latter two types of failure are determined by a comparison of stress-strain curves of the materials. Some of the specimens reported here failed in this manner.

The following discussion, which illustrates these failures, is divided into four sections. The first three sections deal with failure due to wrinkling of the facings, and the fourth section deals with compression failures in the facings and cores. A few specimens that fail as columns are found among those of sections 2 and 3.

The mathematical development in sections 1 through 11 of part I was based on the elastic behavior of the facing and core materials. The predicted maximum loads are those due to the elastic instability of the individual facings. In order to check experimentally this part of the development, it was necessary to use data from specimens that reached their maximum loads at stresses in their facings less than the proportional-limit stress and that did not appear to fail in their cores before their maximum loads were attained. Section 1 of this part of the report deals with the results obtained from tests of such sandwich constructions.

In sections 12 through 14 of part I, the mathematical development is given for sandwich constructions whose facings are not perfectly flat. It is assumed that the facings are perfectly elastic and that failure takes place in the cores due to tensile stresses normal to the facings caused by the growth of the initial irregularities in the facings, To illustrate this part of the development, it was necessary to use data from specimens that reached their maximum loads at stresses in their facings less than the proportional-limit stress and in which failure[8] took place between the facings and the core. Section 2 of this part of the report deals with the results obtained.

Section 15 of part I extends the mathematical development into the plastic range by the use of a reduced modulus of elasticity for the facings. The maximum loads are limited by tension failure between the facings and the cores. The results of some of the tests reported in Forest Products Laboratory Report No. 1561 illustrate this manner of failure; and they are compared in section 3 with results obtained from the analysis.

Section 4 of this part of the report discusses tests of a number of sandwich constructions, previously reported in Forest Products Laboratory Report No. 1561, in which failure was not caused by wrinkling of the facings, but by stresses in either the facings or cores that were equal to their compressive strengths.

---

[8] These failures were in the core adjacent to the glue line. A thin skin of the core material adhered to the glue on the facing. Such failures are common at glued joints and probably occur at this location because of stress concentrations. The glue increases the elastic properties of the material which it penetrates.

The sandwich constructions, for which results are cited in sections 1 through 4, included four facing materials having moduli of elasticity from 2 to 30 million pounds per square inch; and eight core materials having moduli of elasticity varying from 420 to 536,000 pounds per square inch, and moduli of rigidity varying from 330 to 15,000 pounds per square inch. The thicknesses of the facings varied from 0.005 to 0.032 inch, and the thicknesses of cores varied from 1/4 to 2-1/2 inches. The compressive stresses in the facings at maximum load varied from 8,000 to 95,000 pounds per square inch.

Tests to Show Manner in Which Different Sandwich Constructions Failed

1. Teste Illustrating Elastic Instability of the Facings

Materials

The materials used in these sandwich constructions were aluminum facings on cores of two compositions of granulated-cork board, and steel facings on a third composition. The facings were 24ST clad aluminum alloy in sheets 0.012-, 0.020-, and 0.032-inch thick. The steel was blue-tempered and polished 0.70 to 0.80 carbon spring steel, 0.010 inch thick and 1-1/4 inches wide. Each composition of cork board, according to the manufacturer, contained the "fine" particle size of granulated cork of a clean, soft grade, thoroughly bonded with a protein glue. The densities of the boards were about 22, 28, and 41 pounds per cubic foot, Boards 1/2, 3/4, and 1 inch thick of each composition were used.

Sandwich Specimens

The sandwich constructions having aluminum facings and cork cores were made 12 inches square. The rolled direction of the facing on one side was placed parallel to that on the other. The facings were bonded to the core by means of a primary and a secondary glue. The primary glue was sprayed and baked on the facings, and the secondary glue was applied to the cores with a brush. The assembly was pressed at 15 pounds per square inch at room temperature. Sandwich specimens 2 inches wide were machined from each of the 12- by 12-inch panels. Five specimens of each construction were cut to lengths equal to four times their thickness plus 1 inch. Their end8 were cast in disks about 3-1/2 inches in diameter and 1/2 inch thick. The disks were made of a mixture of resin and wood flour. Five additional

specimens of each construction were cut to lengths equal to about four times their thickness, The ends of these specimens were not cast in disks

The sandwich constructions having steel facings and cork cores were made into individual specimens. The steel of this particular quality was available only in strips 1-1/4 inches wide. Consequently, the facings were cut to length and assembled in a jig with their respective core materials as individual flat plates. The facings were bonded to the cores by the same gluing procedure as that used to bond aluminum facings to cork. After the facings were bonded to their cores, the bearing ends of the steel facings were ground smooth and parallel; and the bearing ends of the core were undercut prior to the attachment of disks. Five specimens of each construction were fabricated for testing.

Method of Test -- Sandwich Specimens

The sandwich specimens were tested in compression in a direction parallel to the rolled direction of the facings. The load was applied through a spherical bearing block properly centered on the specimen to distribute the load uniformly. Distribution of the load was checked by measuring the strains in the facings. If the strains showed a difference greater than 10 percent at about one-half the anticipated maximum load, adjustments were made for better equality. When the load was distributed as uniformly as possible, the final loading of the specimen was made by a continuous motion of the movable head of the testing machine.

Four specimens were tested to observe in detail the wrinkling of the facings. For these specimens the load was applied in increments so that the profile of the surface of each facing at each increment of load could be measured by means of a pair of 1/10,000-inch dials. The apparatus used for this method of test is shown in figure 18. It consists of a pair of 1/10,000-inch dials (A), each secured to a bar (B) that rotates on needle bearings (C) to support bar and dials and to allow precise freedom of movement. Both bars are connected by a wire (D) to a single drum that, when revolved by crank (E), causes the pointers on the dials (A) to travel along the surface of the specimen. Two 1/1,000-inch dials (F) were also connected to the bars by means of wires and pulleys to provide a method for measuring the location of the 1/10,000-inch dials with respect to a horizontal position. Since it was desired to traverse the surface of the facings during a reasonable interval (about 7 seconds), a 35-mm. motion picture camera was used to record all the dial readings during the continual traverse, This record of lateral deflection on the 1/10,000-inch dials and of vertical position on the 1/1,000-inch dials was

tabulated and then corrected for the circular motion of the dials. The corrections were made to take into account the distance between the arc and a vertical line tangent to the arc.

Methods of Test -- Core Materials

Mechanical tests of the core materials were made according to the methods set forth in Forest Products Laboratory Report No. 1555, revised October 1948. Initial tangent moduli were determined in compression and shear, but only maximum stress was determined in tension. The compression modulus in the flatwise direction, perpendicular to the plane of the sandwich, was determined according to the method in paragraphs 5 to 11 of Report No. 1555, which relates to stacking 2- by 2-inch flat sections of core material. The strains were measured by Tuckerman optical extensometers. The modulus of elasticity in edgewise compression parallel to the direction of applied load and parallel to the plane of the sandwich, was obtained according to the method in paragraphs 12 to 18 of Report No. 1555. The shear modulus in the transverse plane was obtained according to the method in paragraphs 36 to 41 of Report No. 1555, which describes testing a 1/2- by 2- by 6-inch specimen between steel plates. The pendulum method was tried, but the damping factor of the cork was so high that the pendulum stopped swinging immediately. The maximum tensile stress was obtained according to the method in paragraphs 19 to 23 of Report No, 1555. Typical stress-strain curves obtained in compression and shear are shown in figures 19 and 20, respectively, for the three compositions of cork.

Results of Tests

The results of the tests on sandwich constructions and on their core materials are presented in tables 2, 3, and 5. Tables 2 and 3 present the data obtained from sandwich constructions having aluminum facings and cork cores. Table 4 presents the data obtained from sandwich constructions having steel facings and cork cores. Table 5 presents a summary of the mechanical properties of the core materials. The data in tables 2, 3, and 4 are arranged in sequence with respect to increasing ratios of core thickness to facing thickness of the constructions. The thicknesses of the materials comprising each sandwich construction are listed. The term "free" height of the specimen refers to the distance between disks, or, if disks were not used, it refers to the total height of the specimen.

The observed maximum compressive load of each specimen is listed in pounds per inch of width and in pounds per square inch of compressive area of the

facings. These observed stresses in the facings were computed according to the following relationship, by which it is assumed that at a given load the strain in the core is equal to the strain in the facings and that the ratio of modulus of elasticity of the facings to that of the core is constant throughout the test.

$$p_f = \frac{P_m}{2f + \frac{(Ex)_c}{(Ex)_f} c} \qquad 2.1.1$$

The values of stress in the facings that were obtained by the two methods of test, with and without disks at the bearing ends, are so nearly equal that the effect of the end condition could not be determined. The values also show that slight variations in length do not affect the maximum stress. Since these values of stress for a given construction are in fair agreement with each other, the 10 values are averaged for comparison with theoretical values.

The wrinkling of the facings was observed in detail on four specimens having aluminum facings and cork cores, The profiles obtained from measurements are shown in figures 21, 22, 23, and 24. Figures 25, 26, 27, and 28 are enlarged pictures of these specimens taken on 35 mm. film after they had failed.

Figures 21, 22, 23, and 24 show that the specimens were originally slightly thicker at their centers than at their ends, and that as load was applied short waves became visible, as predicted by the theory discussed in part L

The half waves associated with failure are indicated by crosses placed at the points of contraflexure on the profile preceding failure. In figures 21 and 22 the lengths of these half-waves were found to be 0.90 and 0.86 inch. The half-wave length of the critical wave calculated by use of figure 6 of part I is 0.895 inch. Similarly, the measured half-wave lengths in figures 23 and 24 are 0.43 and 0.46 inch, and the calculated length is 0.424 inch. The agreement between the measured and calculated values is reasonable.

The photographs taken of these specimens after failure had occurred, figures 25, 26, 27, and 28 show the type of failure, but do not indicate the wave pattern of the facings that existed prior to failure.

All of the specimens reported in this section reached their maximum loads without fracturing in a discernible manner. Further, the stresses in the facings at the maximum loads did not exceed the proportional-limit stress of the material. It can be assumed, therefore, that the maximum loads

obtained closely approximated the critical loads of the specimens. The stresses in the facings at the maximum loads are compared with the computed critical stresses in figures 29 and 30. The curves in these figures are drawn according to the methods described in sections 8, 9, and 10 of part I. Each plotted point represents an average of 10 test values. It is evident that the theory yields a good estimate of the test values obtained.

2. Tests Illustrating Failure in the Core Due to Initial Irregularities in the Facings

Materials

Sandwich constructions consisting of steel facings and cellular cellulose acetate cores were used to illustrate this manner of failure. The steel facings were the same as those described in section 1 of part II. The cellular cellulose acetate (C.C.A.) was a cellular form of cellulose acetate containing a small portion of glass fibers as strength-imparting filler material. Microscopic observations of the cells showed that the diameters in the extruded direction were one-half the diameters in the width and thickness directions. The C. C. A. weighed 6 to 7 pounds per cubic foot. It had been manufactured in strips approximately 5/8 inch thick, 2-5/8 inches wide, and of random lengths. The strips were machined to about 1/2-inch thickness and 2-3/8-inch width,

Two methods were used to orient these strips in the sandwich. First, the C. C. A. was oriented "flatwise." This term is used to indicate that the plane of the manufactured material described by the extruded length and width directions was oriented parallel to the plane of the facings. The extruded direction was parallel to the length of the specimen. Cores more than 1/2 inch thick were made up of two strips, equal in thickness and glued together at the center of the specimen. The plane of the glue line was parallel to that of the facings and midway between.

Second, the C. C. A. was oriented "edgewise." This term is used to indicate that the plane of the manufactured material described by the extruded length and width directions was oriented perpendicularly to the plane of the facings. The extruded direction was parallel to the length of the specimen. Cores were made by assembling unglued strips, cut from 1/2-inch thick material, of proper length, width, and thickness in relation to the dimensions of the sandwich. The length was four times the sandwich thickness plus 1 inch, the width was 1-1/4 inches, obtained by assembling two strips and a half strip, and the thickness was 1/2 to 1 inch, depending on the construction. The strips were not glued together.

Sandwich Specimens

The sandwich specimens were made of 0.010-inch steel facings and various thicknesses of C. C. A., as listed in tables 6 and 7. The specimens were fabricated and prepared as individual plates in the same manner as those specimens having steel facings and cork cores described in section 1, part II. Only four specimens were made, however, for each construction instead of five; and the disks were made of plaster instead of the mixture of resin and wood flour.

Methods of Tests -- Sandwich Specimens

The sandwich specimens were tested in edgewise compression in a direction parallel to the rolled direction of the facings. The load was applied through a spherical bearing block properly centered on the specimen to distribute the load uniformly. Equal distribution of the load between the two facings of each specimen having a flatwise core was obtained by partially loading the specimen and lightly tapping the spherical block to slightly shift its position. When tapping caused no change in the applied load, as indicated by the weighing device of the test machine, the loading was continued to failure. The distribution of the load between the two facings of each specimen having an edgewise core was checked by means of strain gages as previously described. When the distribution was fairly equal, the loads were applied in increments so that profiles of the facings could be obtained by the apparatus described in section 1, part II.

Method of Test -- Core Materials

Mechanical tests of C. C. A. were made according to the methods described in Forest Products Laboratory Report No. 1555, revised October 1948. The flatwise C. C. A. core, due to its orientation in the sandwich, was tested to determine the modulus of elasticity in compression perpendicular to the plane of the facings according to the procedure described in paragraph 9 of Report No. 1555 relating to the stacking of unglued specimens and to measuring the strains with filar microscopes. The edgewise C. C. A. core, due to its orientation in the sandwich, was tested differently to determine the modulus perpendicular to the plane of the facings, because the flatwise direction of the sandwich was the edgewise direction of the core. Normally, tests of core materials are conducted on materials that are matched to those in the sandwich. These flatwise tests were conducted, however, on the same strips that were used in the sandwich. This was accomplished by testing

strips of C. C. A. 1/2 by 2 inches by a length equal to that of the facings. These strips were tested in compression for only the modulus of elasticity by applying loads not exceeding the proportional limit. The load was applied on the strip in the direction parallel to the 2-inch dimension, and the strains were measured by a Marten's-mirror compressometer. After the load-deformation data had been obtained, the central portion of each strip between the knife edges of the compressometer was cut into a strip the width of which was equal to the thickness of the core required. Each strip was then used for the core of the sandwich construction as previously described. The C. C. A. was also tested for modulus of elasticity in compression parallel to the extruded direction according to paragraphs 12 to 18 of Report No. 1555. Typical stress -strain curves, as obtained in these three directions, are shown in figure 19.

The torsion pendulum shear test, paragraphs 30 to 35 of Report No. 1555, was used to determine the modulus of rigidity associated with strains in the plane perpendicular to the facings and parallel to the extruded direction.

The maximum tensile strength in the flatwise direction was made according to paragraphs 19 to 23 of Report No. 1555.

Results of Tests

The results of the tests are presented in tables 5, 6, and 7 and in figures 31 and 32. The tables have the same column headings and the figures have the same coordinates as those used in section I, part II.

Figures 33 to 37 show typical examples of the profiles of the facings taken during test. The datum lines of these curves are not vertical because the specimens were very slightly slanted in the testing machine, and the fineness of the measurements magnified this slant. Because the profiles were measured over only limited portions of the specimens, near their centers, it is not possible to determine the positions of the datum lines. The curves show, however, the growth of the initial irregularities in the facings as the load is applied. This is discussed in section 13 of part I. The irregularities grow, but do not change greatly in general shape. Failure took place at loads below the critical loads and, therefore, the growth of the waves having the critical half-wave length could not be detected.

Most of the specimens failed in tension between the facings and the cores. It is necessary, therefore, to determine an appropriate value of K from figure 16, according to the discussion in section 14 of part I. For the

specimens having flatwise C. C. A. cores, a value of 0.05 was chosen. Curves for K = O and K = 0.05 are drawn in figure 31. The plotted points represent the experimental data obtained, It is seen that the plotted points, with the exception of the two to the left, are in reasonable agreement with the theory.

The two points at the left are to the left of the cut-off point, and, therefore, the specimens represented by them would not be expected to fail due to face wrinkling. Observation of the specimens during test indicated that they may have failed as columns. The curve to the left on figure 31 represents stresses associated with critical column loads for these specimens. It is drawn according to equation 30 of Forest Products Laboratory Report No. 1583 applied to an infinitely wide plate for specimens having column lengths four times their thicknesses. The experimental points are in fair agreement with the curve.

The appropriate value of K for specimens having edgewise C. C. A. core8 lies between 0.05 and 0.10. Curves for these values are shown in figure 32. The plotted points represent experimental results and agree reasonably well with the curves.

3. Tests Illustrating Core Failure at Stresses in the Facings Above the Proportional Limit

Materials

The data used were taken from previous experimental work reported in "Preliminary Report on the Strength of Flat Sandwich Plates in Edgewise Compression," Forest Products Laboratory Report No. 1561, May 1947. The constructions of present interest are those that develop stresses in the facings in excess of the elastic-limit stress. Sandwich constructions having cores of balsa wood, cellular cellulose acetate (C. C. A.), or cellular hard rubber (C. H. R.) were tested more extensively than other materials. The constructions having aluminum facings and these cores were used, therefore, for purposes of illustration.

Specimens

Descriptions of test specimens, fabrication, methods of test, and data are reported in Forest Products Laboratory Report No. 1561. These tests were

made at a time previous to that of the present report and before the great importance of uniformity in the tensile strength of the bond between the core and facings was fully realized. The results previously given in this report show less scatter than those taken from Report No. 1561, partly because of the greater care exercised in the preparation and inspection of the specimens.

Discussion of Results of Tests

All of the specimens failed in tension between the core and the facings or as columns. The results of the tests are compared with the theoretical limiting stresses discussed in section 15 of part I and with column loads discussed in Forest Products Laboratory Report No. 1583.

The reduced modulus of elasticity used for the facings at stresses above the proportional-limit stress is given by:

$$E_r = \frac{4\,E_f E_t}{(\sqrt{E_f} + \sqrt{E_t})^2}$$

A smoothed stress-strain curve of the facings was obtained from an experimental curve by the three-parameter method given in National Advisory Committee for Aeronautics Report No. 902, and the formula given in that report for the reduced modulus in terms of stress was used. The formula obtained and a curve plotted from it are given in figure 17. The accuracy of the curve is questioned above a stress of 70,000 pounds per square inch.

Theoretical curves relating the stresses in the facings at failure to the ratio of the core thickness to the face thickness for the various combinations of materials are shown in figures 38, 39, and 40, together with plotted points representing the results of experiments, and are discussed in the following examples. Two of the constructions in example 1 follow the theoretical curves reasonably well. The rest of the data scatters rather badly, probably for the reasons subsequently pointed out.

Example 1: Aluminum -- Balsa-wood constructions. --Curves for the stress in the facings at failure, computed for values of K of 0, 1.0, and 2.0 according to the method described in section 15 of part I, are plotted in figure 38. Average experimental values are plotted as points. These values were taken from tables 1 and 2 of Forest Products Laboratory Report No. 1561, and the pertinent values are also given in table 8 of the present report.

The curve to the left on figure 38 represents stresses associated with critical column loads computed according to equation (30) of Forest Products Laboratory Report No. 1583. This curve applies to specimens whose lengths are four times their thicknesses, which is approximately true for the specimens tested.

The points representing the test data from specimens having facings 0.0050 and 0.0125 inch thick are nearly included between the curves for K = 1.0 and K = 2.0. Insufficient data were obtained to determine the proper curves for the other specimens. A smaller value of K is indicated.

The stresses in some of the specimens were evidently limited by the column critical stress. Others exceeded this limiting value, The facings of these may have contained initial irregularities that opposed column failure.

The value of K contains the ratio of the modulus of elasticity of the core material to the tensile strength of the bond between the facings and the core as a coefficient (section 14, part I). Maximum and minimum values of this ratio were obtained from the data reported in Forest Products Laboratory Report No. 1561. They were found to be 2,690 and 172. Thus the highest value of K might readily be $\frac{2,690}{172} = 15.65$ times the lowest value. The greatest and least values of K were obtained from the data plotted in figure 38, but omitting the point furthest to the left because its position was probably influenced by its proximity to the column critical-stress curve. These values are 2.00 and 0.12. Their ratio, 16.65, agrees very well with the ratio previously obtained. It seems likely, therefore, that the scatter of the points representing tests in figure 38 may be due in part to variations in the mechanical properties of the materials in the specimens.

Example 2: Aluminum -- cellular cellulose acetate. --The curves in figure 39 are similar to those in figure 38 applying to example 1, but they are plotted for sandwich constructions having aluminum facings and cellular cellulose acetate cores. Curves for values of K of 0, 0.07, 0.20, and 0.50 are shown.

The plotted points representing the results of tests scatter a great deal and seem to bear little relation to the curves. However, the ratios of the modulus of elasticity of the facings to the strength of the bond between the facings and the core as determined from the data of Forest Products Laboratory Report No. 1561, vary from 967 to 29, which yield a ratio of 33.4. Values of K determined from the experimental data plotted in figure 39, omitting those points to the left of the column critical curve, vary from 1.10 to 0.04, which yield a ratio of 27.4. These two ratios are in fair agreement, and it seems likely, therefore, that the wide scatter of the test points may be due

in part to variations in the mechanical properties of the materials in the specimens.

Example 3: Aluminum -- cellular hard rubber. --Figure 40 is a curve sheet for aluminum facings and cellular hard-rubber cores similar to figures 38 and 39 given for examples 1 and 2. The plotted points, representing experimental values, seem to have little relation to the curves drawn. The greatest and least values of the modulus of elasticity of the cores to the tensile strength of the bond between the core and the facings were obtained from the data of Forest Products Laboratory Report No. 1561 and are found to be 514 and 58, which yield a ratio of 8.87. The greatest and least values of K obtained from the data plotted in figure 40 are 1.00 and 0.04, which yield a ratio of 25. It seems that the scatter of the points may not be entirely due to variations in the modulus of elasticity of the core material and the tensile strength of the bond. Possibly, variations in the other mechanical properties of the core material contributed to the scatter.

4. Facings or Cores Fail in Compression at Loads Insufficient to Cause Failure Because of Face Wrinkling

Three examples are given of sandwich constructions that fail because of direct compression in the facings or in the cores. The illustrative data are taken from Forest Products Laboratory Report No. 1561.

Example 1: Glass-cloth-laminate facings on balsa-wood cores. --Stresses in the facings of sufficient magnitude to cause failure by face wrinkling were computed according to the method described in section 14 of part I. It is not necessary to use a reduced modulus of elasticity of the facings, as described in section 15 of part I, because the stress-strain curve of glass-cloth laminate, figure 41, is substantially a straight line to failure, The computed critical stress in the facings for the various constructions of sandwich tested are all about 20 times the compressive strength of the glass-cloth laminate. It is thought, therefore, that failure was due to direct compression of the facings.

The values of the stress in the facings of the sandwich at failure are presented in table 9 for comparison with the compressive strength of the facing material. This comparison shows that the stresses in the facings of the sandwich specimens at failure agree reasonably well with the strength of the facing material.

Example 2: Papreg facings on end-grain balsa-wood cores. --Stress in the facings of sufficient magnitude to cause failure by face wrinkling was computed according to the method described in section 15 of part I. Because the stress-strain curve of papreg has considerable curvature (fig. 41), it is necessary to use the reduced modulus. The computations indicated that the limiting stress due to face wrinkling is equal to the Compressive strength of the papreg. The value of this strength, given in table 6 of Forest Products Laboratory Report No, 1561, is 19,150 pounds per square inch. Values of the stresses in the facings of the sandwich specimens tested taken from table 4 of Report No. 1561 are 18,200, 19,250, and 20,500 pounds per square inch. These values are in reasonable agreement with the previous one.

Example 3: Papreg facings on balsa-wood cores, with the grain direction of the balsa in the direction of the applied stress. --The limiting values of the stresses in the papreg facings were computed according to the method described in section 15 of part I; and as in example 2, they were found to be equal to the compressive strength of the papreg. The strains at the maximum compressive strength of the facing and core material, however, must also be investigated, The strain of the balsa-wood cores at the maximum compressive stress of 2,600 pounds per square inch is 0.0039 inches per inch. These values are averages of those given in table 7 of Forest Products Laboratory Report No. 1561. The stress in the papreg at this strain, taken from the stress-strain curve in figure 41, is 7,800 pounds per square inch. It is assumed, therefore, that the limiting value of stress is 7,800 pounds per square inch instead of 19,150 pounds per square inch. Table 10 shows the values of the strengths of the sandwich constructions computed in accordance with the lowest stress value. In the computations it was assumed that the values of stress in facings and core, given above, occurred at failure in the sandwich specimens.

The computed loads are seen to be conservative. The differences between the test loads and computed loads are roughly constant and may be due to the strengthening effect of the glue used to bond the facings to the cores.

Conclusions

1. Sandwich constructions subjected to an edgewise compressive stress may fail in a number of ways. They will fail by face wrinkling only when the stress required to cause such failure is less than that required to cause failure in any of the other ways.

2. If a sandwich construction fails by face wrinkling and if the component materials have such properties that face wrinkling can occur without causing failure between the core and the facings, the maximum stress in the facings is the critical wrinkling stress as determined by sections 8, 9, and 10 of part I of this report. Test values of maximum stress are compared with the computed critical values in figures 29 and 30.

3. If a sandwich construction fails by face wrinkling combined with failure between the core and the facings, the maximum stress in the facings can be estimated by means of the method given in part III and in section 14 of part I. Test values of the maximum stress are compared with estimated values in figures 31 and 32.

4. If a sandwich construction fails by face wrinkling at a stress in the facings above the proportional-limit stress, the maximum stress can be estimated by the use of a reduced modulus of elasticity for the facings as described in section 15 of part I. Test values of the maximum stress are compared with estimated values in figure 38. Test values for sandwich constructions having facings of different thickness are shown. It is probable that different values of the parameter K apply to the different thicknesses of facings.

5. Variations in the strength between the core and the facings and variations in the properties of the core result in marked variation in the maximum stress in the facings because of their effect on the value of the parameter K as introduced in section 14 of part I and discussed in part 111. This is illustrated by the scatter of the points representing test data in figures 38, 39, and 40. When the values of these properties are accurately known, the test data do not scatter greatly. This is illustrated by figures 29, 30, 31, and 32.

PART 111. DESIGN CRITERIA FOR FACE WRINKLING OF SANDWICH PANELS

Introduction

It is the purpose of this part of the report to outline the problem that confronts the designer and a method by which an approximate solution to it may be obtained. If two opposite edges of a sandwich panel are subjected to uniformly distributed loads acting in the plane of the sandwich and directed perpendicularly to the edges, the panel may fail in a number of ways. Each manner of failure should be examined independently, and the lowest of the loads determined should be used in design. The possible manners of failure are:

(1) The sandwich panel may become elastically unstable as a whole due to the action of the applied loads, Failure will take place due to the formation of buckles that induce bending stresses or shear stresses greater than those which the sandwich can withstand.

(2) If the elements of the panel in the direction of the load are not originally straight, deflections will occur at low loads and will grow as the load is increased. Thus bending stresses or shear stresses greater than those which the sandwich can withstand may occur at a load less than that required to cause elastic instability of the panel as a whole.

(3) As load is applied, the compressive stress in the facings or core of the sandwich may reach the compressive strength of the materials at a load less than that required to cause failure in the manner described under (1) and (2) and thus cause failure due to direct compression.

(4) The facings of the sandwich may act as columns elastically supported by the core, If the facings are perfectly straight, the load on the sandwich will be limited by the critical loads of the elastically supported facings. If the facings are not perfectly straight, they will deflect at low loads; and the deflections will grow as load is applied and thus induce stresses in the core that may cause failure before the critical loads of the facings are reached.

Discussion of Wrinkling Failure

Design criteria for the first three types of failure are dealt with elsewhere. The following discussion is limited to the fourth type of failure, which will be called wrinkling failure.

It is assumed that the over-all shortenings of the two facings of the sandwich panel are equal. Ideally, the wave patterns shown in figures 1, A or 1, B will form when the critical load is reached. If the core is sufficiently thick, the wave patterns in the two facings will be independent of each other, and either pattern will lead to the same critical load. In this case the strains introduced into the core by the formation of the waves in one facing die out before they reach the other facing. For sandwiches having thinner cores, the strains in the core introduced by one facing influence the wave pattern in the other facing and it is found that, usually, the wave pattern illustrated by figure 1, A leads to lower critical loads than that illustrated by figure 1, B.

The facings of sandwich panels are never perfectly flat. The initial irregularities increase in amplitude as load is applied. They grow until the core

is stressed to its breaking point, and then failure occurs. Therefore the critical load is never reached. It may, however, be closely approached if certain combinations of materials are used. An exact analysis requires knowledge of the form of the original irregularities in the facings so that they may be reduced to their Fourier components. Such information, of course, is not available for each panel entering a structure, nor would it be practical to design by a method requiring it even if it were.

1. Tests for Effect of Irregularities in Facings

A method of approximating the average effect of the original irregularities of the facings is described. It involves tests of short columns of sandwich construction made of the materials to be used in design. The use of the information obtained from these tests in connection with the mathematical development given in part I allows the design of other sandwich constructions of these materials.

The tests described in part II indicate that the irregularities in the facings are created largely in the fabrication of cores and facings into sandwich panels. Pressure normal to the surfaces of the facings is applied to effect bonds between the facings and cores, This pressure causes the core to be compressed transversely. During the time that the pressure is applied, a certain amount of plastic deformation occurs in the core. Recovery from this deformation is not complete when the pressure is relieved. Because the core materials are not perfectly uniform throughout their volumes, the recovery from plastic deformation is not uniform. Thus slight variations in the thickness of the core of the sandwich result. These variations cause irregularities or waves in the facings. The amplitude of the waves is, therefore, roughly proportional to the thickness of the core. This fact is taken into account in section 14 of part I (equation 1.14.13).

The facings continually tend to resume their initial form, and therefore, introduce stresses in the core tending to diminish the amplitude of the irregularities. This tendency increases with the thickness of the facings, so that it is likely that the amplitude of the irregularities in the facings is more nearly proportional to the ratio of the core thickness to the facing thickness than to the core thickness alone, The accuracy of this assumption should be verified for commercially manufactured panels, however, by designers interested in using these panels. Its accuracy will normally be verified in the use of the design criteria described here.

The design criteria are based on the family of curves shown in figure 16. The abscissa is:

$$q = \frac{c}{f}\,\mu\left(\frac{\lambda}{E_f E_c \mu}\right)^{1/3} \qquad 3.1.1$$

The ordinate is:

$$Q = p\left(\frac{\lambda}{E_f E_c \mu}\right)^{1/3} \qquad 3.1.2$$

The value, which is constant along any one of the curves, is:

$$K = \frac{a}{c}\frac{E_c}{t} \qquad 3.1.3$$

in which [9]

c = core thickness
f = face thickness
μ = modulus of rigidity of the core material associated with shear strains in planes perpendicular to the facings and parallel to the direction of the applied load
E_f = modulus of elasticity of the facings in the direction of the applied load
E_c = modulus of elasticity of the core in the direction normal to the plane of the facings
p = stress in the facings when failure takes place between the facings and the core
t = tensile strength of the core material in the direction normal to the facings or the strength of the bond between the core and the facings, whichever is the lesser
a = initial amplitude of the buckling wave in the facings
$\lambda = 1 - \sigma_{xz}\,\sigma_{zx}$ in which σ_{xz} and σ_{zx} are Poisson's ratios of the facings
σ_{xz} = the ratio of the extension in the plane of the facing perpendicular to the direction of the load to the contraction due to a stress in the direction of the load
σ_{zx} = the ratio of the extension in the direction of the load to the contraction due to a compressive stress in the plane of the facing perpendicular to the direction of the load

---

[9] The symbols used in these expressions are the same as those used in Part I of the report except that a number of the subscripts have been omitted. The definitions of the symbols given here should be used rather than those in the table of nomenclature in part I.

The uppermost curve in figure 16 defines the critical stress in the facings for sandwich panels of various constructions. The curves below this one define the greatest stress obtainable in the facings because of failure between the core and the facings due to the presence of initial irregularities in the facings. Each curve is labeled with the appropriate value of K. All of the curves start at definite points at the left. The significance of these points will be discussed subsequently,

2. Design Curves for Combinations of Materials

Curves for design purposes for various combinations of materials can be obtained from the curves of figure 16, provided some results from edgewise-compression tests on specimens of sandwich panels made of these materials are available. For these specimens the stress in the facings at failure is known and, therefore, values of q and Q can be computed by means of equations 3.1.1 and 3.1.2. If the stresses are above the proportional-limit stress of the facings, a reduced modulus of elasticity of the facings should be used. The reduced modulus used is given by:

$$E_r = \frac{4\,E_f E_t}{(\sqrt{E_f} + \sqrt{E_t})^2} \qquad 3.2.1$$

in which:

E_r = the reduced modulus of elasticity
E_t = the tangent modulus of elasticity of the facings
E_f = the usual modulus of elasticity of the facings

The values of Q and q obtained in this manner are then plotted on figure 16 and, from their position, the particular curve is selected that is associated with the specimens. It is important to be certain that these specimens actually failed due to face wrinkling.

The selected curve of figure 16 may be used for design purposes, however, if the stresses that are obtained in the facings are above the proportional-limit stress, the modulus of elasticity of the facings is a function of the stress, and it is necessary to resort to a cut-and-try process to determine the stress at failure for any particular sandwich construction. It may be more convenient to replot the particular curve of figure 16 to coordinates of stress and of the ratio of the thickness of the core to that of the facings. To do this, a stress is assumed and the reduced modulus of elasticity of the facings

associated with it is computed. These values are substituted in equation 3.1.2 to obtain a value of Q. The selected curve of figure 16 then yields a value of q, and the associated value of $\frac{c}{f}$ is obtained from equation 3.1.1. Thus the desired curve can be plotted point by point. The method of section 15 of part I is useful for the determination of the range in which the stresses should be chosen. Thus a design curve for sandwich constructions made of a particular combination of materials is obtained.

If a considerable amount of test data is available, associated values of q and Q can be calculated and plotted, A curve drawn through the points may be used for design purposes. In plotting, different symbols should be used for sandwich constructions having different thicknesses of facings, since the value of K may vary with face thickness. The plotted points may scatter considerably, due to variations in the elastic properties of the core material and in the strength of the core material or of the bond between the core and facings. Data from specimens that failed in a manner other than face wrinkling should not be plotted.

By these methods a series of curves may be obtained for design purposes. Each curve will apply to sandwich constructions made of a single combination of materials.

The curves of figure 16 give, approximately, the stress in the facings when failure in the core occurs due to antisymmetrical wrinkling of the facings (fig. 1, A), and, therefore, the design curves obtained by the methods described are also such curves. In general, they yield the least stress that will cause failure due to face wrinkling. In some cases, however, symmetrical wrinkling (fig. 1, B) leads to lower stresses than these. These cases may occur if the value of κ given by the following equation is less than one-half. This may be true of some sandwich constructions having honeycomb cores. If it be true, these design criteria may not be applicable and tests of these particular sandwich constructions should be made.

$$\kappa = \frac{\sqrt{E_c E_x}}{2\mu} - \sigma_c \sqrt{\frac{E_c}{E_x}} \qquad 3.2.2$$

in which

E_x = modulus of elasticity of the core in the direction of the applied load

σ_c = Poisson's ratio of the core and is the ratio of the extension in the direction perpendicular to the plane of the facings to the contraction in the direction of the load due to a compressive stress in that direction

This equation is obtained from equation 1.4.3 of part I.

The curves come in from infinity to the right and end at a cut-off point. Each point on a curve is associated with the particular wave length that leads to failure in the core at the lowest possible stress in the facings. These wave lengths are short for points to the right and longer for points at the left. To the left of the cut-off point, wrinkling failure will not occur and failure will take place in some one of the other ways previously discussed.

Table 1.--Typical values of parameters used to predict the wrinkling stress in facings

Material	Core: Specific gravity	Core: Parameters: E	Core: Parameters: β	Core: Parameters: σ	Sandwich: Parameters: Aluminum facing: $\bar{E}$	Sandwich: Parameters: Aluminum facing: x	Sandwich: Parameters: Steel facing: $\bar{E}$	Sandwich: Parameters: Steel facing: x	Sandwich: Parameters: Papreg or glass-cloth: $\bar{E}$	Sandwich: Parameters: Papreg or glass-cloth: x
		1,000 p.s.i.			1,000 p.s.i.		1,000 p.s.i.		1,000 p.s.i.	
Cork[1]	0.35	0.78	0.421	0.090	[2] 12.0	[2] 0.0275	17.6	0.0187	7.32	0.0450
	.45	2.23	.439	.080	[2] 24.8	[2] .0395	35.3	.0278	14.6	.0671
	.66	8.19	.415	.134	55.0	.0618	[2] 81.0	.0420	33.7	.1010
Cellular cellulose acetate (flatwise)[1]	.10	8.90	.448	.175	88.4	.0450	[2] 131.0	[2] .0310	54.0	.0739
Cellular cellulose acetate(edgewise)[1]	.10	11.34	.394	.438	102.0	.0440	[2] 150.0	[2] .0298	62.3	.0720
Balsa (end grain)[3]	.12	65.60	.229	.164	[2] 431.0	[2] .0348	636.0	.0236	[2] 264.0	[2] .0570
Cellular cellulose acetate (flatwise)[3]	.10	23.00	.152	.160	[2] 112.0	[2] .0312	166.0	.0210	69.8	.0500
Cellular hard rubber[3]	.10	13.83	.282	.520	[2] 102.0	[2] .0382	151.0	.0260	62.6	.0620

[1] Parameters computed from values determined in present investigation.

[2] Parameters computed from values taken from Forest Products Laboratory Report No. 1561.

[3] Sandwich parameters for combinations of facing and core materials that have been tested.

Table 2.--Edgewise compressive strength of sandwich specimens having aluminum facings and granulated-cork cores (0.35 sp. gr.)

Thickness of material			Ratio	Free	Observed maximum compressive strength	
Face	Nominal core	Total	c/f	height	Load	Stress in facing
f	c	h				
(1)	(2)	(3)	(4)	(5)	(6)	(7)
Inch	Inch	Inch		Inch	Lb./inch of width	1,000 p.s.i.
0.0196	1	1.045	51.3	3.66	387	9.87
		1.042	51.2	3.81	358	9.10
		1.040	51.2	3.68	377	9.60
		1.040	51.2	3.72	390	9.93
		1.039	51.2	3.68	389	9.90
		1.053	51.3	1/3.63	383	9.75
		1.050	51.3	1/3.63	380	9.67
		1.048	51.3	1/3.63	394	10.03
		1.049	51.3	1/3.69	384	9.77
		1.053	51.3	1/3.68	393	10.00
Av.		1.046	51.3	3.68	384	9.76
0.0120	3/4	.780	63.0	3.04	277	11.50
		.779	62.9	3.01	299	12.41
		.778	62.8	3.04	294	12.20
		.778	62.8	2.85	301	12.50
		.788	63.7	2.93	274	11.37
		.786	63.5	1/2.87	263	10.91
		.781	63.1	1/2.87	261	10.83
		.780	63.0	1/2.87	263	10.91
		.782	63.2	1/2.87	250	10.37
		.788	63.7	1/2.87	219	9.09
Av.		.782	63.2	2.92	270	11.21
0.0120	1	1.031	84.0	3.97	259	10.75
		1.030	83.9	3.85	290	12.04
		1.033	84.0	3.81	279	11.58
		1.035	84.2	3.89	281	11.66
		1.037	84.4	3.92	267	11.10
		1.032	84.0	1/3.85	236	9.80
		1.031	84.0	1/3.85	264	10.95
		1.034	84.1	1/3.85	250	10.37
		1.035	84.2	1/3.85	242	10.05
		1.036	84.3	1/3.85	263	10.92
Av.		1.033	84.1	3.87	263	10.92

1/ Free height is total height of specimen.

Table 3.--Edgewise compressive strength of sandwich specimens having aluminum facings and granulated-cork cores (0.45 sp.gr.)

Thickness of material			Ratio	Free	Observed maximum compressive strength	
Face	Nominal core	Total			Load	Stress in facing
f	c	h	c/f	height		
(1)	(2)	(3)	(4)	(5)	(6)	(7)
Inch	Inch	Inch		Inch	Lb./inch of width	1,000 p.s.i.
0.0322	1	1.066	31.1	3.90	1,500	23.20
		1.055	30.9	3.91	1,461	22.60
		1.066	31.1	3.95	1,462	22.61
		1.067	31.1	3.81	1,560	24.11
		1.068	31.1	3.98	1,574	24.31
		1.049	30.5	±3.14	1,390	21.50
		1.063	30.9	±3.14	1,425	22.02
		1.064	31.0	±3.14	1,406	21.72
		1.064	31.0	±3.15	1,436	22.20
		1.064	31.0	±3.15	1,346	20.80
Av.		1.063	31.0	3.53	1,456	22.51
0.0196	3/4	.801	38.8	2.96	608	15.44
		.798	38.7	2.91	631	16.02
		.798	38.7	2.90	590	14.98
		.798	38.7	2.96	602	15.29
		.799	38.8	2.89	603	15.31
		.798	38.7	±2.80	613	15.56
		.797	38.7	±2.80	582	14.78
		.795	38.6	±2.80	544	13.81
		.796	38.6	±2.80	484	12.30
		.797	38.7	±2.80	612	15.50
Av.		.798	38.7	2.86	587	14.90
0.0120	1/2	.537	42.7	1.91	478	19.85
		.535	42.6	1.94	461	19.15
		.537	42.7	1.89	444	18.45
		.540	43.0	2.00	480	19.95
		.525	41.8	1.99	344	14.28
		.530	42.1	±2.00	387	16.07
		.530	42.1	±2.00	460	19.15
		.530	42.1	±2.00	407	16.90
		.537	42.7	±2.00	462	19.20
Av.		.533	42.4	±1.97	436	18.11

Table 3.--Edgewise compressive strength of sandwich specimens having aluminum facings and granulated-cork cores (0.45 sp.gr.) (continued)

Thickness of material			Ratio c/f	Free height	Observed maximum compressive strength	
Face f	Nominal core c	Total h			Load	Stress in facing
(1)	(2)	(3)	(4)	(5)	(6)	(7)
Inch	Inch	Inch		Inch	Lb./inch of width	1,000 p.s.i.
0.0196	1	1.048	51.4	3.65	758	19.20
		1.048	51.4	3.61	728	18.45
		1.049	51.5	3.67	772	19.55
		1.050	51.6	3.60	855	21.65
		1.050	51.6	3.67	727	20.95
		1.050	51.6	[1]3.51	807	20.45
		1.050	51.6	[1]3.51	782	19.80
		1.050	51.6	[1]3.56	785	19.87
		1.050	51.6	[1]3.75	824	20.78
Av.		1.049	51.5	3.61	793	20.08
0.0120	3/4	.786	63.5	2.93	433	17.90
		.784	63.4	3.00	448	18.52
		.784	63.4	2.92	439	18.15
		.786	63.5	2.96	439	18.15
		.787	63.6	2.93	423	17.49
		.786	63.5	[1]2.87	423	17.49
		.786	63.5	[1]2.87	441	18.23
		.784	63.4	[1]2.87	409	16.90
		.786	63.5	[1]2.87	429	17.74
		.785	63.4	[1]2.87	412	17.03
Av.		.785	63.5	2.91	430	17.76
0.0120	1	1.032	84.0	4.00	582	23.95
		1.030	83.9	3.82	565	23.25
		1.029	83.9	3.84	588	24.20
		1.029	83.9	4.05	604	24.85
		1.027	83.6	3.94	589	24.22
		1.021	83.1	[1]3.99	550	22.61
		1.022	83.2	[1]3.99	522	21.48
		1.020	83.0	[1]3.99	472	19.42
		1.020	83.0	[1]3.99	465	19.14
		1.018	82.8	[1]3.99	489	20.11
Av.		1.025	83.4	3.96	543	22.32

[1] Free height is total height of specimen.

Table 4.--Edgewise compressive strength of sandwich specimens having steel facings and granulated-cork cores (0.66 sp. gr.)

Thickness of material			Ratio	Free	Observed maximum compressive strength	
Face	Nominal core	Total			Load	Stress in facing
f	c	h	c/f	height		
(1)	(2)	(3)	(4)	(5)	(6)	(7)
Inch	Inch	Inch		Inch	Lb./inch of width	1,000 p.s.i.
0.010	19/64	0.321	30.1	1.33	1,200	59.60
		.322	30.2	1.14	1,408	70.00
		.318	29.8	1.15	1,320	65.60
		.315	29.5	1.15	1,328	66.00
		.315	29.5	1.13	1,112	55.25
Av.		.318	29.8	1.18	1,274	63.29
0.010	25/64	.423	40.3	1.58	1,320	65.40
		.427	40.7	1.52	1,340	66.40
		.428	40.8	1.47	1,240	61.50
		.426	40.6	1.48	1,480	73.40
		.423	40.3	1.49	1,448	71.80
Av.		.425	40.5	1.51	1,366	67.70
0.010	1/2	.521	50.1	1.80	1,440	71.20
		.530	51.0	2.20	1,344	66.40
		.526	50.6	1.90	1,352	66.80
		.523	50.3	2.08	1,460	72.20
		.531	51.1	2.01	1,188	58.75
Av.		.526	50.6	2.00	1,357	67.07

Table 5.--Mechanical properties of core materials used to predict wrinkling stresses in the facings

Core material	Specific gravity	Compression: Modulus of elasticity: Flatwise E_y	Compression: Modulus of elasticity: Edgewise E_x	Shear: Modulus of rigidity μ_{xy}	Tension: Maximum stress t	Poisson's ratio σ_{xy}	Poisson's ratio σ_{xz}	Poisson's ratio σ_{zy}	Poisson's ratio σ_{yx}
		1,000 p.s.i.	1,000 p.s.i.	1,000 p.s.i.	P.s.i.				
Cork[1]	0.35	0.52	1.18	0.33	42	[2]0.136	0.10	.....	0.06
	.45	1.40	3.55	.98	51	[2].127	.11	.....	.05
	.66	4.89	13.70	3.40	87	[2].224	.21	.....	.08
Cellular cellulose acetate(flatwise)[1]	.10	17.28	4.58	3.99	180	.09	.21	0.39	.....
Cellular cellulose acetate(edgewise)	.10	23.59	5.44	4.47	180	.21	.09	.....	.....
Balsa wood (Eg) (edge grain)[2]	.12	536.00	8.01	15.00	880	.02	.50	.02	.40
Cellular cellulose acetate(flatwise)[2]	.10	40.70	12.98	3.50	201	.09	.21	.39	.....
Cellular hard rubber[2]	.10	27.50	6.95	3.90	240	.26	.40	.....	.19

[1]Average values obtained in this investigation.

[2]Values computed by $\sigma_{xy} = \frac{E_x \sigma_{yx}}{E_y}$.

[3]Average values obtained from tables in Forest Products Laboratory Report No. 1561.

Table 6.--Edgewise compressive strength of sandwich specimens having steel facings and cellular-cellulose-acetate cores (flatwise

Thickness of material			Ratio c/f	Free height	Observed maximum compressive strength	
Face f	Nominal core c	Total h			Load	Stress in facing
(1)	(2)	(3)	(4)	(5)	(6)	(7)
Inch	Inch	Inch		Inch	Lb./inch of width	1,000 p.s.i.
0.010	1/4	0.262	24.2	0.83	960	47.85
		.251	23.1	.94	1,217	60.75
		.273	25.3	.95	1,135	56.60
		.255	23.5	.89	960	47.85
Av.		.260	24.0	.90	1,068	53.26
0.010	3/8	.382	36.2	1.41	1,258	62.70
		.383	36.3	1.39	1,477	73.80
		.367	34.7	1.38	1,660	82.50
		.354	33.4	1.42	1,278	63.80
Av.		.372	35.2	1.40	1,418	70.70
0.010	1/2	.493	47.3	1.80	1,650	82.20
		.491	47.1	1.83	1,576	78.70
		.503	48.3	1.88	1,637	81.70
		.489	46.9	1.84	1,366	68.20
Av.		.494	47.4	1.89	1,557	77.70
0.010	5/8	.600	58.0	1.93	1,908	95.40
		.582	56.2	1.96	1,475	73.80
		.595	57.5	1.95	2,082	104.00
		.593	57.3	1.90	1,934	96.50
Av.		.592	57.2	1.94	1,850	92.43
0.010	3/4	.738	71.8	2.20	1,631	81.60
		.734	71.4	2.25	1,740	87.00
		.742	72.2	2.25	2,020	101.00
		.734	71.4	2.30	1,645	82.25
Av.		.737	71.7	2.25	1,759	87.96
0.010	7/8	.883	86.3	3.35	1,653	82.20
		.895	87.5	3.38	1,616	80.50
		.883	86.3	3.35	1,814	90.20
		.847	82.7	3.36	1,545	76.70
Av.		.877	85.7	3.36	1,657	82.40
0.010	1	.946	92.6	3.90	1,456	72.30
		.961	94.1	3.85	1,430	71.00
		.965	94.5	3.88	1,550	77.00
		.932	91.2	3.70	1,500	74.30
Av.		.951	93.1	3.83	1,484	73.65

Table 7.--Edgewise compressive strength of sandwich specimens having steel facings and cellular-cellulose-acetate cores (edgewise)

Thickness of material			Ratio	Free	Observed maximum compressive strength	
Face	Nominal core	Total			Load	Stress in facing
f	c	h	c/f	height		
(1)	(2)	(3)	(4)	(5)	(6)	(7)
Inch	Inch	Inch		Inch	Lb./inch of width	1,000 p.s.i.
0.010	1/2	0.514	49.4	1.93	1,693	84.20
		.522	50.2	1.97	1,888	94.00
		.515	49.5	2.05	1,534	76.30
Av.		.517	49.7	1.98	1,705	84.83
0.010	5/8	.658	63.8	2.50	1,832	91.20
		.651	63.1	2.49	1,880	93.40
		.655	63.5	2.51	1,712	85.10
		.657	63.7	2.55	1,825	90.70
Av.		.655	63.5	2.51	1,812	90.10
0.010	3/4	.781	76.1	2.97	1,874	93.00
		.773	75.3	3.10	1,897	94.20
		.768	74.8	2.99	1,840	91.30
		.768	74.8	2.90	1,848	91.80
Av.		.772	75.2	2.99	1,865	92.57
0.010	7/8	.896	87.6	3.55	1,664	82.50
		.888	86.8	3.50	1,874	93.00
		.892	87.2	3.38	1,754	87.00
		.900	88.0	3.49	1,680	83.30
Av.		.894	87.4	3.48	1,743	86.45
0.010	1	1.005	98.5	4.05	1,638	81.10
		1.009	98.9	4.07	1,680	83.20
		1.008	98.8	4.02	1,628	80.60
		1.013	99.3	3.93	1,680	83.20
Av.		1.009	98.9	4.02	1,656	82.02

Table 8.--Recapitulation of edgewise compressive strength of sandwich specimens having aluminum facings as reported in Forest Products Laboratory Report No. 1561

Core material	Nominal thickness: Face f	Nominal thickness: Core c	Total thickness h	Ratio c/f	Observed maximum compressive strength: Load	Observed maximum compressive strength: Stress in facing
(1)	(2)	(3)	(4)	(5)	(6)	(7)
	Inch	Inch	Inch		Lb./inch of width	1,000 p.s.i.
Balsa (end grain)	0.0050	1/4	0.255	49.0	362	34.60
		1/2	.506	99.2	402	37.20
		3/4	.769	151.8	282	25.73
		1	1.019	201.8	270	22.94
	.0125	1/4	.282	20.5	1,173	46.15
		1/2	.527	40.1	1,168	45.40
		5/8	.645	49.6	919	35.95
		3/4	.778	60.2	1,081	41.75
		1	1.030	80.2	1,059	40.45
		1-1/4	1.271	99.6	839	31.45
		1-7/8	1.869	147.5	594	22.65
		2-1/2	2.470	195.5	478	17.76
	.0185	1/4	.297	14.0	2,166	58.00
		1/2	.544	27.4	2,197	58.00
		3/4	.788	40.5	1,914	51.80
		1	1.035	53.9	1,641	42.90
	.0200	7/16	.448	20.4	2,803	70.00
		1/2	.567	26.4	2,578	64.40
	.032	1/4	.325	8.9	3,178	49.62
		1/2	.468	13.3	3,192	49.68
		3/4	.821	24.3	3,856	59.98
		1	1.068	32.1	4,184	64.55
Cellular cellulose acetate	.0050	1/4	.249	47.8	213	20.45
		1/2	.501	98.1	244	22.40
		3/4	.726	147.5	294	26.25
		1	.980	194.0	284	23.92
	.0125	1/4	.278	20.2	1,111	45.30
		1/2	.514	39.1	1,095	42.25
		5/8	.568	43.5	689	27.70
		3/4	.780	60.5	972	37.20
		1	1.019	79.5	1,107	42.10
		1-1/4	1.209	94.9	1,043	42.00
		1-7/8	1.844	145.5	848	34.10
		2-1/2	2.455	194.5	957	38.50

Table 8.--Recapitulation of edgewise compressive strength of sandwich specimens having aluminum facings as reported in Forest Products Laboratory Report No. 1561 (continued)

Core material	Nominal thickness		Total thickness	Ratio c/f	Observed maximum compressive strength	
	Face f	Core c	h		Load	Stress in facing
(1)	(2)	(3)	(4)	(5)	(6)	(7)
	Inch	Inch	Inch		Lb./inch of width	1,000 p.s.i.
Cellular cellulose acetate (cont.)	0.0185	1/4	0.280	13.2	1,565	41.95
		1/2	.547	27.6	1,454	38.21
		3/4	.782	40.3	1,446	37.41
		1	1.030	53.6	1,874	48.60
	.0320	1/4	.311	7.7	2,281	35.50
		1/2	.557	15.4	2,244	34.80
		3/4	.887	25.7	2,054	31.70
		1	1.043	30.6	2,505	38.30
Cellular hard rubber	.0050	1/4	.267	51.4	278	26.60
		1/2	.502	98.5	329	31.40
		3/4	.771	152.1	380	35.44
		1	1.019	201.8	459	41.55
	.0125	1/4	.297	21.6	1,013	40.00
		1/2	.537	41.0	1,175	45.85
		5/8	.664	51.1	457	17.90
		3/4	.790	61.2	994	38.60
		1	1.046	81.8	990	33.70
		1-1/4	1.277	100.1	727	27.90
		1-7/8	1.926	152.0	890	34.20
		2-1/2	2.548	202.0	819	30.15
	.0185	1/4	.308	14.6	1,213	32.50
		1/2	.542	27.3	1,549	41.15
		3/4	.800	41.2	1,440	38.30
		1	1.045	54.5	1,473	39.00
	.0320	1/4	.325	7.9	2,156	33.60
		1/2	.580	16.1	2,096	32.60
		3/4	.826	23.8	1,783	27.60
		1	1.081	31.8	1,866	28.80

Table 9.--Edgewise compressive strength of sandwich specimens having facings of glass-cloth laminate and cores of balsa wood (end grain)[1]

Facing thickness	Core thickness	Stress in facings of sandwich at failure	Compressive strength of facing material
Inch	Inch	P.s.i.	P.s.i.
0.016 (four-ply)	1/4	17,170	19,840
	1/2	16,000	
	3/4	17,360	
	1	16,290	
0.032 (eight-ply)	1/4	18,240	20,800
	1/2	19,600	
	3/4	21,000	
	1	20,980	
0.044 (sixteen-ply)	1/4	21,930	22,250
	1/2	20,650	
	3/4	22,560	
	1	23,180	

[1] The table is an abstract from tables 3 and 6 of Forest Products Laboratory Report No. 1561.

Table 10.--Edgewise compressive strength of sandwich specimens having papreg facings on balsa-wood cores with grain direction of balsa in the direction of the applied stress

Facing thickness[1]	Core thickness[1]	Computed load supported by:		Total computed load	Test load[1]	Difference
		Facings	Cores			
Inch	Inch	Lb./inch of edge	Lb./inch of edge	Lb./inch of edge	Lb./inch of edge	Lb./inch of edge
0.009	0.890	140	2,320	2,460	3,030	570
.027	.636	422	1,652	2,074	2,428	354
.042	.366	655	951	1,606	2,050	444

[1] The dimensions and test results are taken from table 4 of Forest Products Laboratory Report No. 1561.

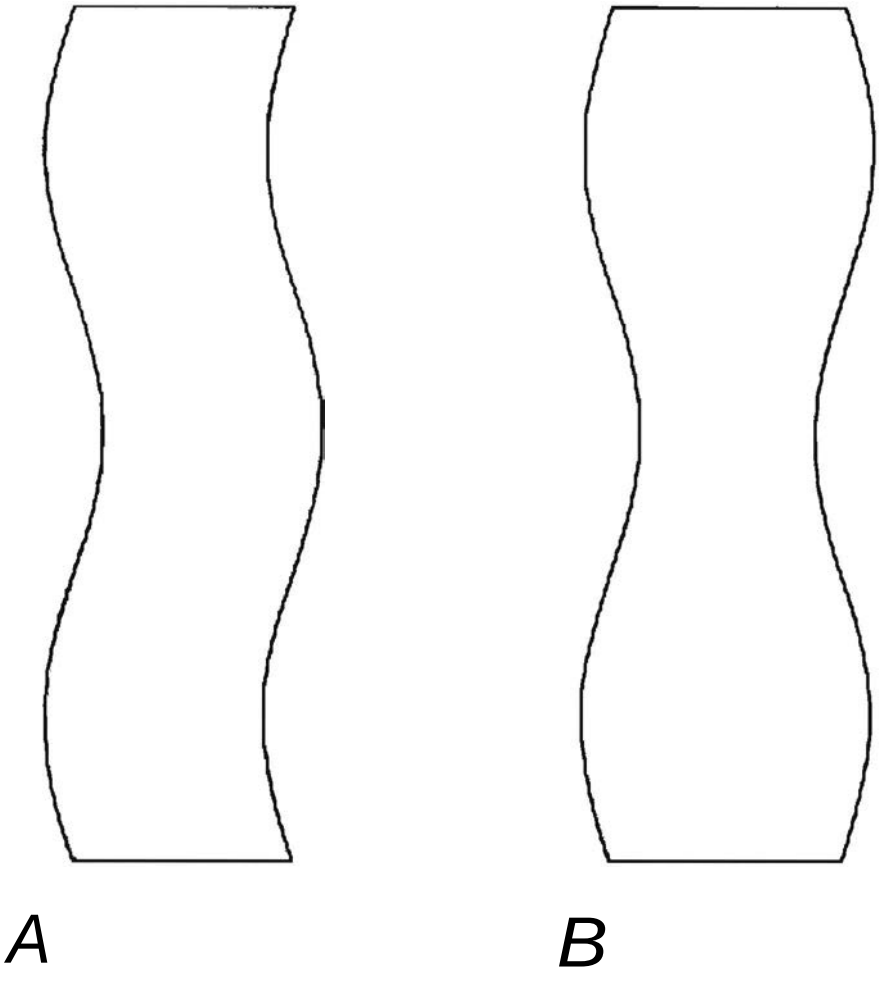

Figure 1.--Types of wrinkling instability; A, antisymmetrical; B, symmetrical.

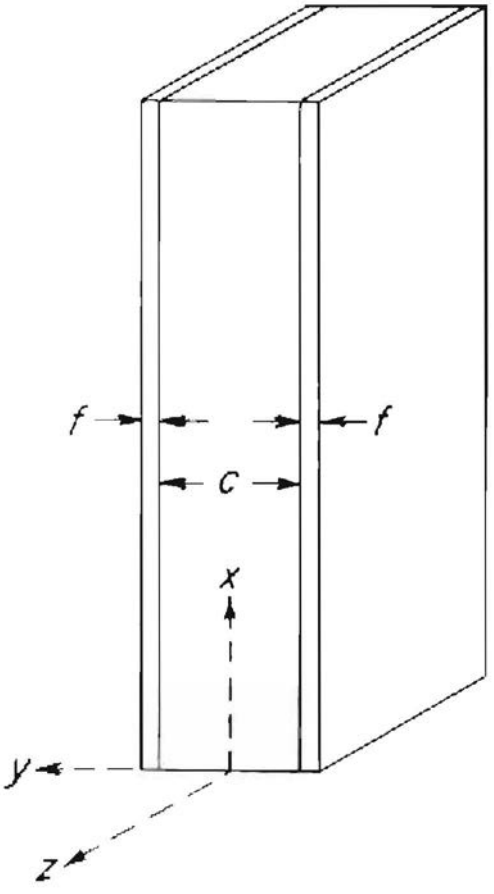

Figure 2.--Section of sandwich column showing orientation of axes.

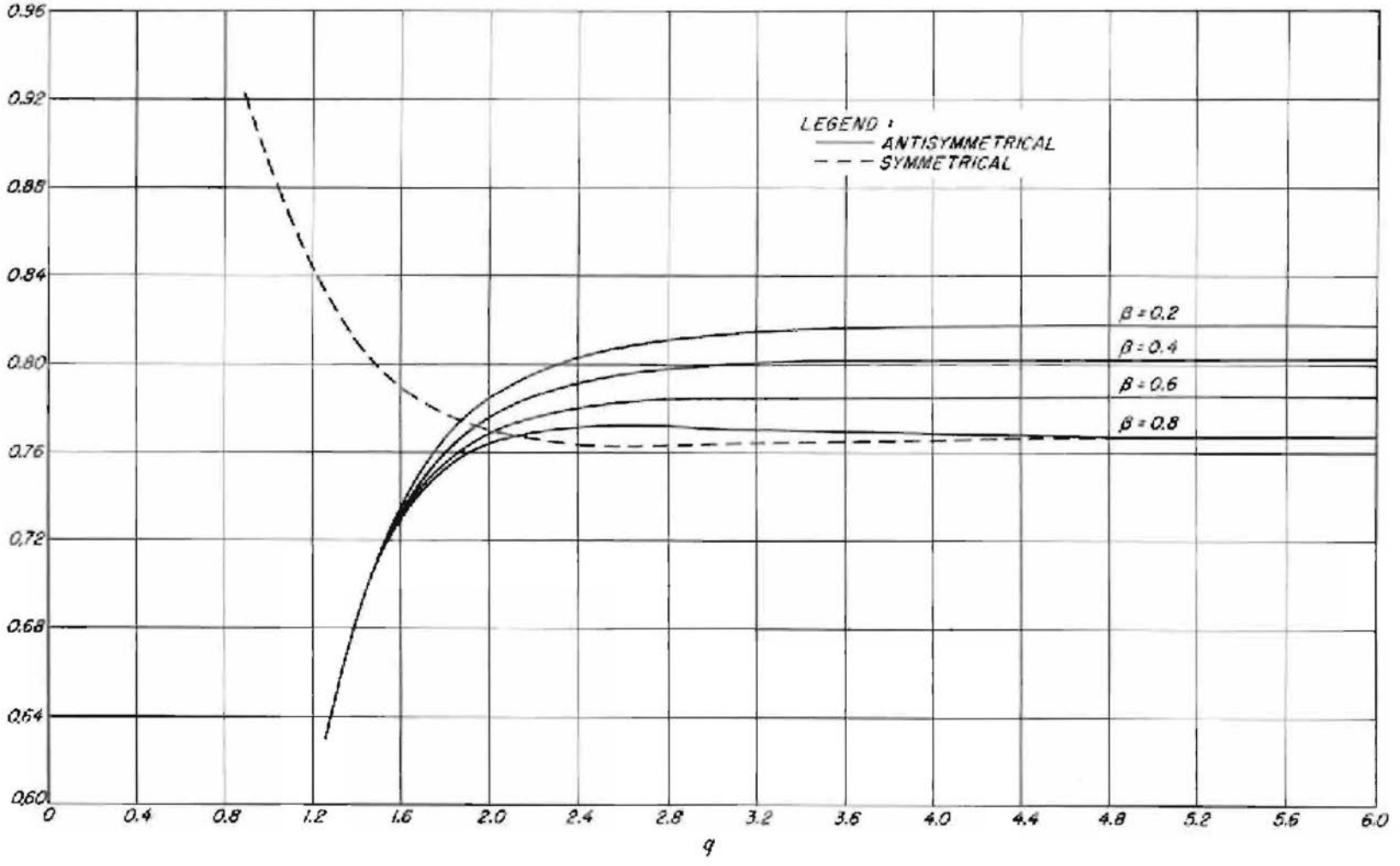

Figure 3.--Q_f vs. q for symmetrical and antisymmetrical wrinkling with $\alpha = 0$; $\beta = 0.2$, 0.4, 0.6, and 0.8.

Z M81736F

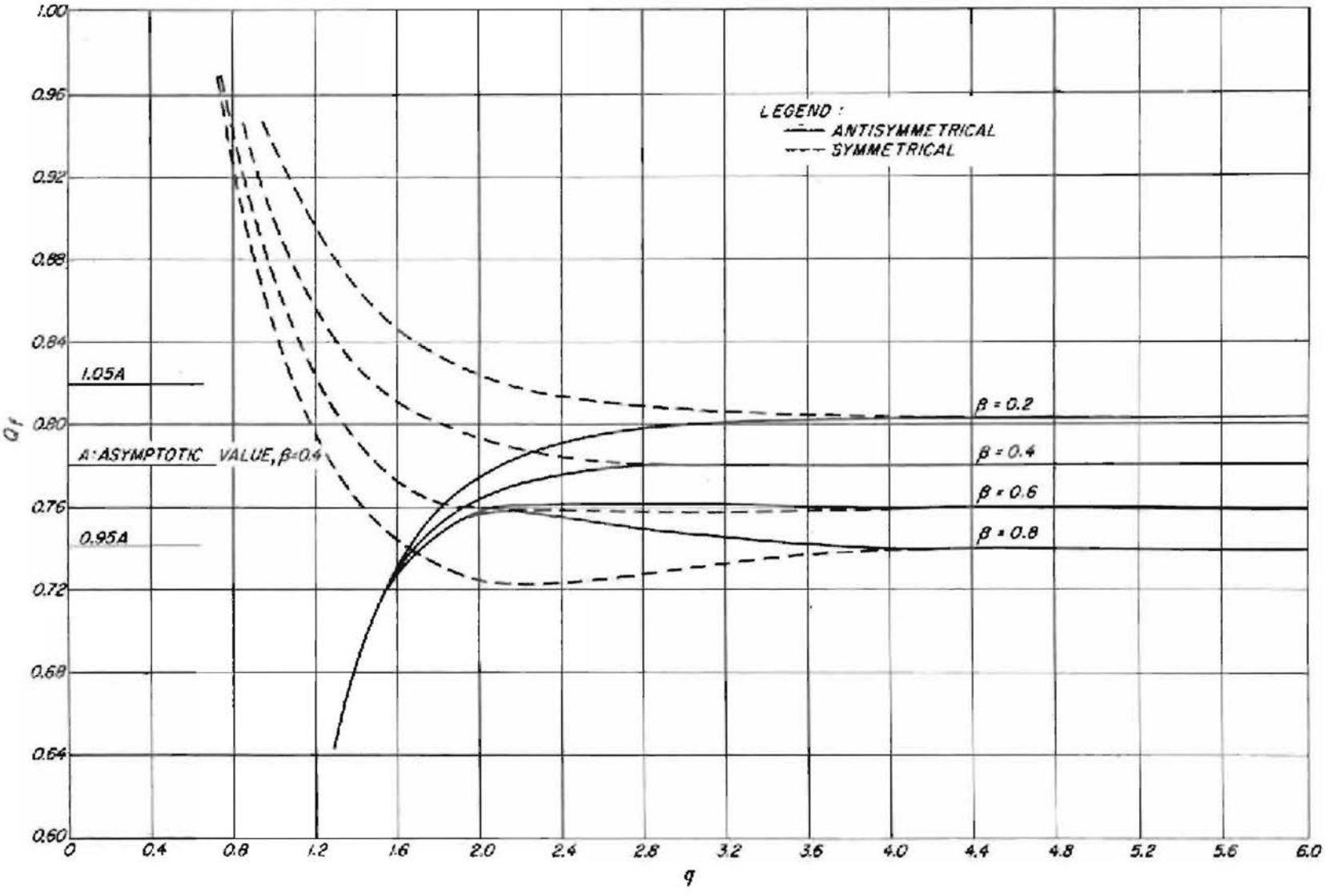

Figure 4.--Q_f vs. q for symmetrical and antisymmetrical wrinkling with $\sigma = 0.25$; $\beta = 0.2$, 0.4, 0.6, and 0.8.

z MS1460F

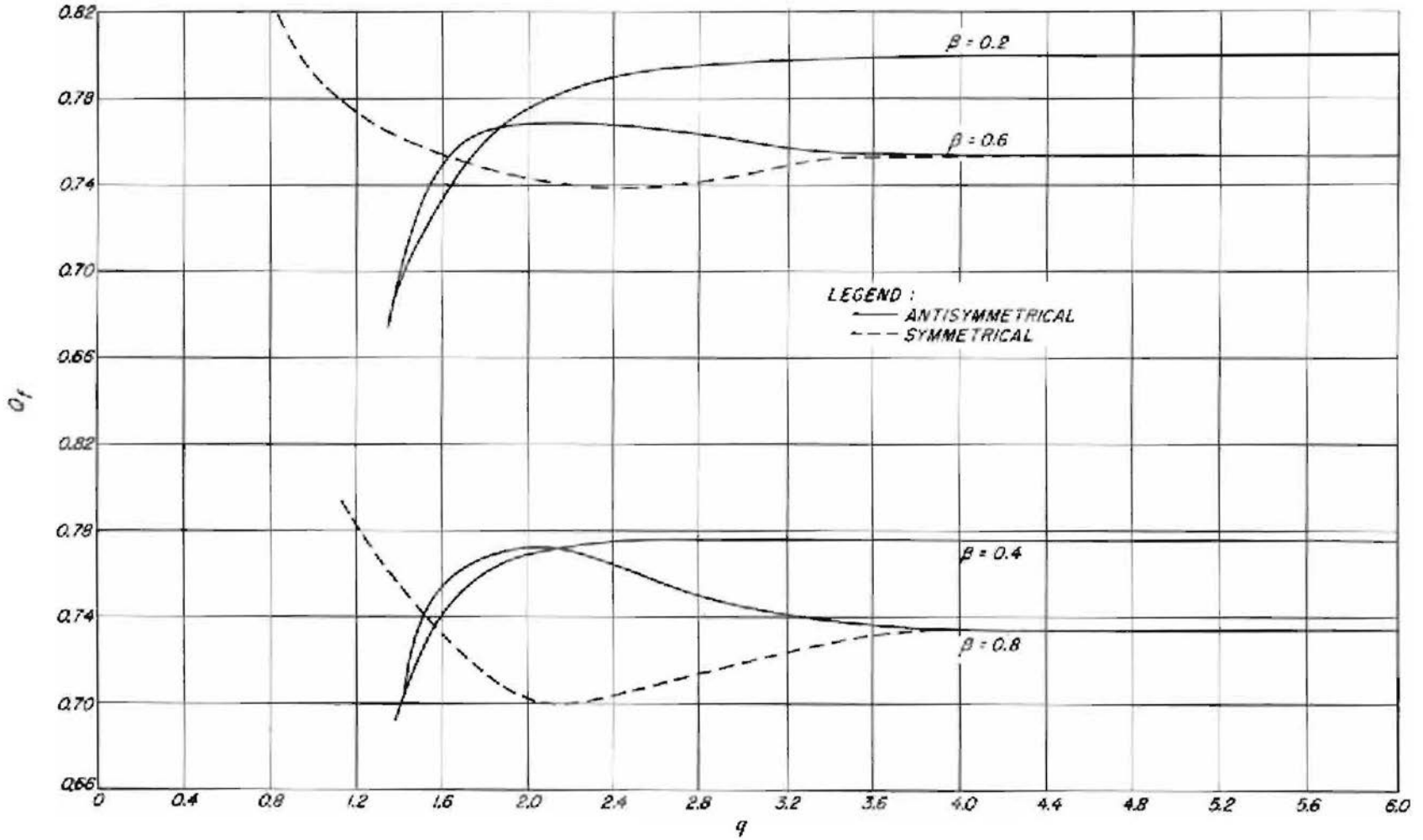

Figure 5.--Q_f vs. q for symmetrical and antisymmetrical wrinkling with $\nu = 0.5$; $\beta = 0.2$, 0.4, 0.6, and 0.8.

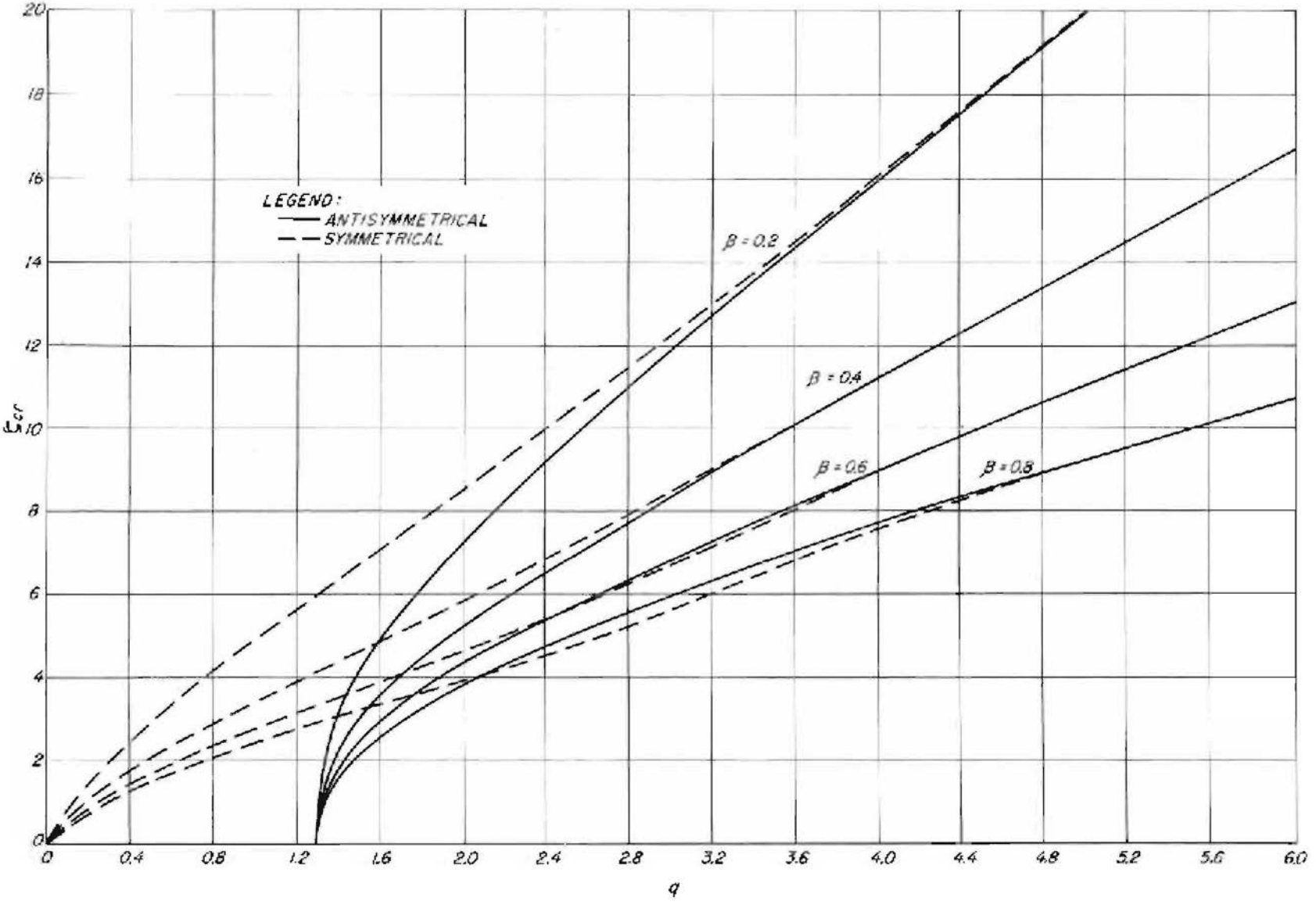

Figure 6.--Critical values of ξ vs. q for symmetrical and antisymmetrical wrinkling with $\sigma = 0.25$; $\beta = 0.2$, 0.4, 0.6, and 0.8.

Z M 82083 F

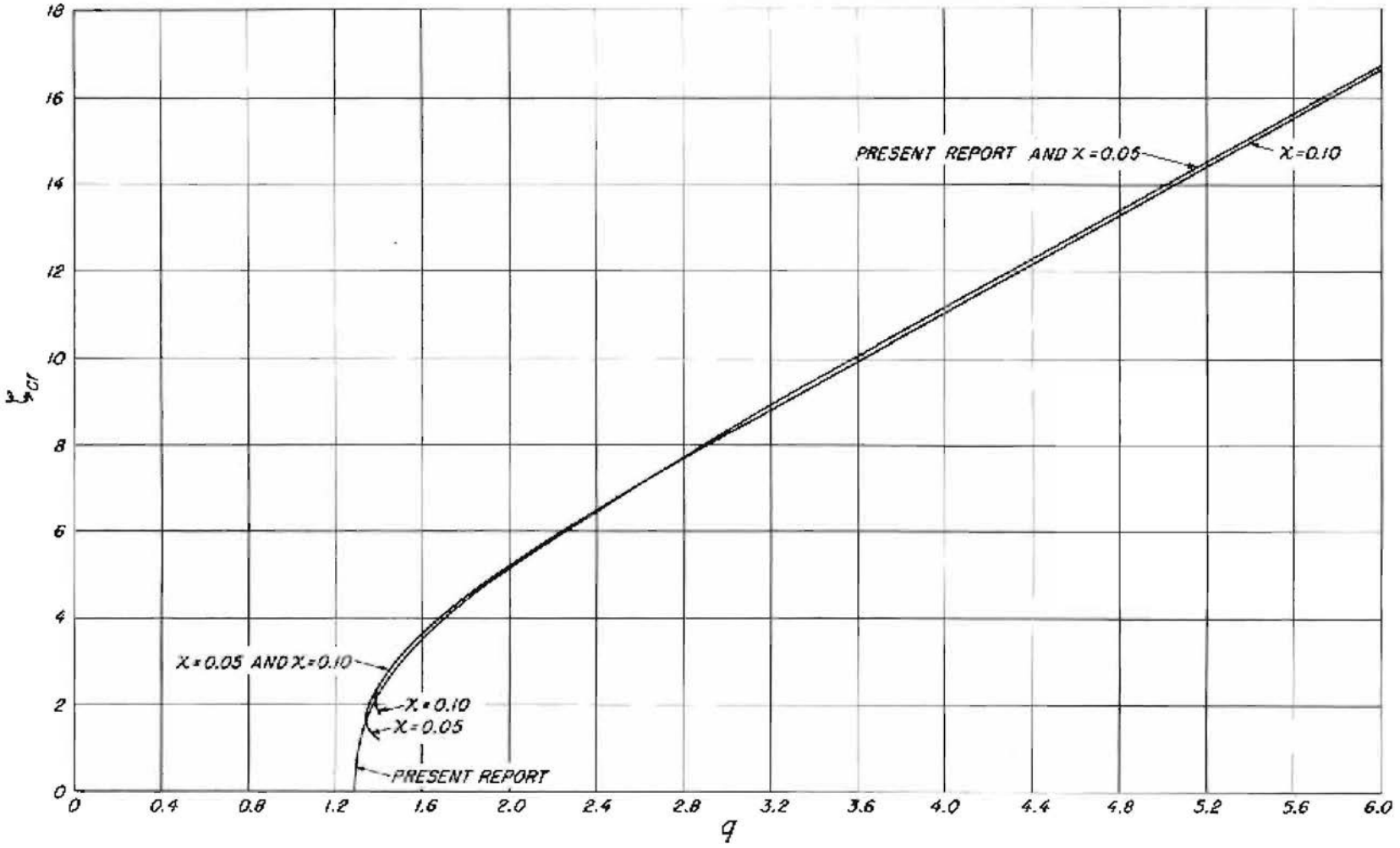

Figure 8.--Comparison of values of ζ_{cr} as obtained by the Cox formula with those obtained by the formula of the present report for antisymmetrical wrinkling with $\nu = 0.25$, $\beta = 0.1$. When ζ is shown as a two-valued function of q, the smaller value corresponds to a relative maximum.

Z M81741F

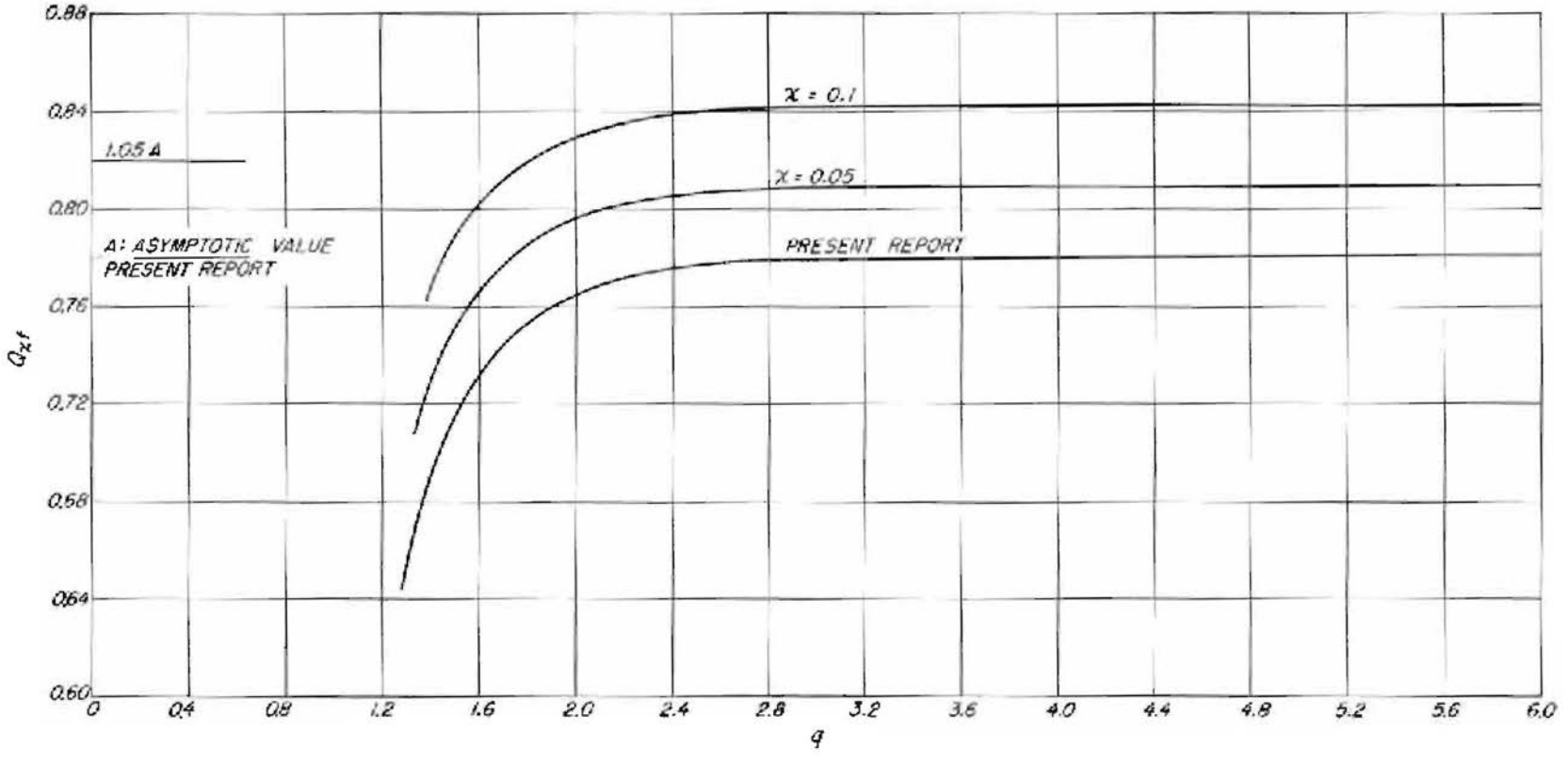

Figure 7.--Comparison of critical values of $Q_{\chi f}$ from the Cox formula with those from the present report for antisymmetrical wrinkling with $\sigma = 0.25$, $\beta = 0.4$.

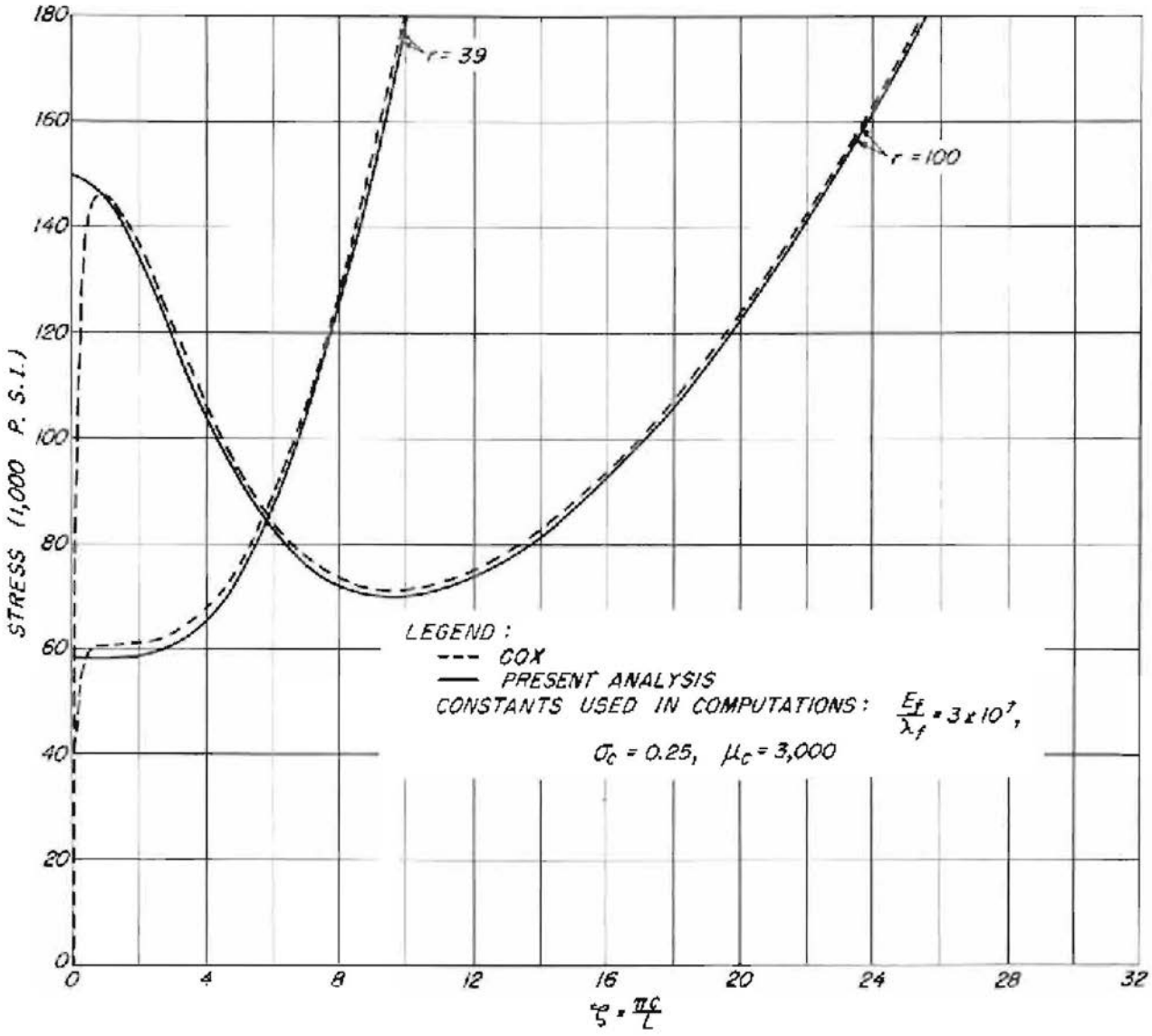

Figure 9.--Comparison of graphs of stress in facings vs. ζ obtained by the Cox formula with those obtained by the formula of the present report. Isotropic facings and core.

Z 881742F

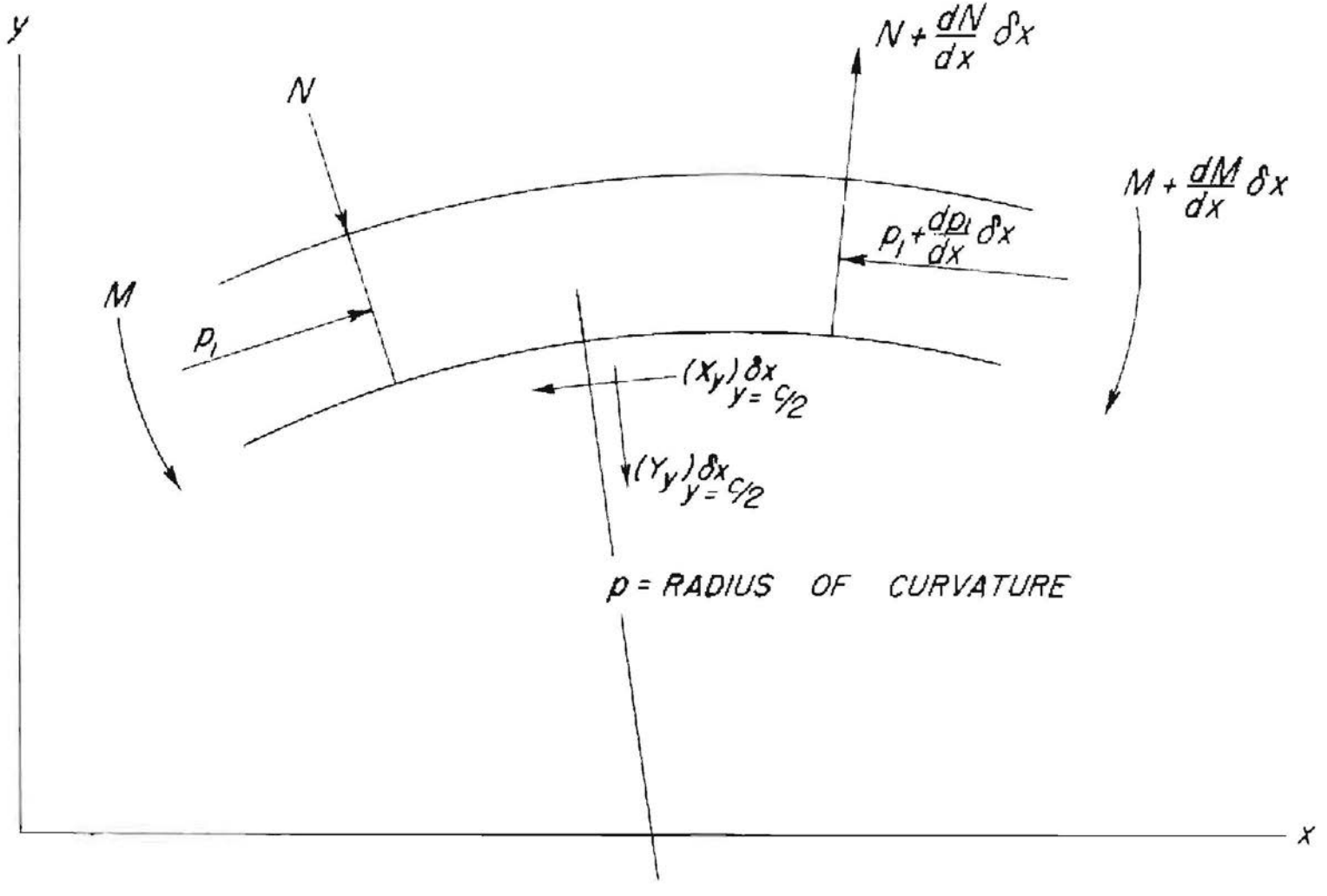

Z M 62064 F Figure 10.--Forces and moments acting upon an element of a face.

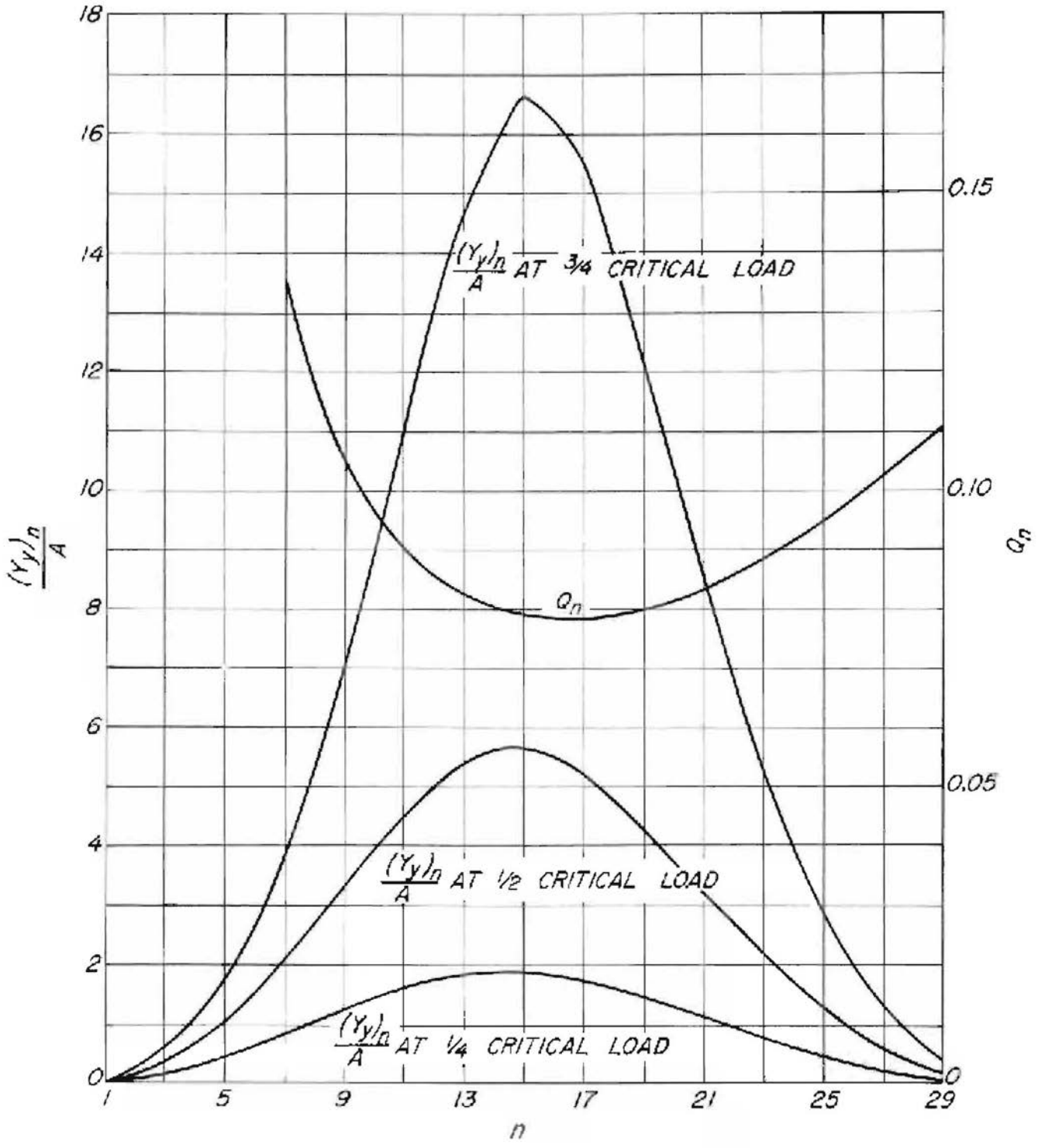

Figure 11.--Values of $\frac{(Y_y)_n}{A}$ and Q_n for various values of n for initial irregularity given by equation 1.13.1.

Z M 82086 F

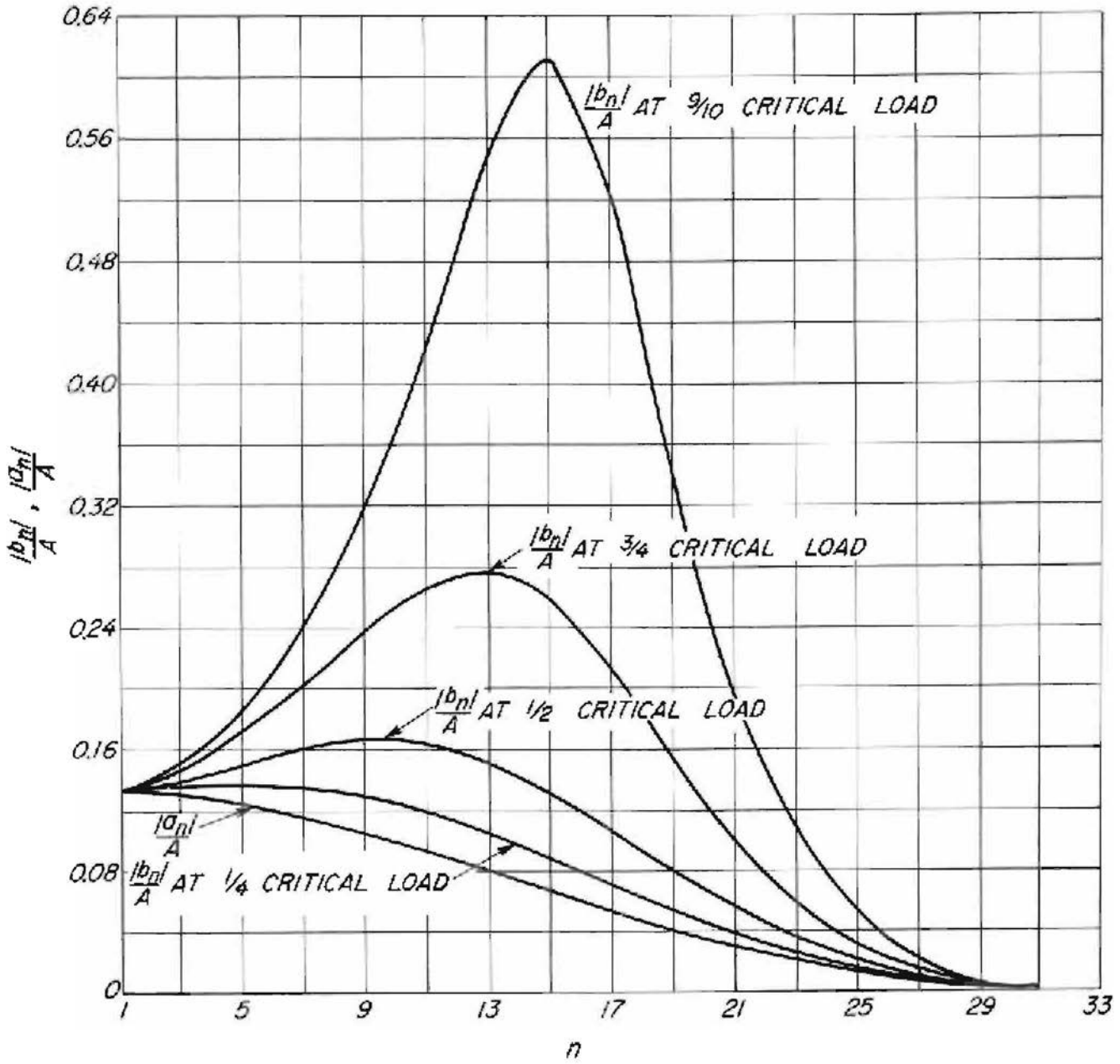

Figure 12.--Values of $\frac{|a_n|}{A}$, $\frac{|b_n|}{A}$ for various values of n for initial irregularity given by equation 1.13.4.

z M 82086 F

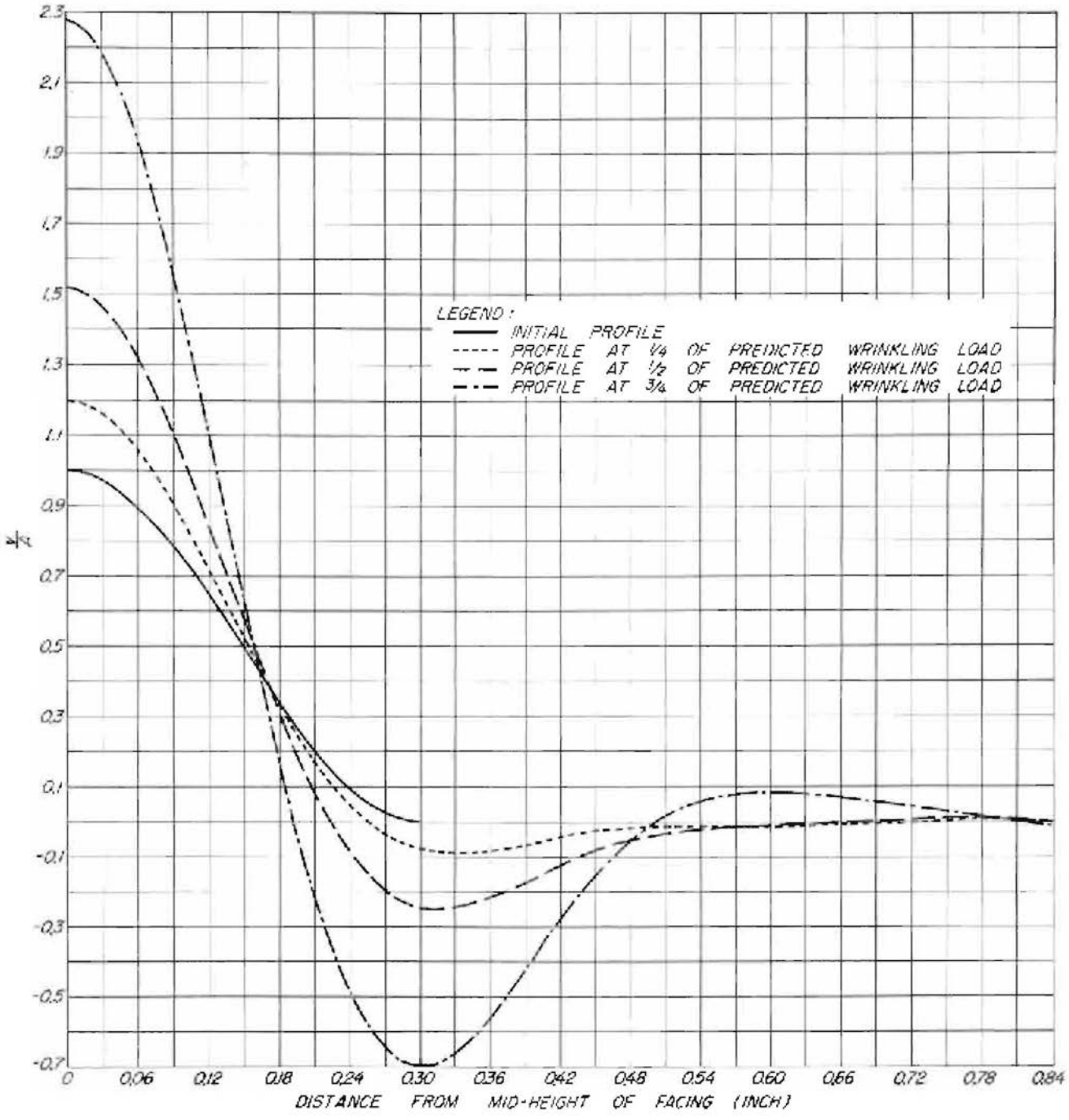

Figure 13.--Profiles at various fractions of the predicted wrinkling load. Initial profile given by equation 1.13.4 with $e = 0.3$ inch, $l = 4.5$ inch.

M 62067 F

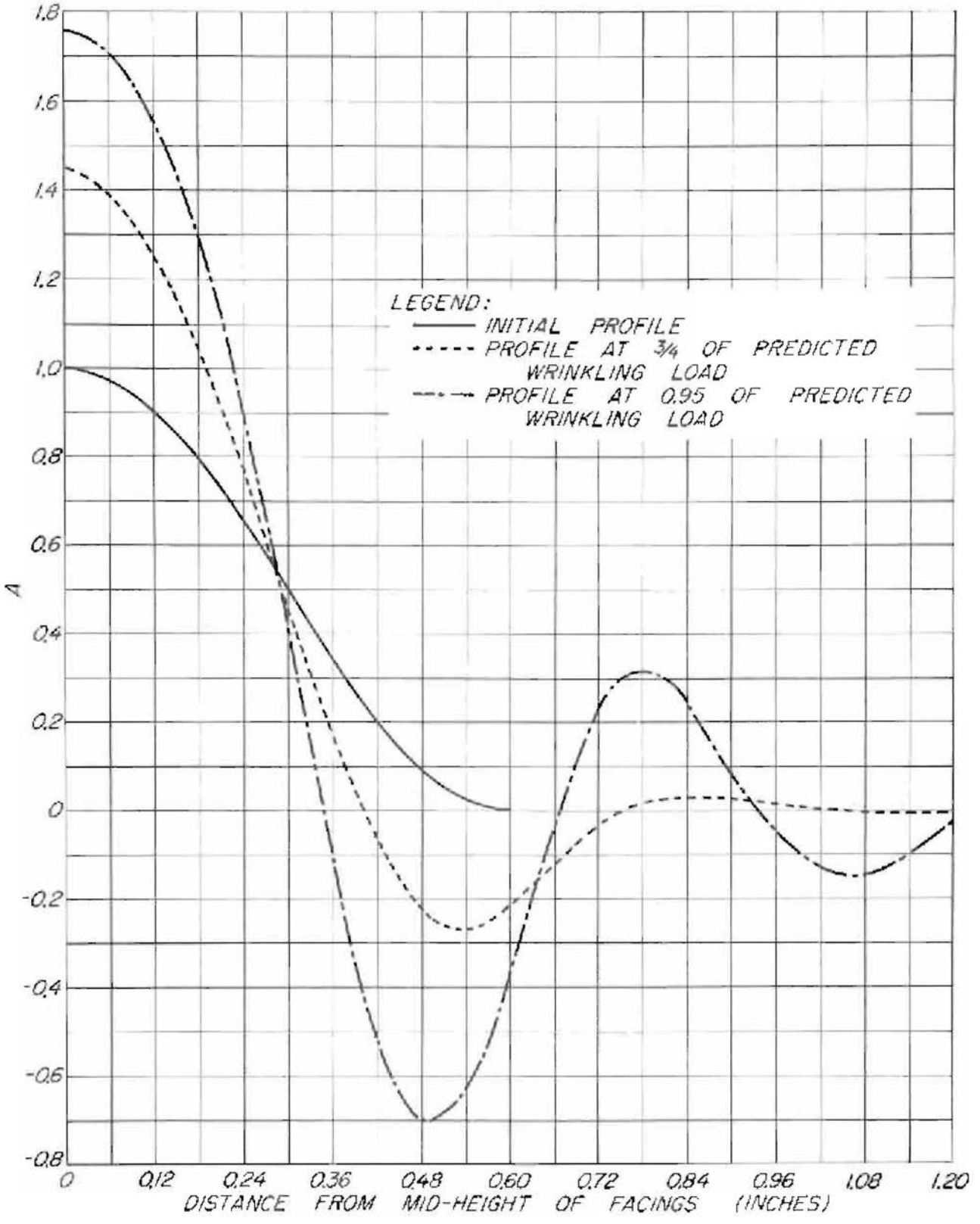

Figure 14.--Profiles at various fractions of the predicted critical load. Initial profile given by equation 1.13.4 with e 0.6, l 4.5 inch.

2 N 82068 F

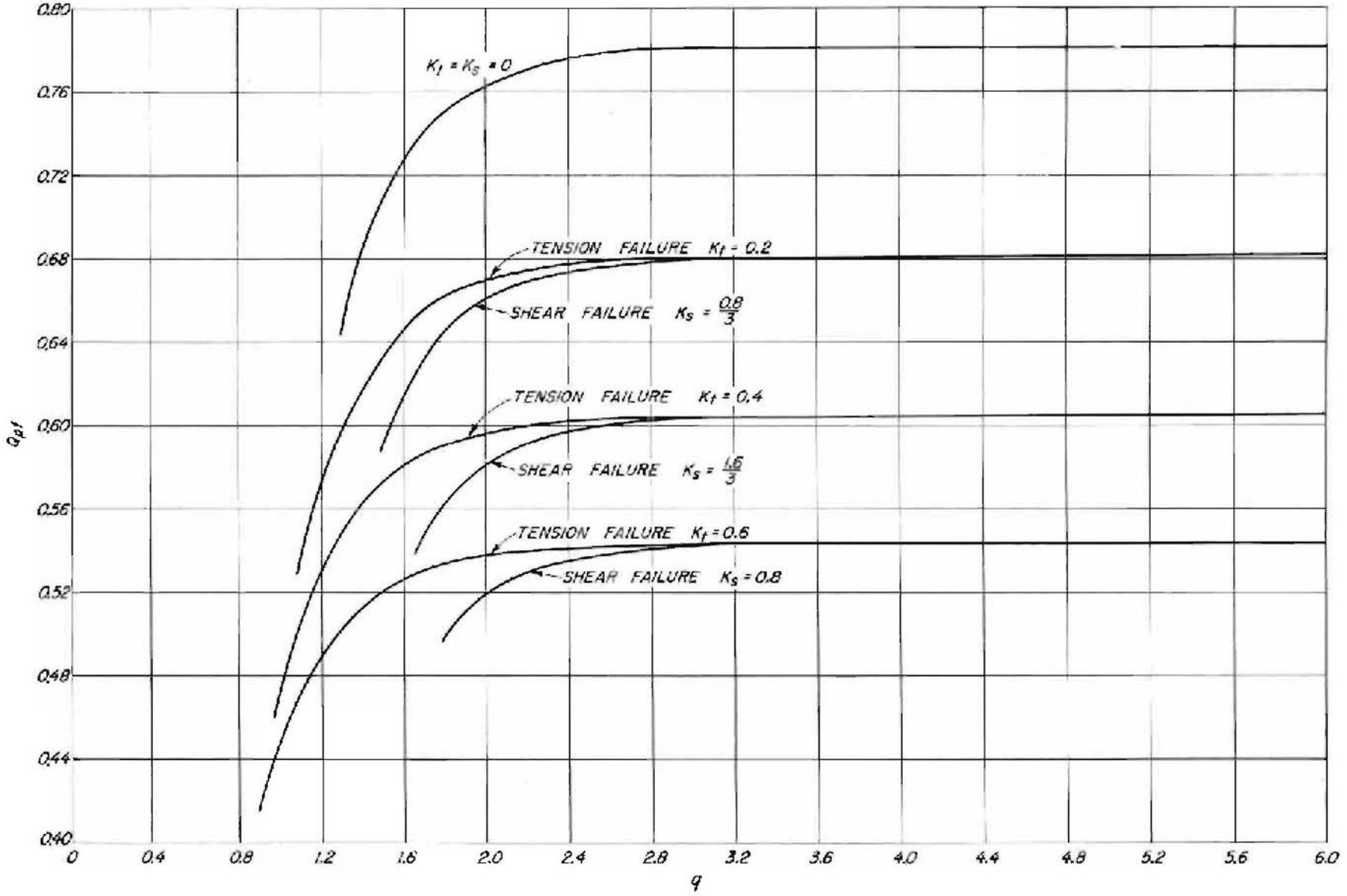

Figure 15.--Q_{pf} vs. q for tension and shear failure in antisymmetrical wrinkling. Initial amplitude proportional to wave length $\tau = 0.25$, $\beta = 0.4$.

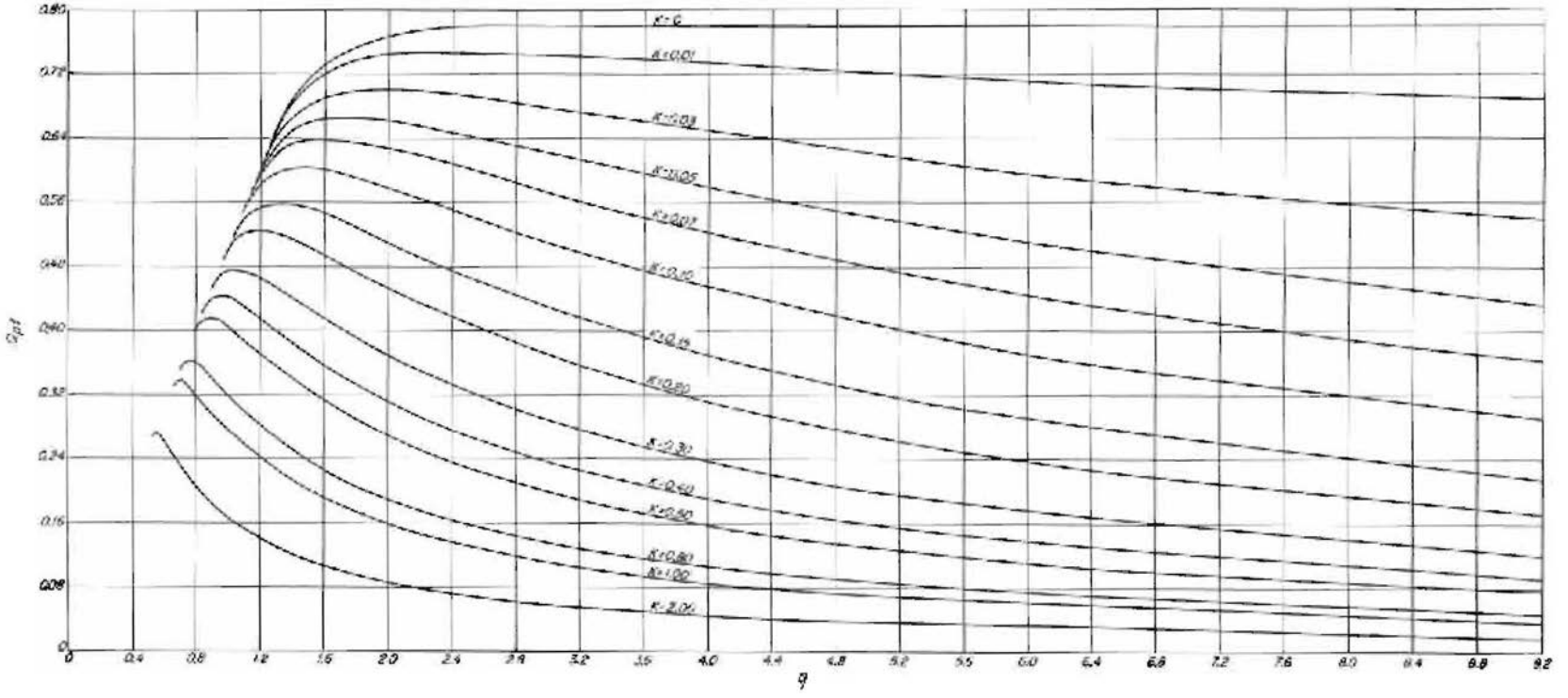

Figure 16.--Plots of Q_{pf} vs. q for various values of K. Initial amplitude proportional to core thickness. $\sigma = 0.25$, $\beta = 0.4$.

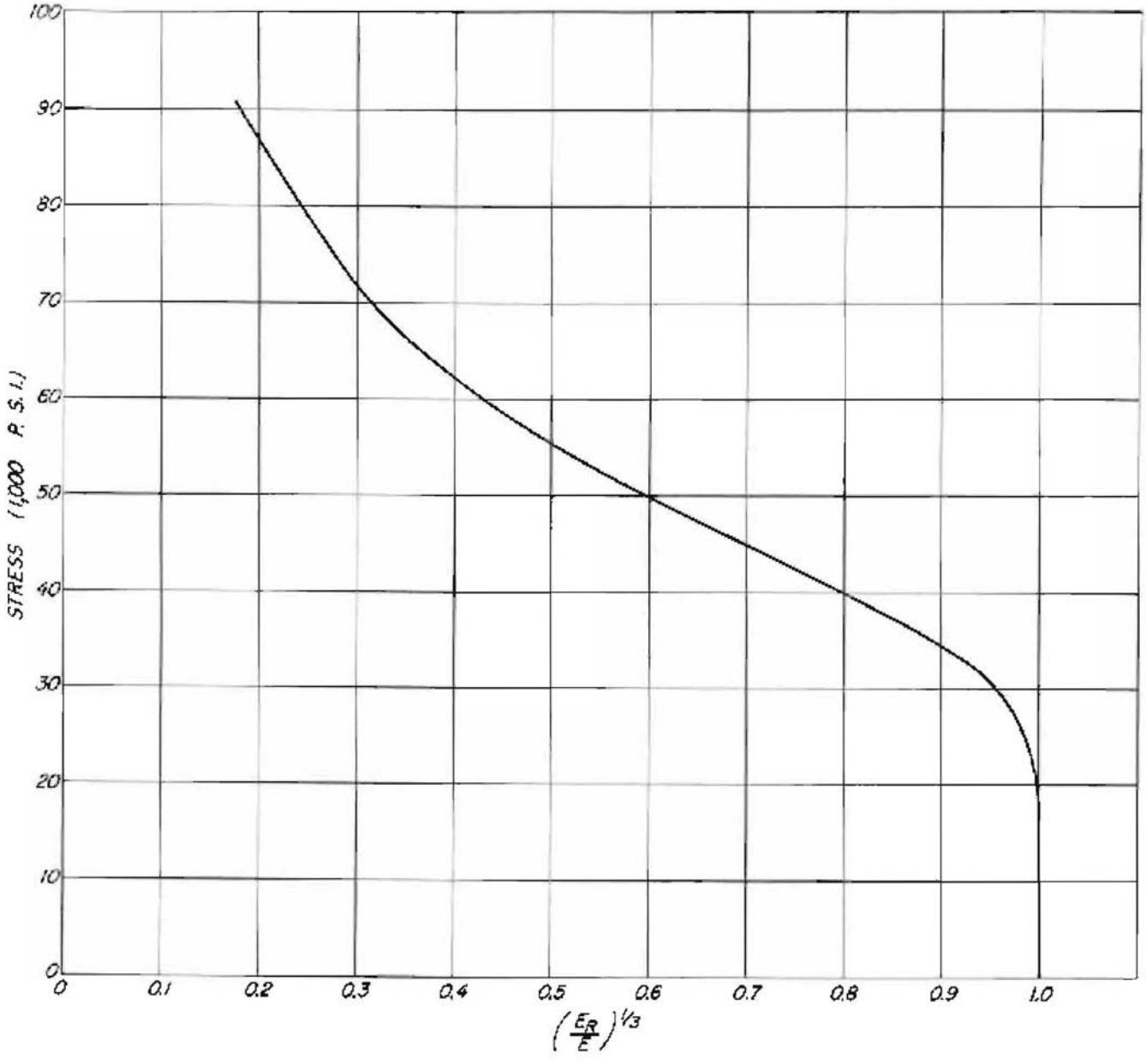

Figure 17.--Reduced modulus-stress curve of 24ST clad aluminum alloy, where

$$\frac{E_r}{E} = \frac{1}{\left(1 + \sqrt{\frac{E}{E_t}}\right)^2}, \text{ and } \left(\frac{S_r}{E}\right)^{2/3} = \left[\frac{1}{\left(2 + \sqrt{2 + \frac{2}{7} \times 7.78\left(\frac{S_r}{S_t}\right)^{5.78}}\right)^2}\right]^{1/3}$$

where S_t = 42,250 pounds per square inch.

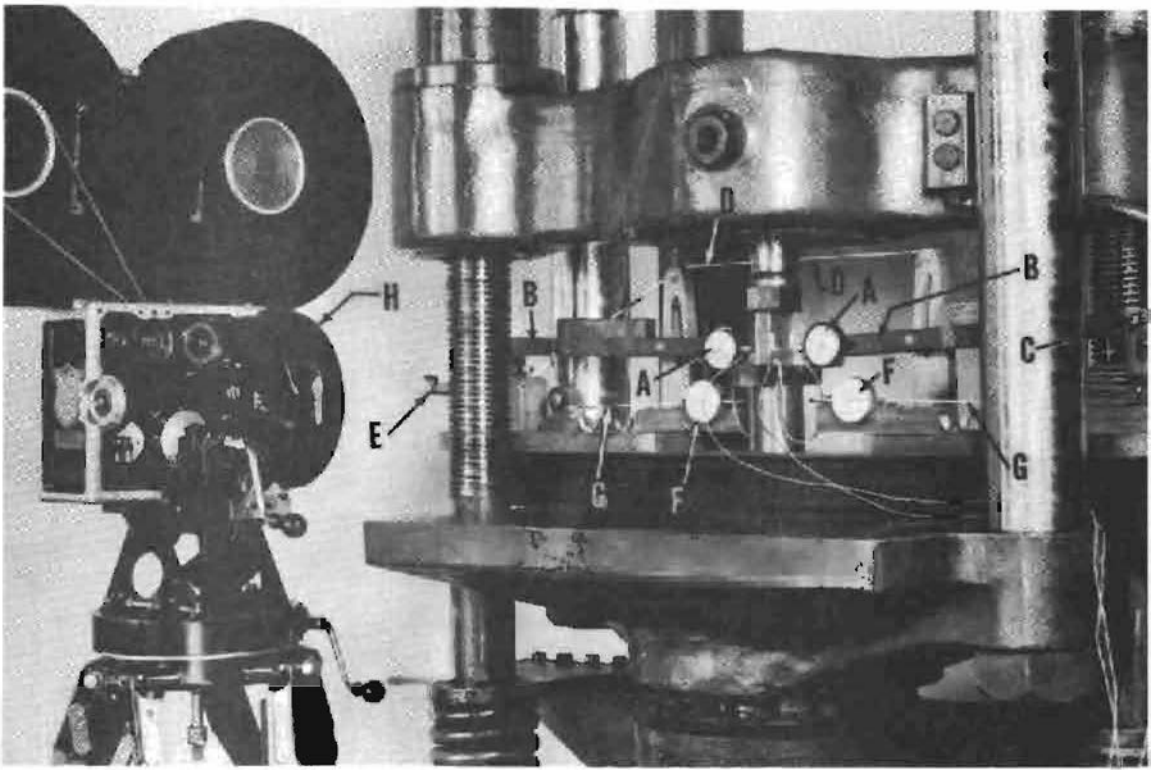

Figure 18.--Apparatus for measuring and film-recording the profile of the surface of the sandwich specimens.

Z M 82085 F

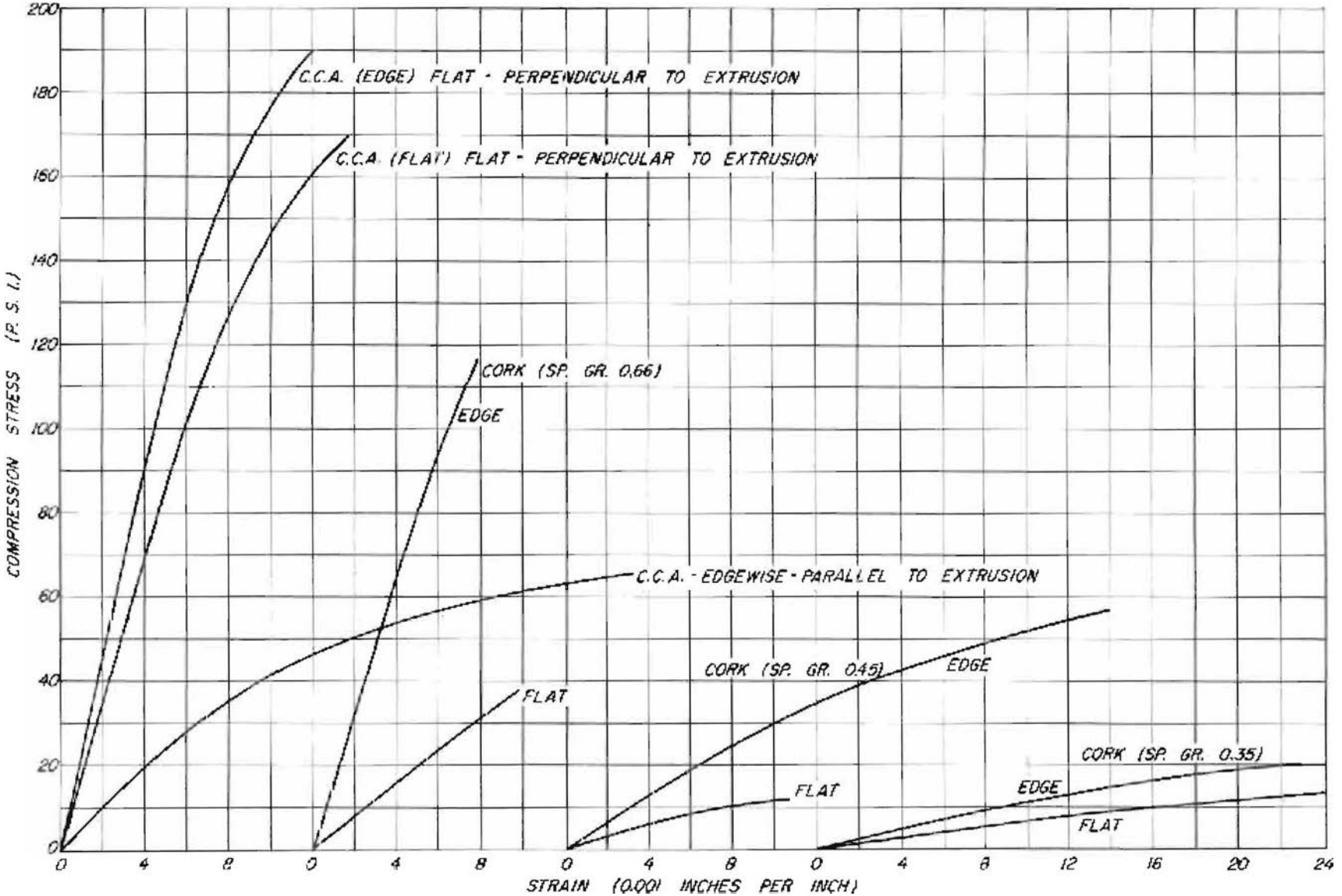

Figure 19.--Typical stress-strain curves of cellular cellulose acetate and composition cork cores in compression.

2 X A2071 F

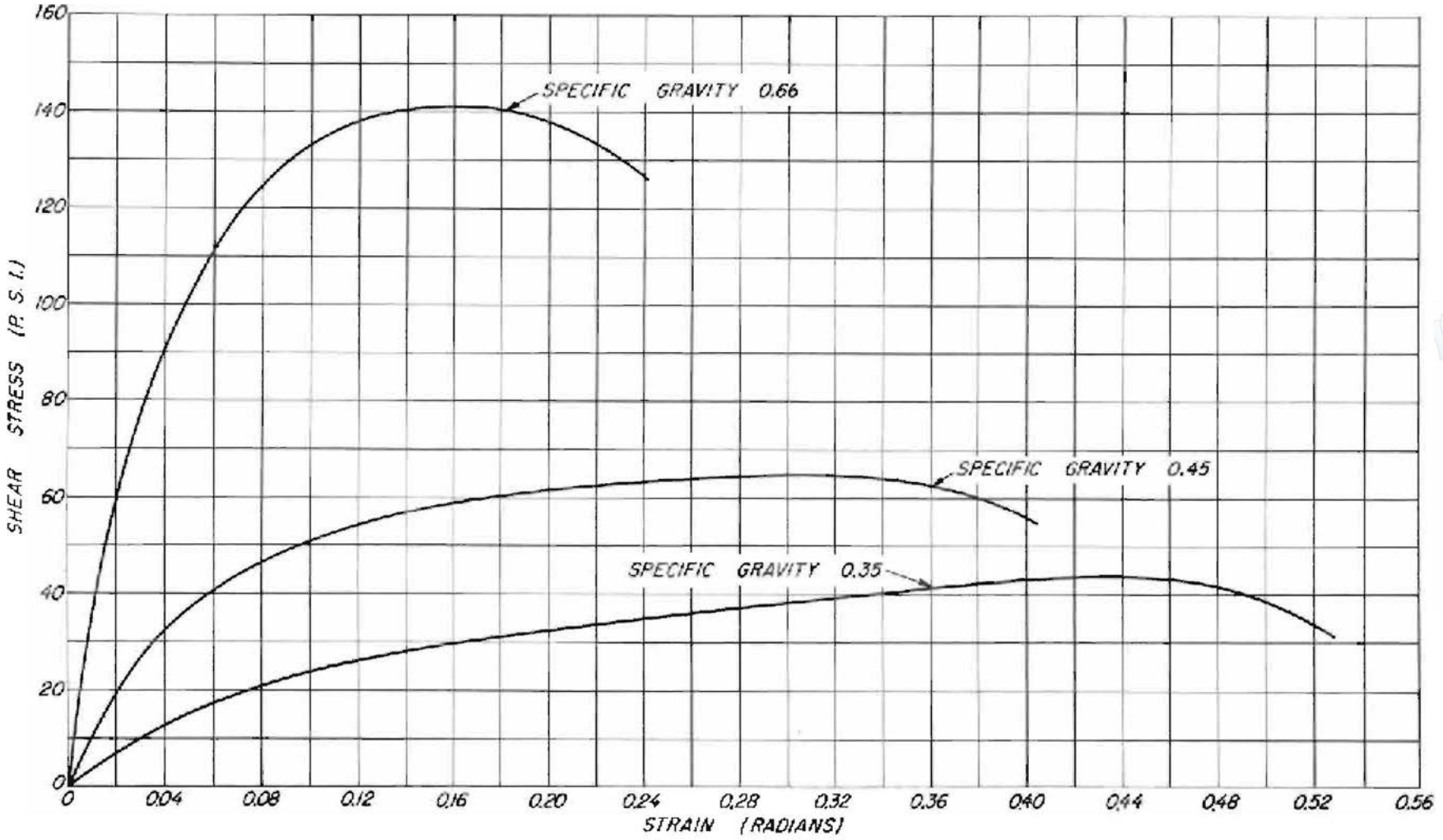

Figure 20.--Typical stress-strain curves of cork cores in shear.

ZN 82072 F

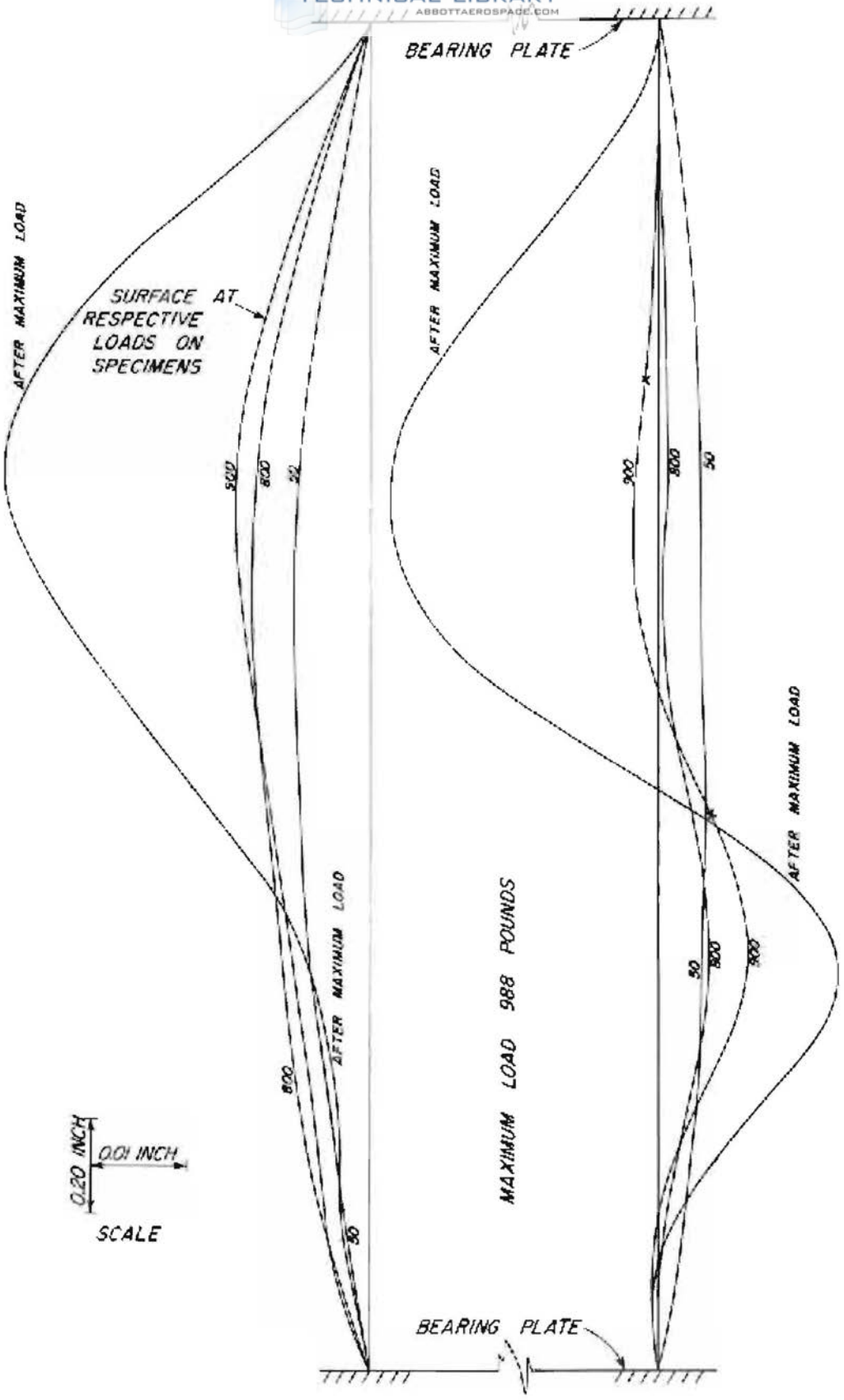

Figure 21.--Profiles of sandwich construction with 0.0196-inch 248F clad aluminum-alloy facings and 3/4-inch cork core (sp. gr. 0.45) shown in figure 25.

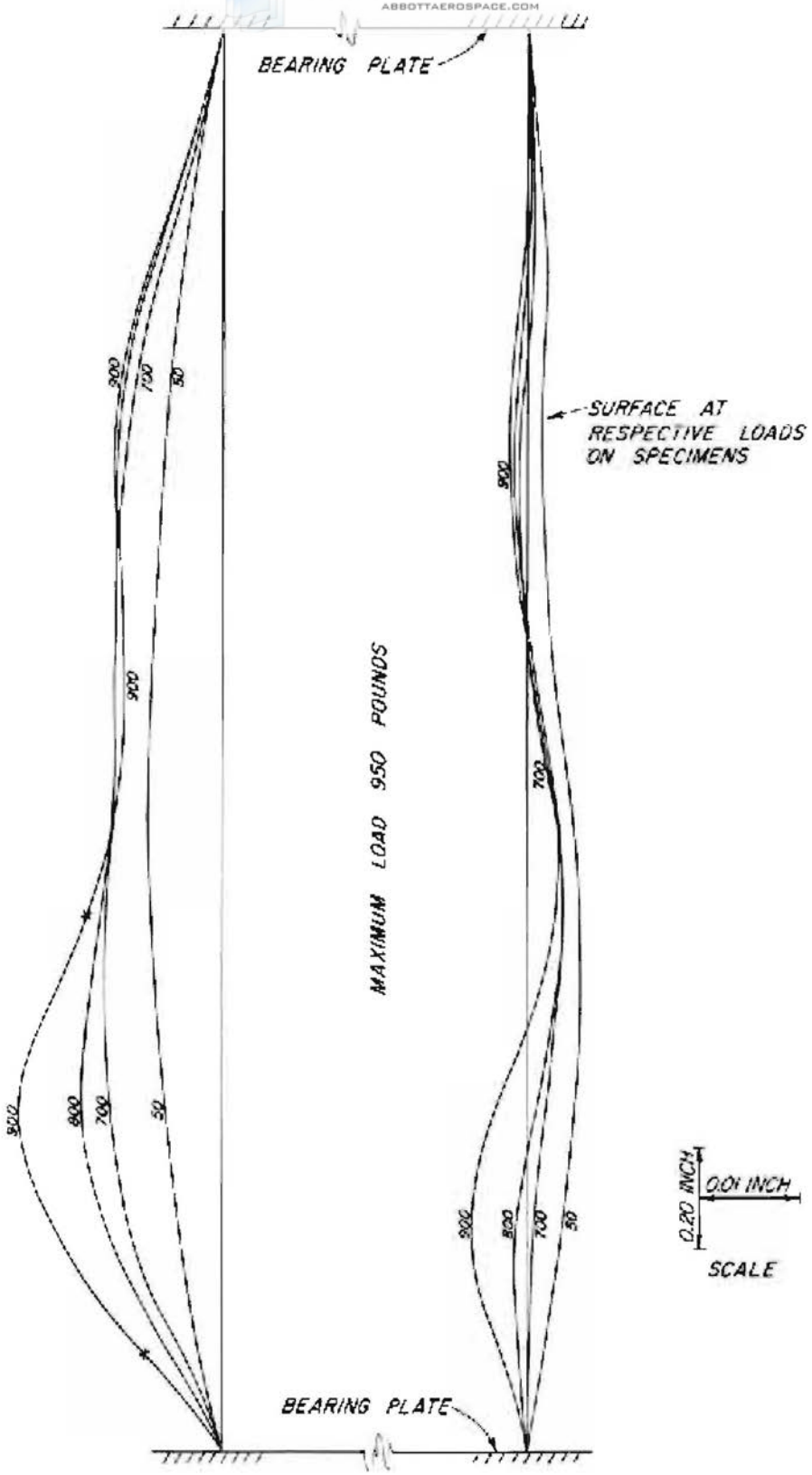

Figure 22.--Profiles of sandwich construction with 0.9196-inch 24ST clad aluminum-alloy facing and 3/4-inch cork core (sp. gr. 0.45) shown in fugure 26.

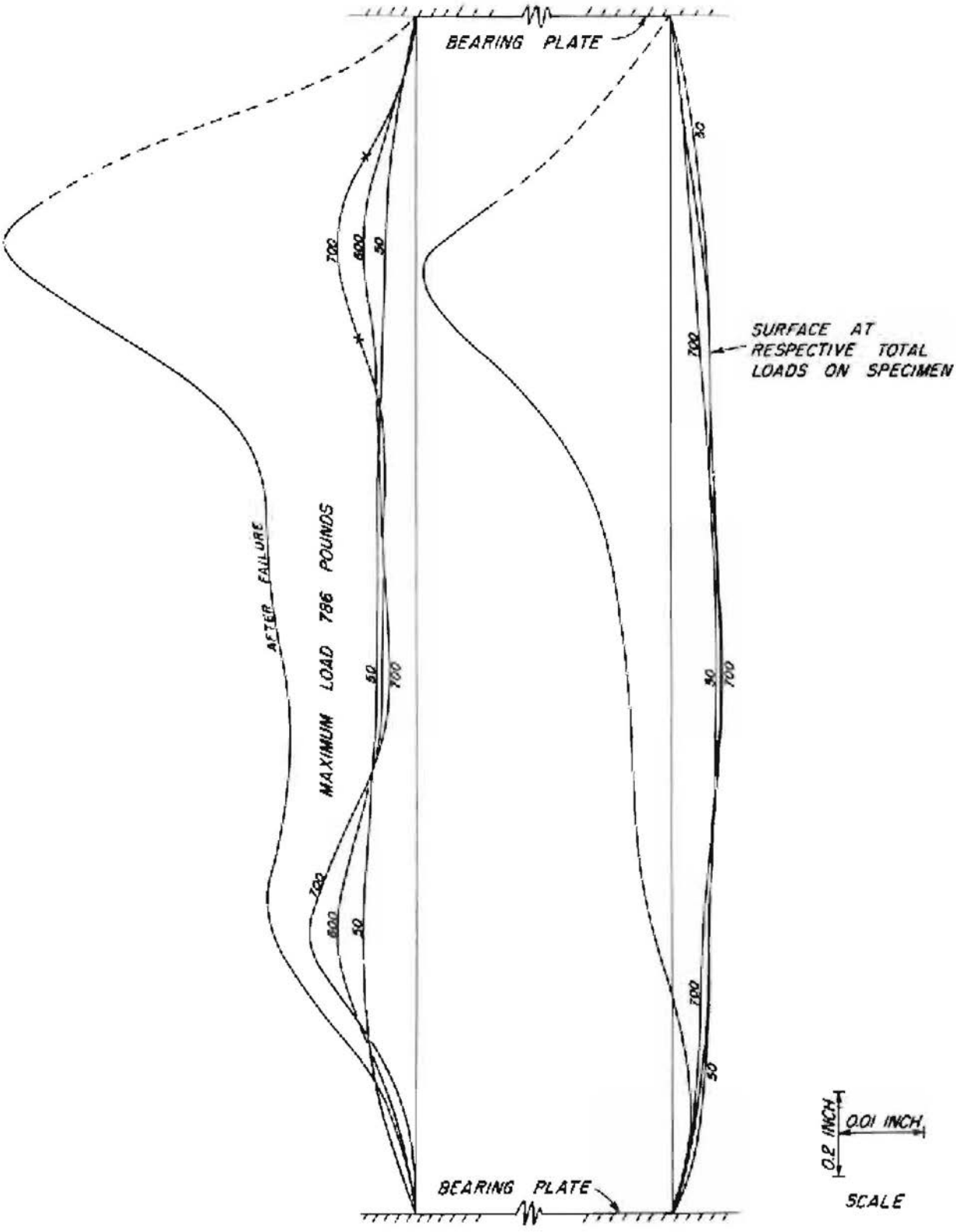

Figure 23.--Profiles of 0.012-inch 248T clad facings and 3/4-inch cork core (0.45 sp. gr.) shown in figure 27.

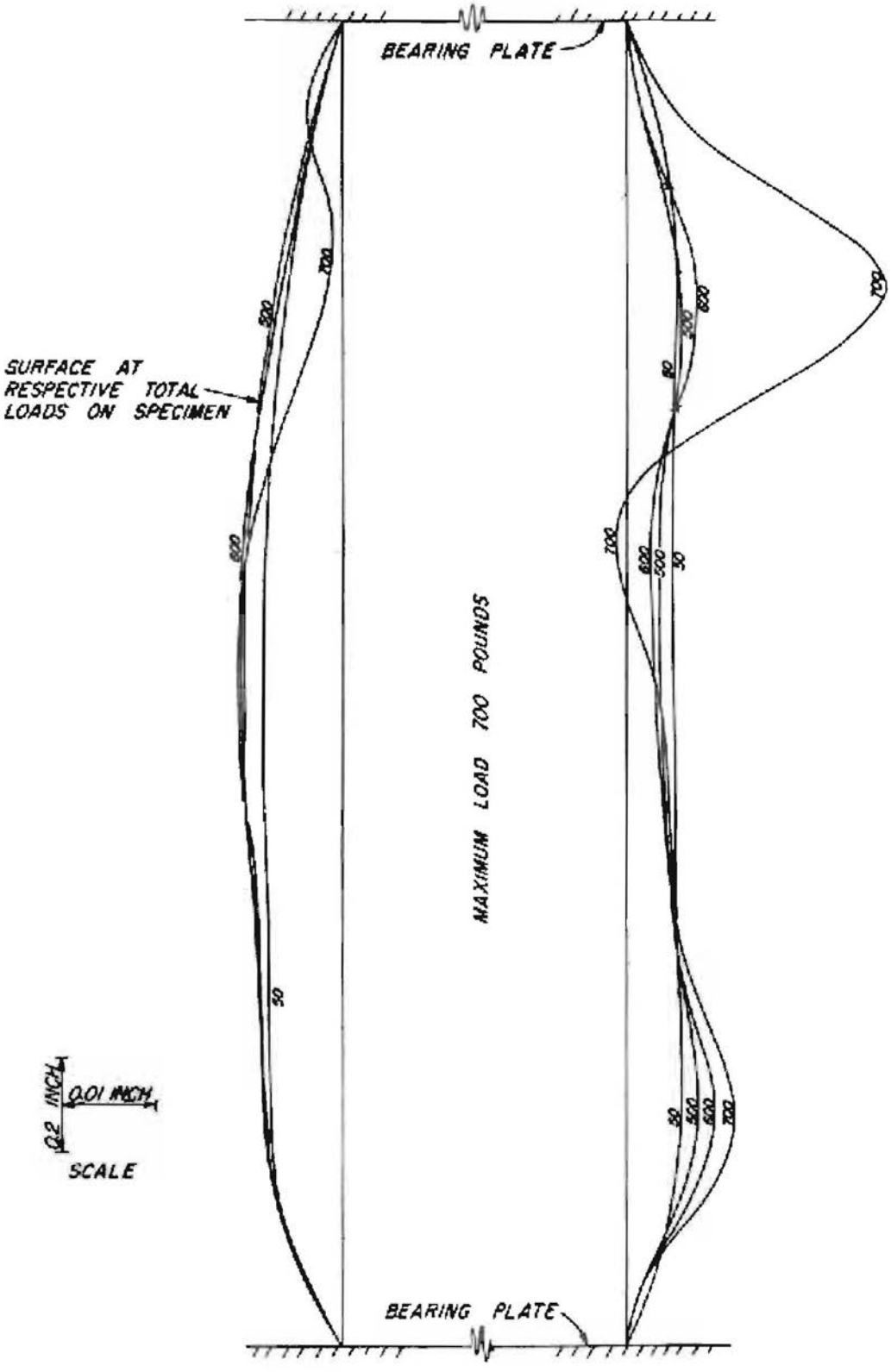

Figure 24.--Profiles of 0.012-inch 24ST clad facings and 3/4-inch cork core (0.45 sp. gr.) shown in figure 28.

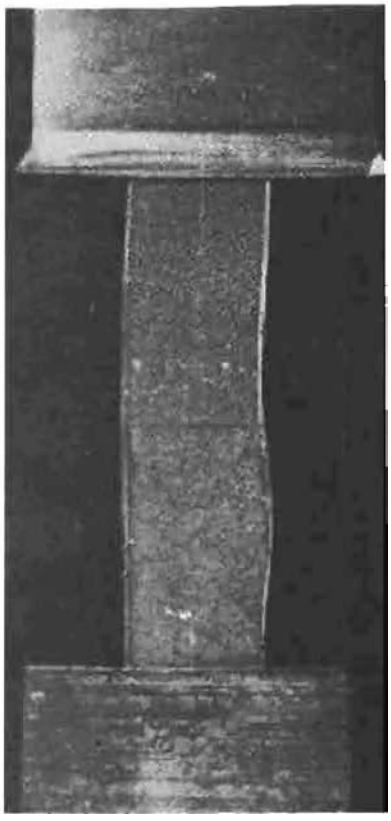

Figure 25.--Photograph of wrinkling failure of sandwich specimen having 0.020-inch 24ST aluminum-clad facings and 3/4-inch, 0.45-specific-gravity cork cores. The measured profile of this specimen is shown in figure 21.

Z M 81872 F

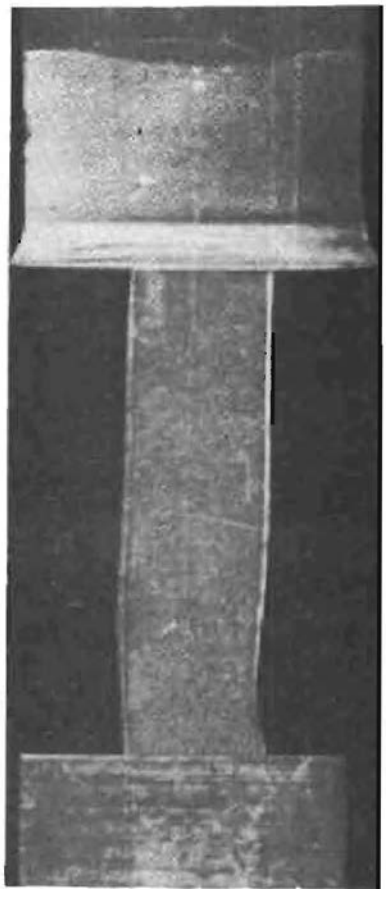

Figure 26.--Photograph of wrinkling failure of sandwich specimen having 0.020-inch 24ST alminum-clad facings and 3/4-inch, 0.45-specific-gravity cork cores. The measured profile of this specimen is shown in figure 22.

ZM 81873 F

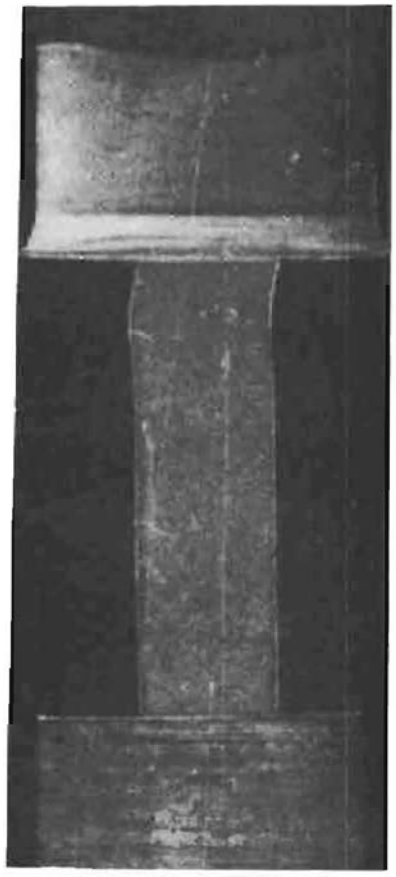

Figure 27.--Photograph of wrinkling failure of sandwich specimen having 0.012-inch 24ST aluminum-clad facings and 3/4-inch, 0.45-specific-gravity cork cores. The measured profile of this specimen is shown in figure 23.

Z M 81874 F

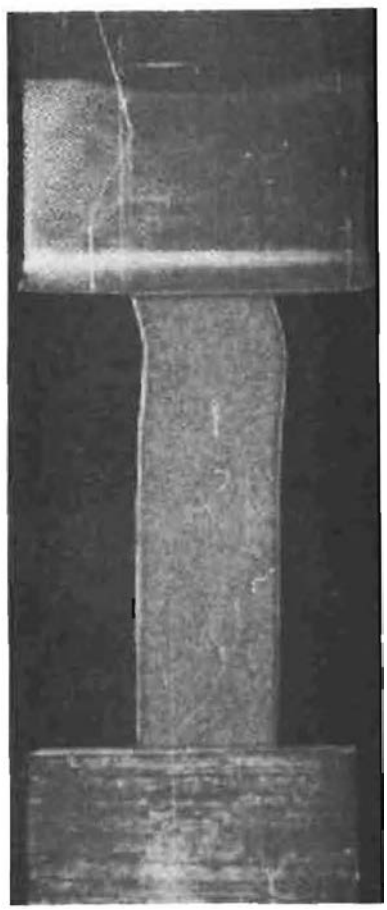

Figure 28.--Photograph of wrinkling failure of sandwich specimen having 0.012-inch 24ST alminum-clad facings and 3/4-inch, 0.45-specific-gravity cork cores. The measured profile of this specimen is shown in figure 24.

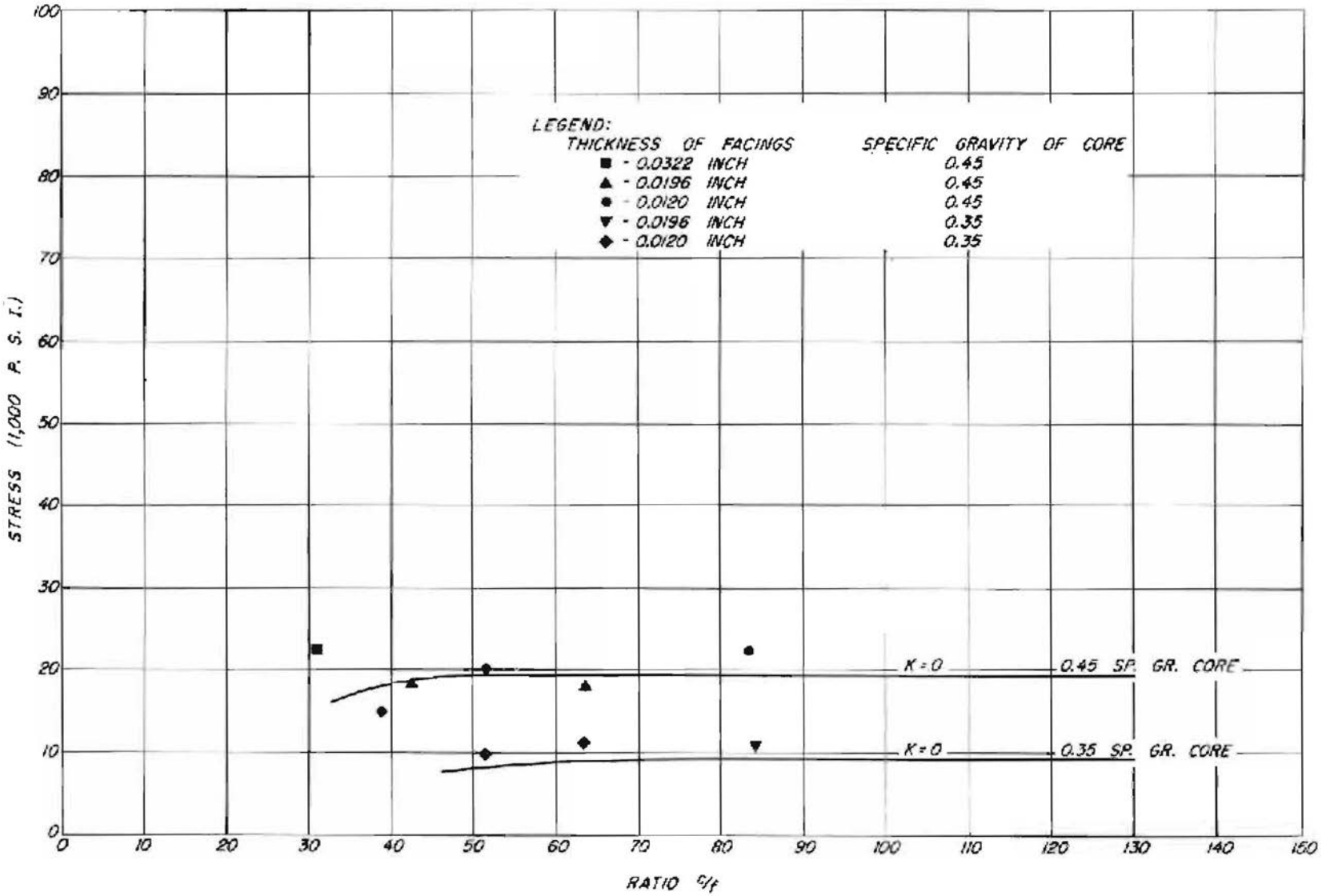

Figure 29.--Sandwich constructions having aluminum facings and cork cores. Curves represent computed values. Each plotted point represents the average of 10 specimens.

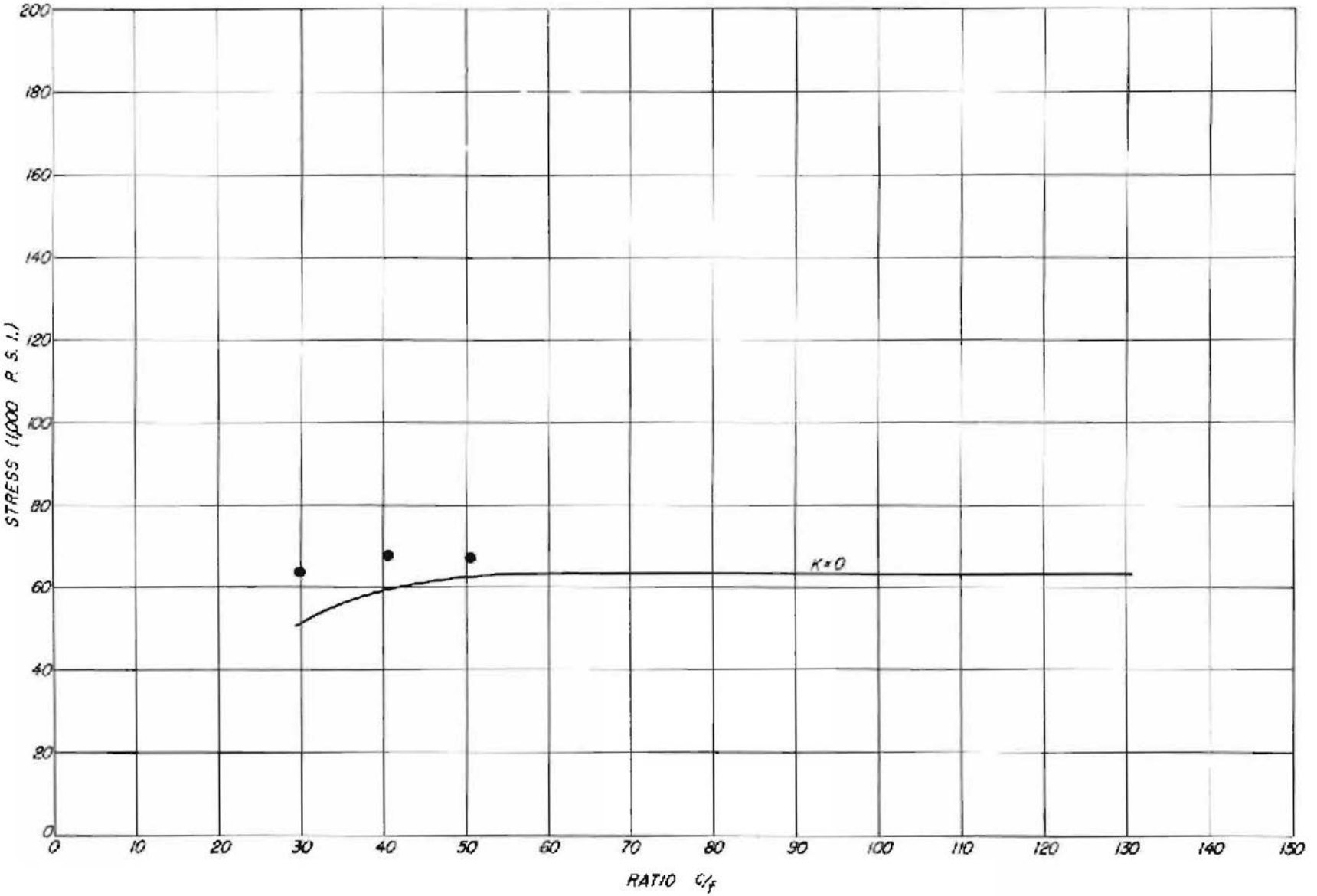

Figure 30.--Sandwich construction with 0.010-inch steel facings and cork (0.66 sp. gr.) core for average of five specimens.

Z K 82075 F

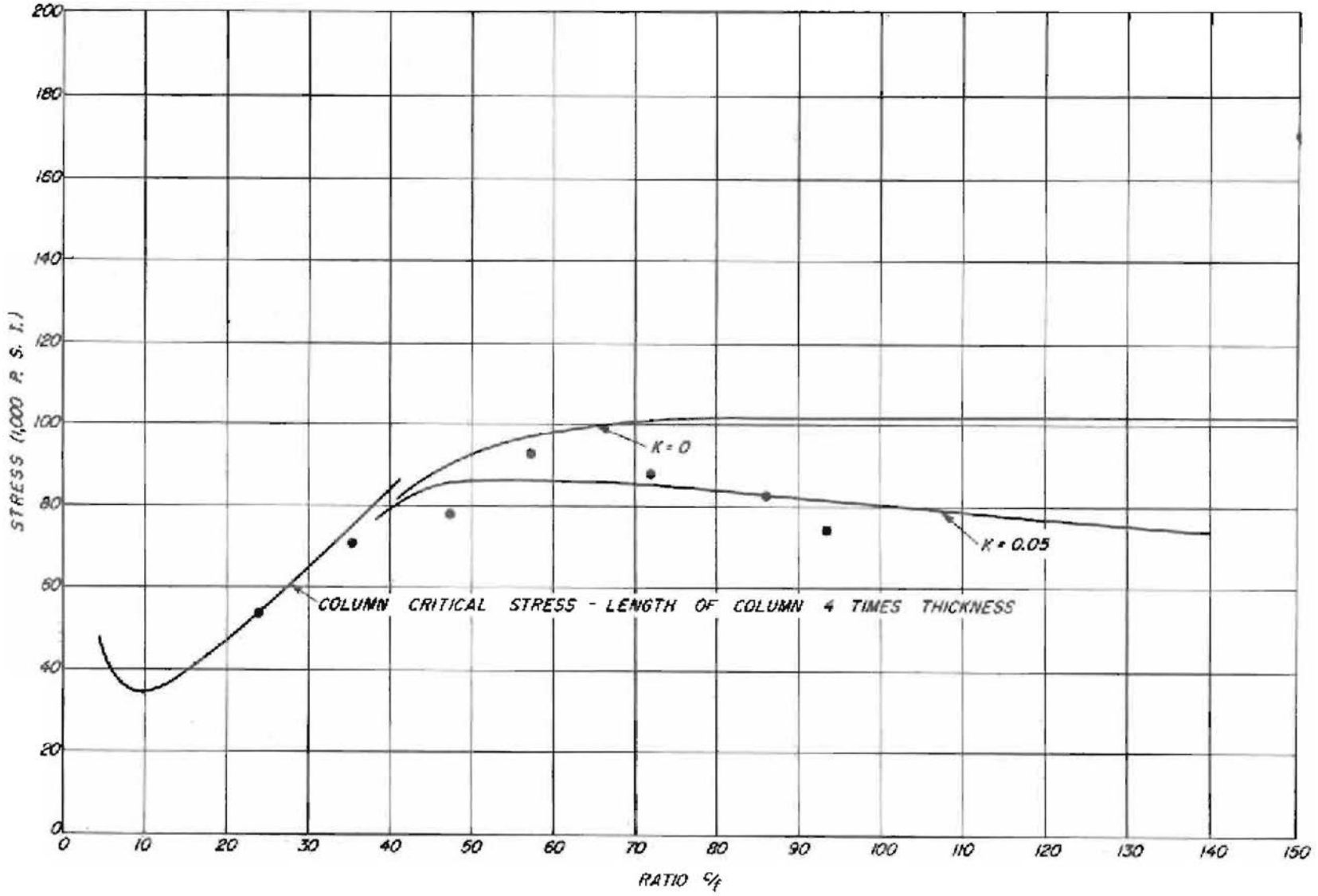

Figure 31.--Sandwich construction of 0.010-inch steel facings and cellular cellulose acetate cores (flatwise). Each plotted point represents average of four specimens.

z M81467F

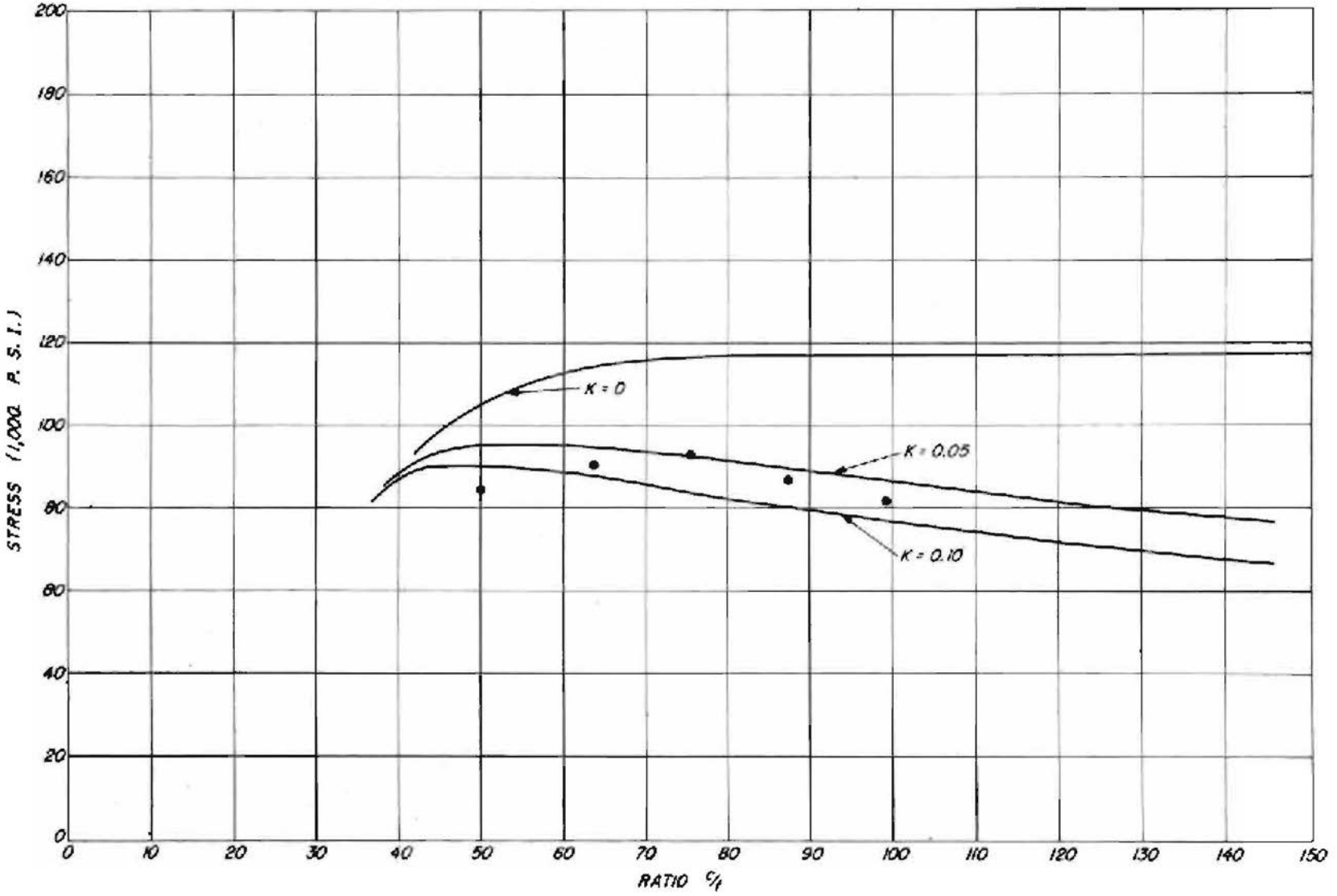

Figure 32.--Sandwich construction of 0.010-inch steel facings and cellular cellulose acetate cores (edgewise). Each plotted point represents average of four specimens.

z M81468F

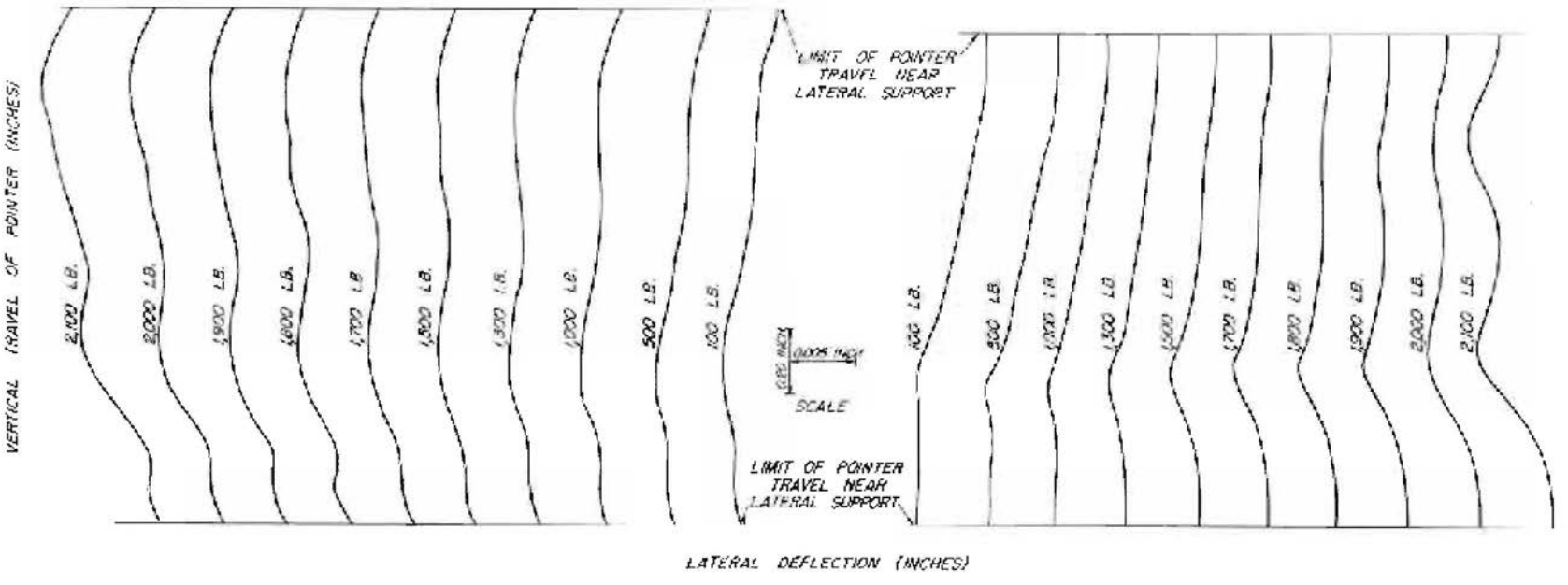

Figure 33.--Profile of facings of sandwich construction with 0.010-inch steel facings and 1/2-inch cellular cellulose core (edgewise).

Z M 62076 F

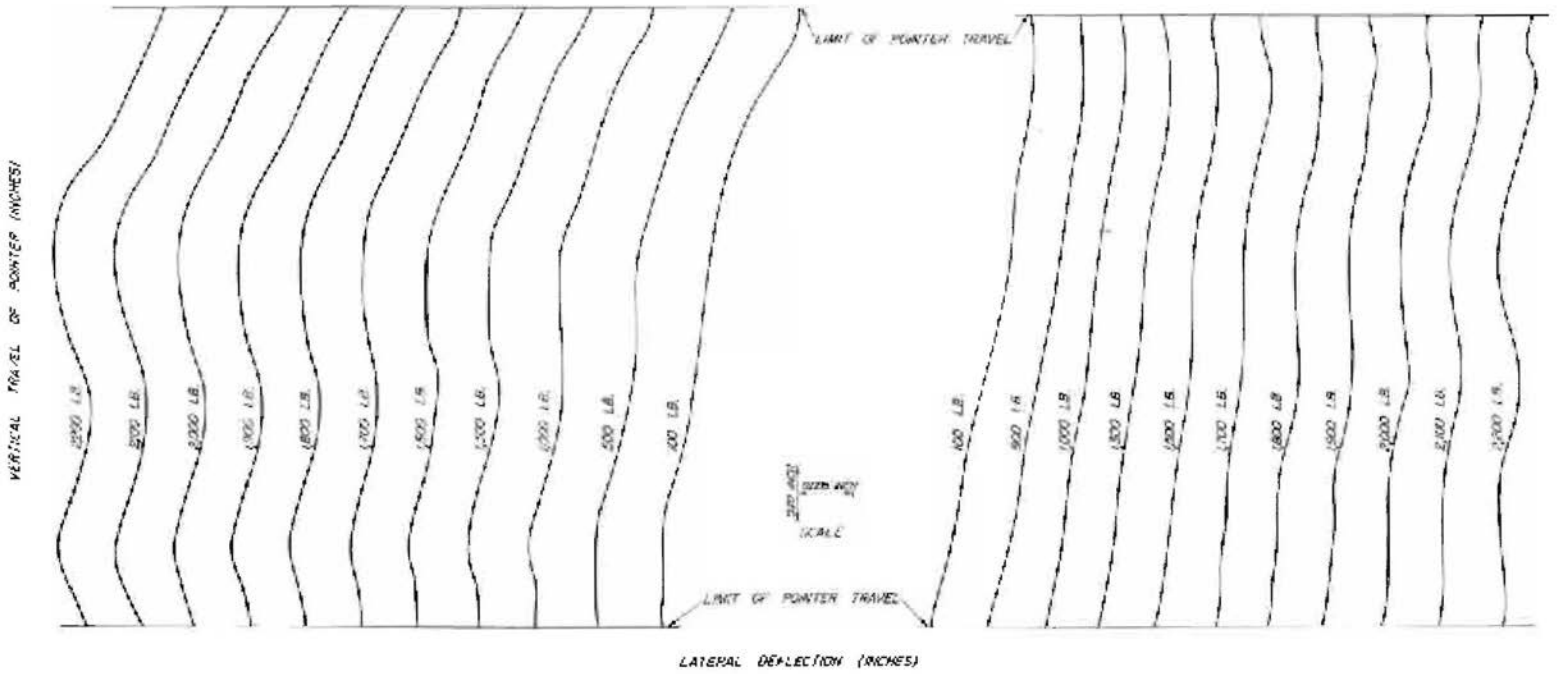

Figure 34.--Profile of facings of sandwich construction with 0.010-inch steel facings and 5/8-inch cellular cellulose acetate core (edgewise).

Z M 82077 F

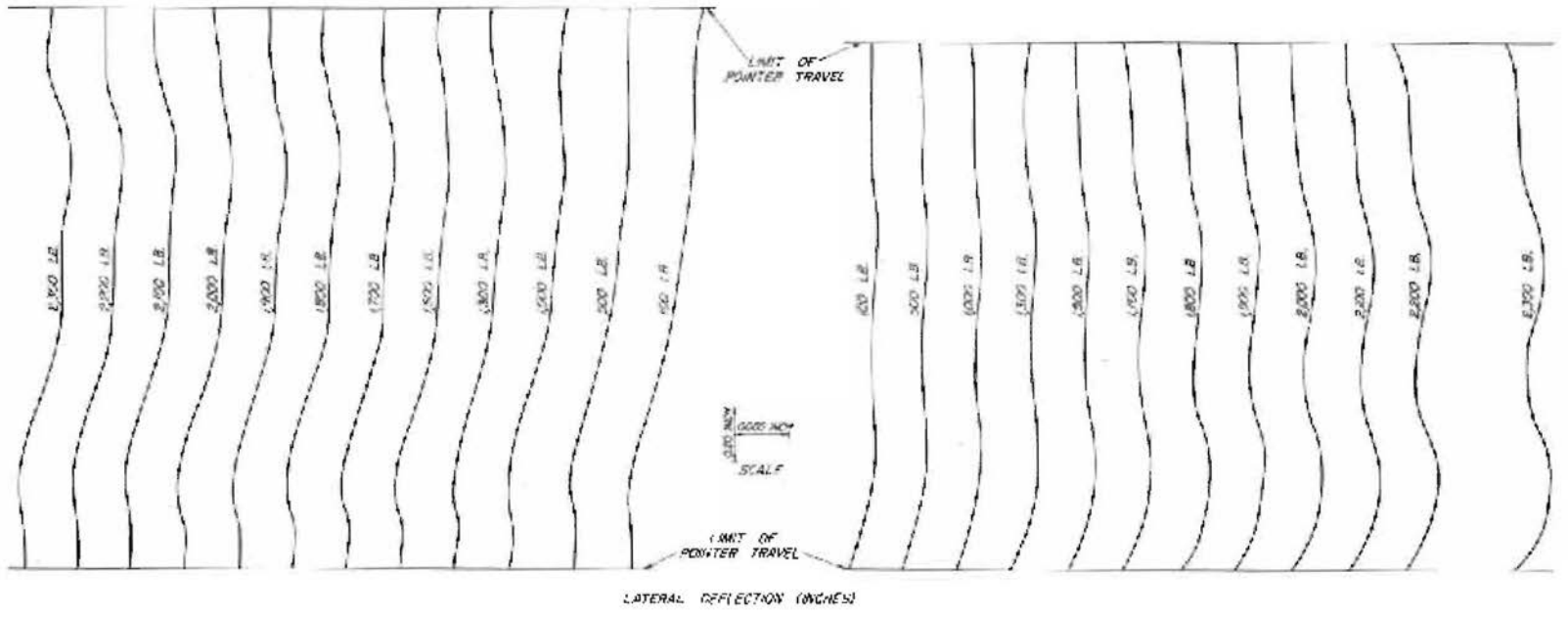

Figure 35.--Profile of facings of sandwich construction with 0.010-inch steel facings and 3/4-inch cellular cellulose acetate core (edgewise).

Z X 82078 F

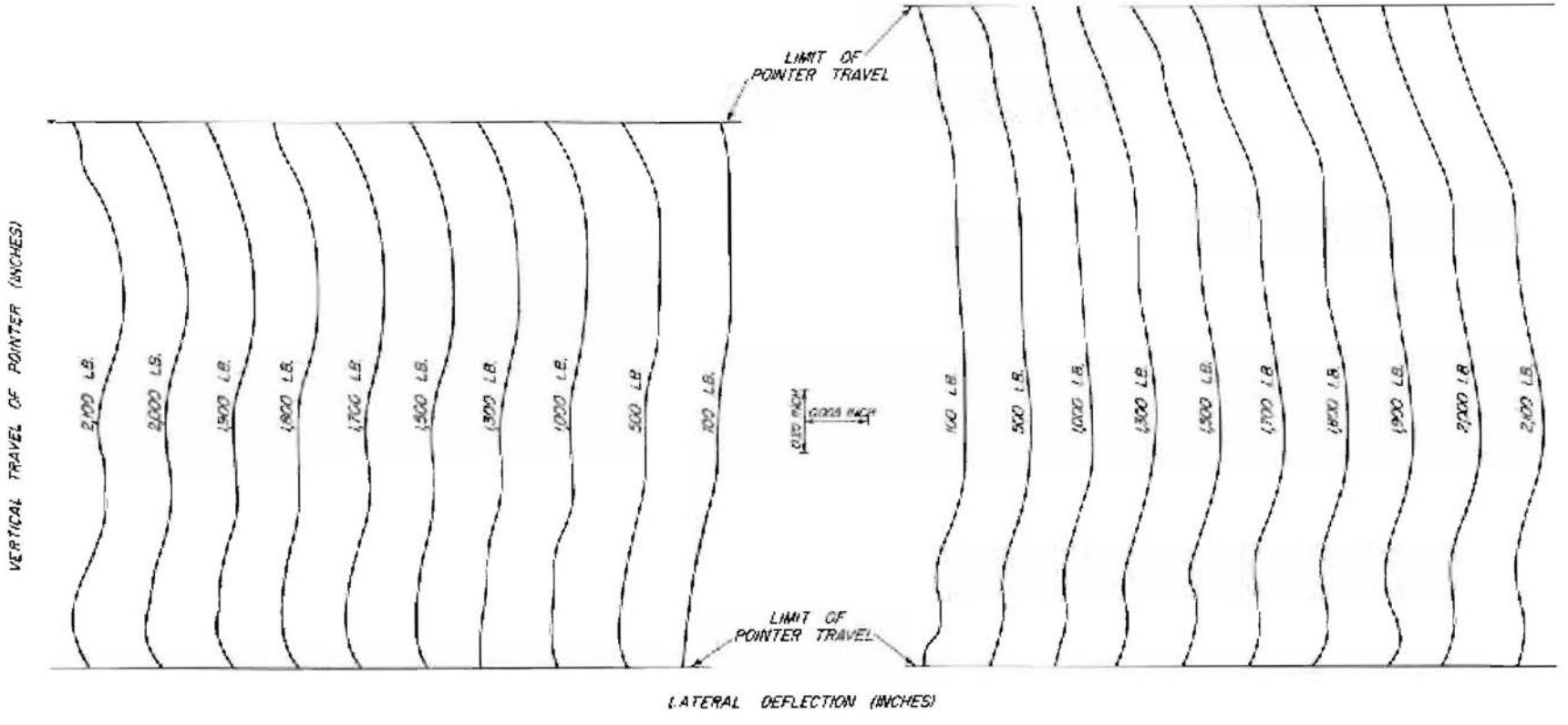

Figure 36.--Profile of facings of sandwich construction with 0.010-inch steel facings and 7/8-inch cellular cellulose acetate core (edgewise).

Z M 62079 F

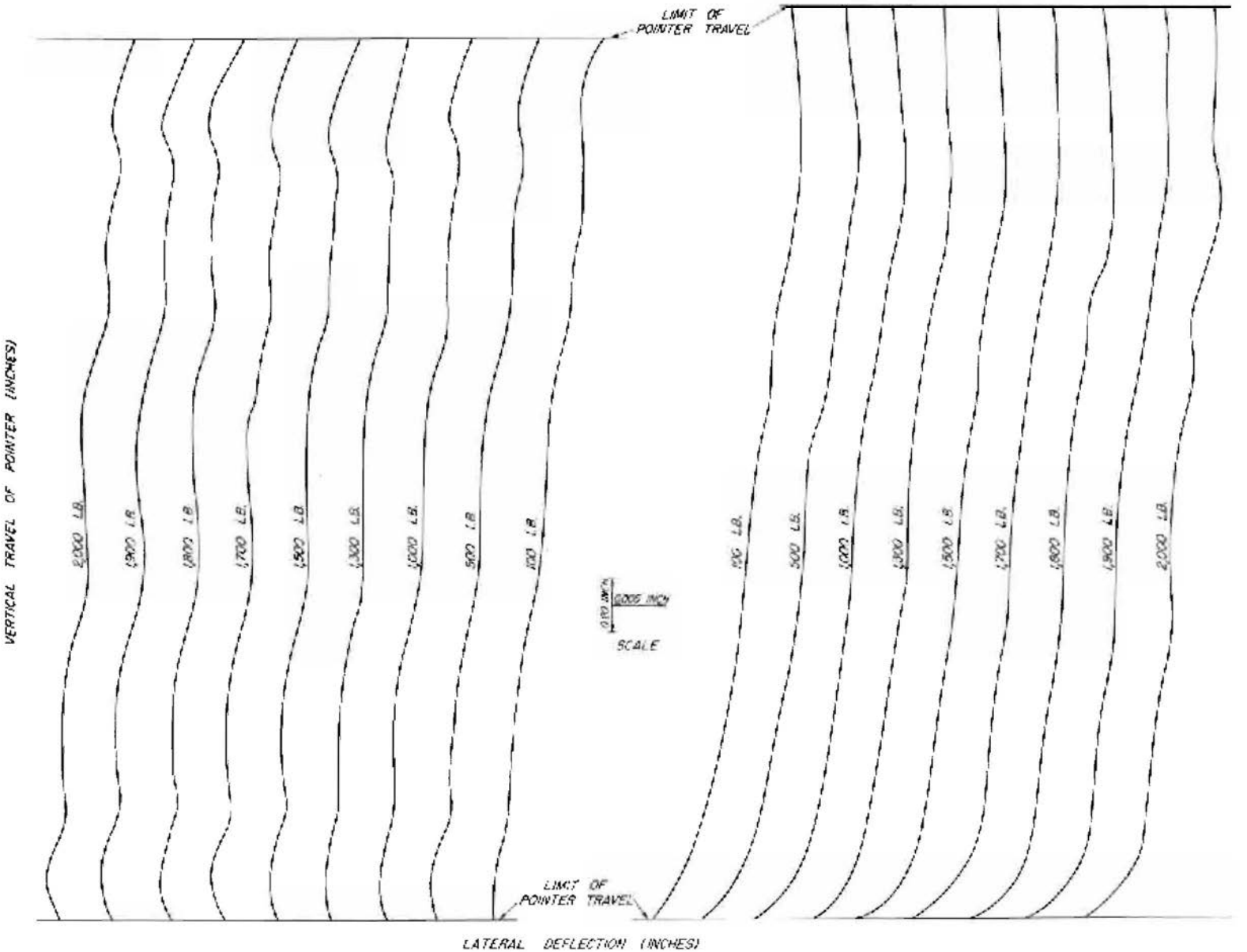

Figure 37.--Profile of facings of sandwich construction with 0.010-inch steel facings and 1-inch cellular cellulose acetate core (edgewise).

Z M 62080 F

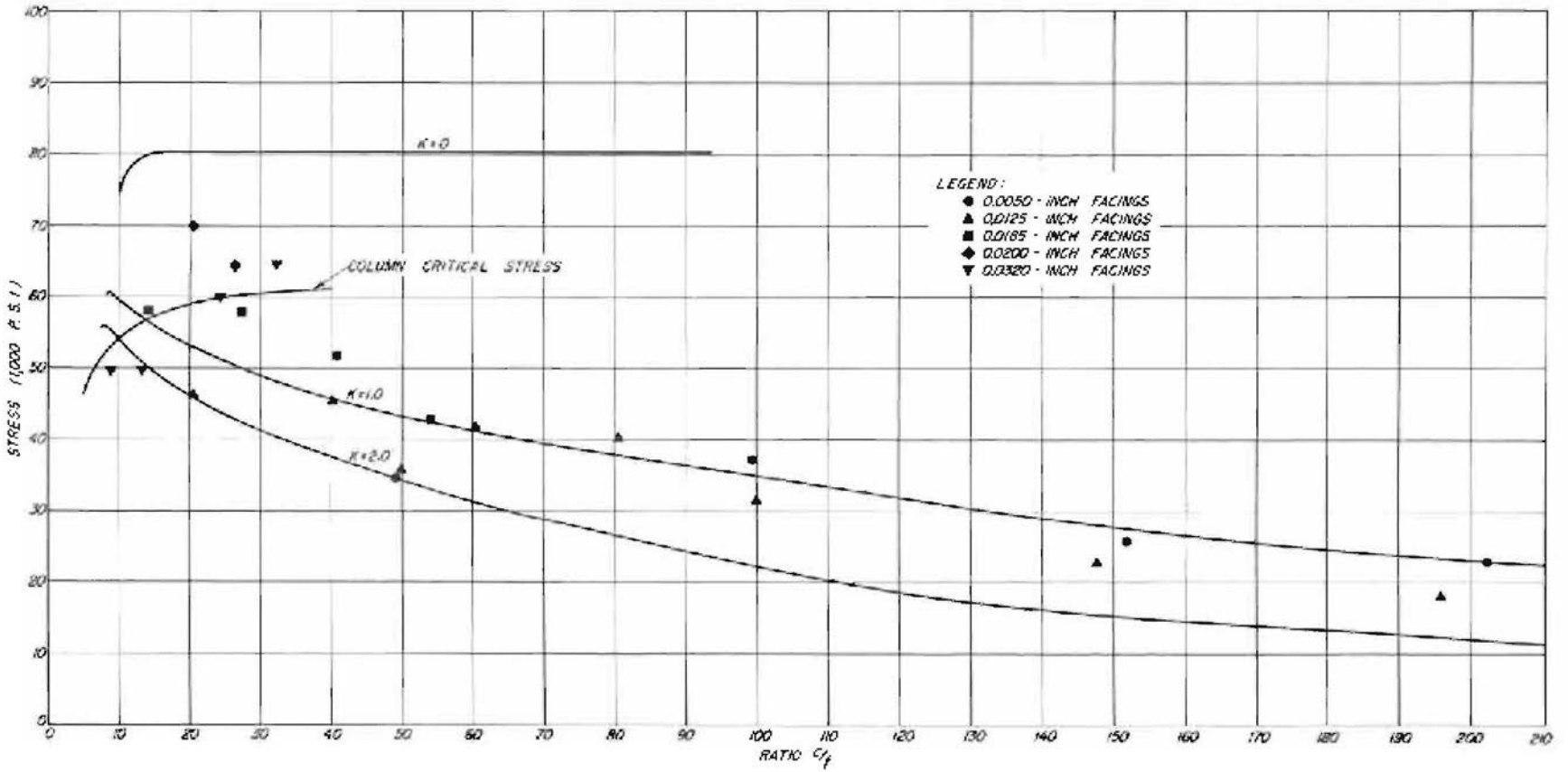

Figure 38.--Sandwich constructions of aluminum facings and balsa core for average of five specimens.

Z M 82081 F

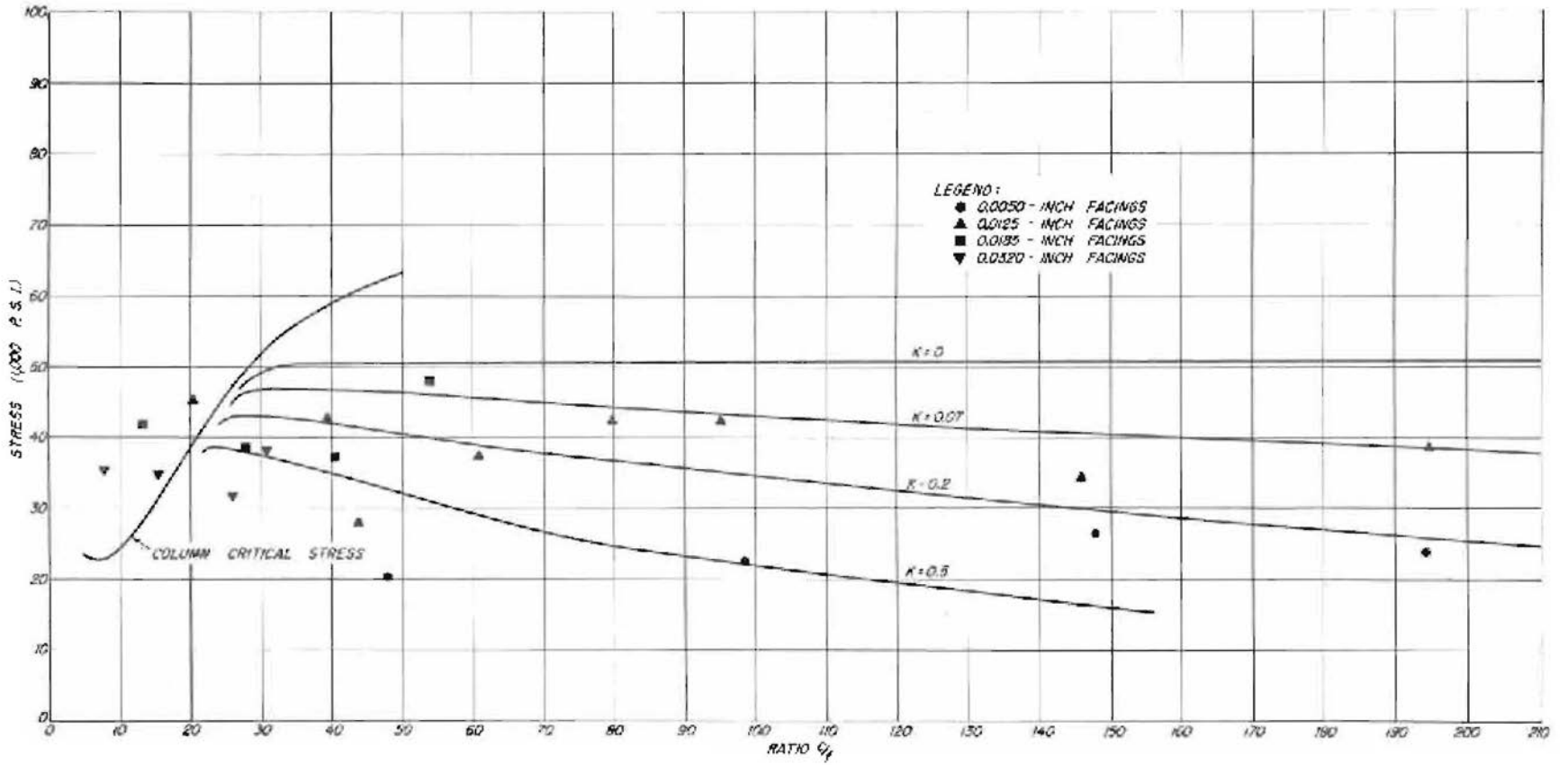

Figure 39.--Sandwich constructions with aluminum facings and cellular cellulose acetate cores for an average of five specimens.

Z M 82082 F

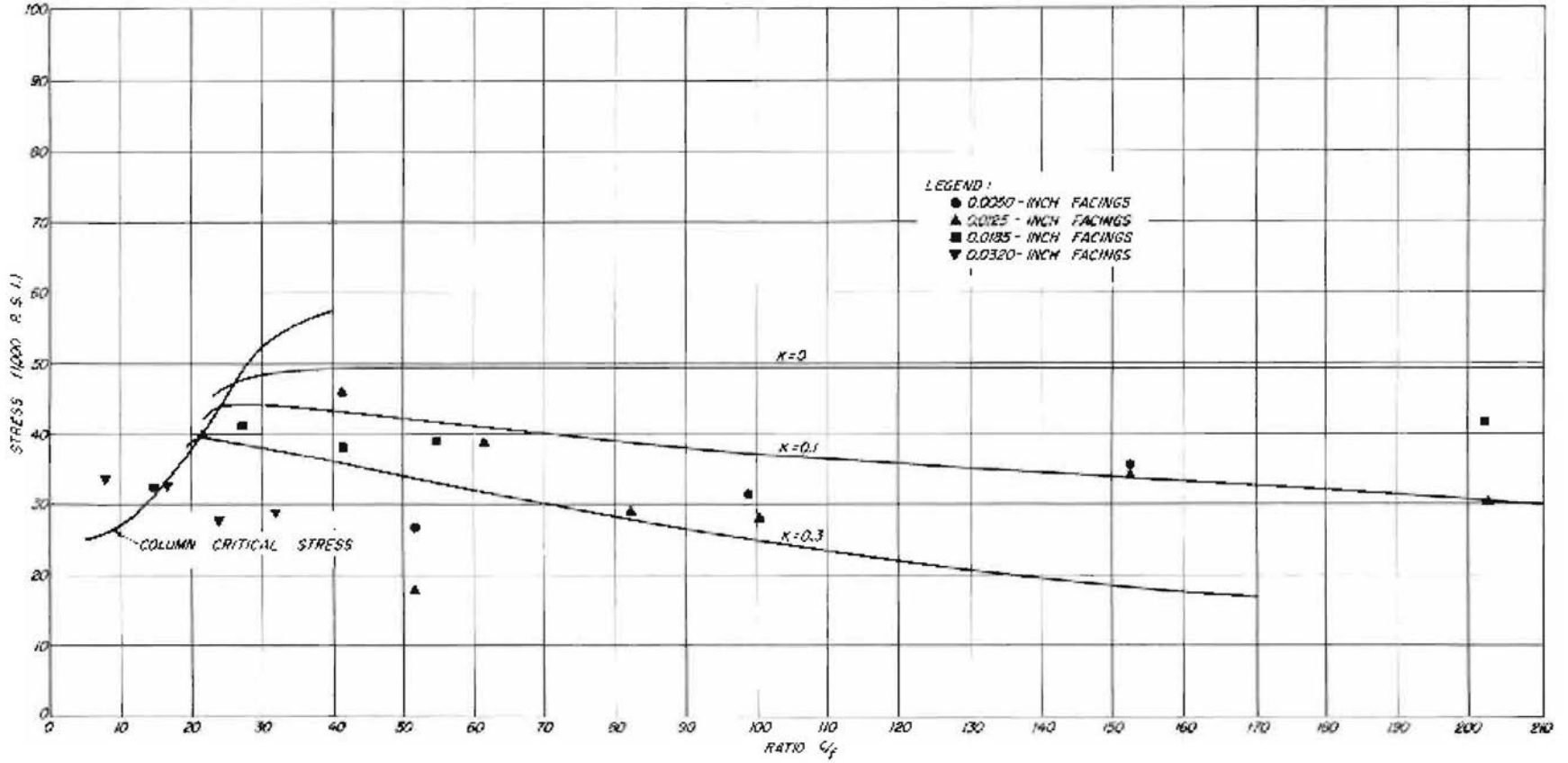

Figure 40.--Sandwich constructions with aluminum facings and cellular hard-rubber core for an average of five specimens.

Z K 82083 F

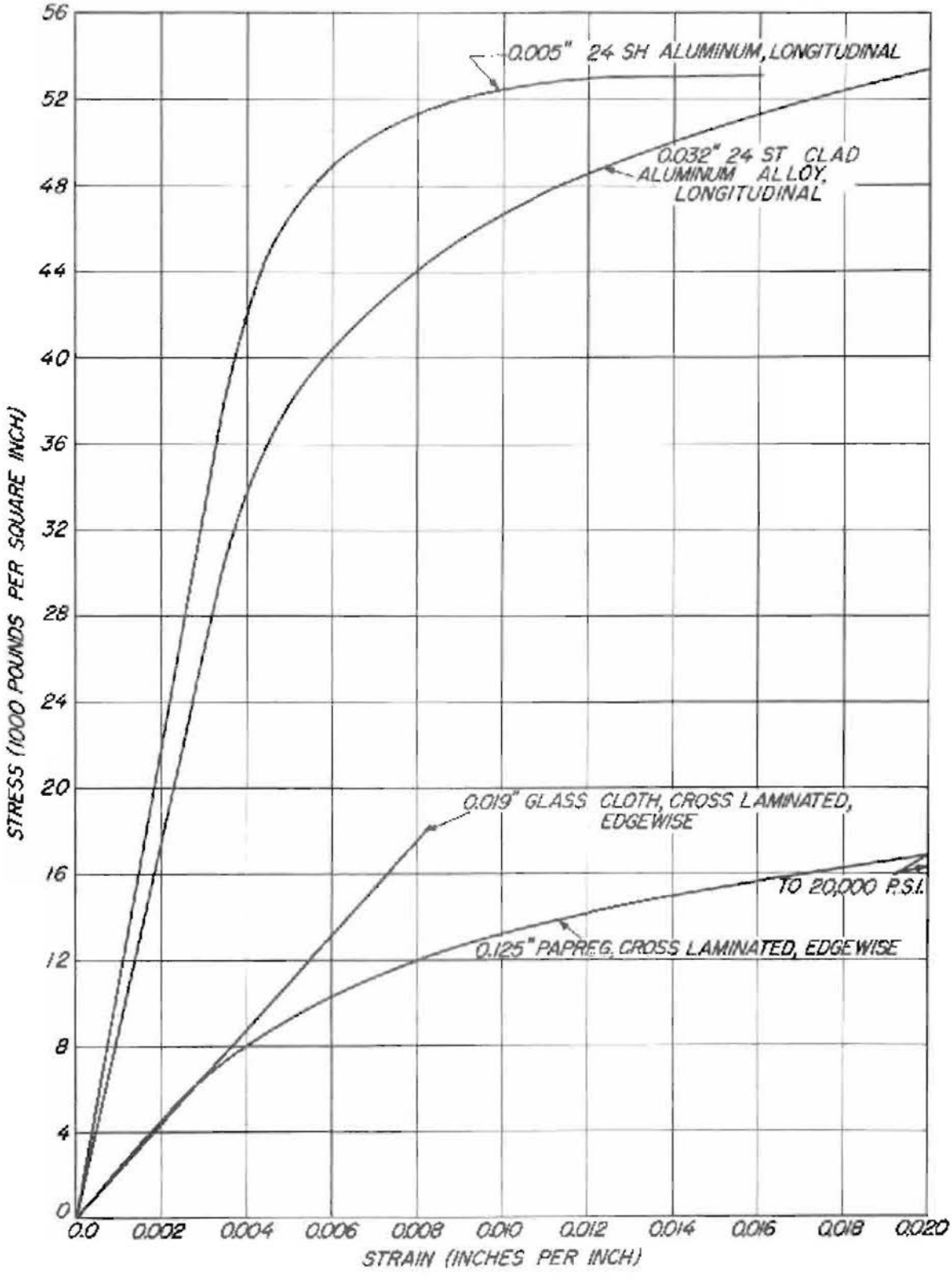

Figure 41.--Typical stress-strain curves of facing materials in edgewisecompresssion.

Z M 82084 F

SUBJECT LISTS OF PUBLICATIONS ISSUED BY THE

FOREST PRODUCTS LABORATORY

The following are obtainable free on request from the Director, Forest Products Laboratory, Madison 5, Wisconsin:

List of publications on Box and Crate Construction and Packaging Data

List of publications on Chemistry of Wood and Derived Products

List of publications on Fungus Defects in Forest Products and Decay in Trees

List of publications on Glue, Glued Products and Veneer

List of publications on Growth, Structure, and Identification of Wood

List of publications on Mechanical Properties and Structural Uses of Wood and Wood Products

Partial list of publications for Architects, Builders, Engineers, and Retail Lumbermen

List of publications on Fire Protection

List of publications on Logging, Milling, and Utilization of Timber Products

List of publications on Pulp and Paper

List of publications on Seasoning of Wood

List of publications on Structural Sandwich, Plastic Laminates, and Wood-Base Aircraft Components

List of publications on Wood Finishing

List of publications on Wood Preservation

Partial list of publications for Furniture Manufacturers, Woodworkers and Teachers of Woodshop Practice

Note: Since Forest Products Laboratory publications are so varied in subject no single list is issued. Instead a list is made up for each Laboratory division. Twice a year, December 31 and June 30, a list is made up showing new reports for the previous six months. This is the only item sent regularly to the Laboratory's mailing list. Anyone who has asked for and received the proper subject lists and who has had his name placed on the mailing list can keep up to date on Forest Products Laboratory publications. Each subject list carries descriptions of all other subject lists.